personal buildup for

Force Motors Ltd.

MTZ worldwide 6/2010, as epaper released on 14.05.2010
http://www.mtz-worldwide.com

content:

www.MTZonline.com

MTZ

WORLDWIDE

06 June 2010 | Volume 71

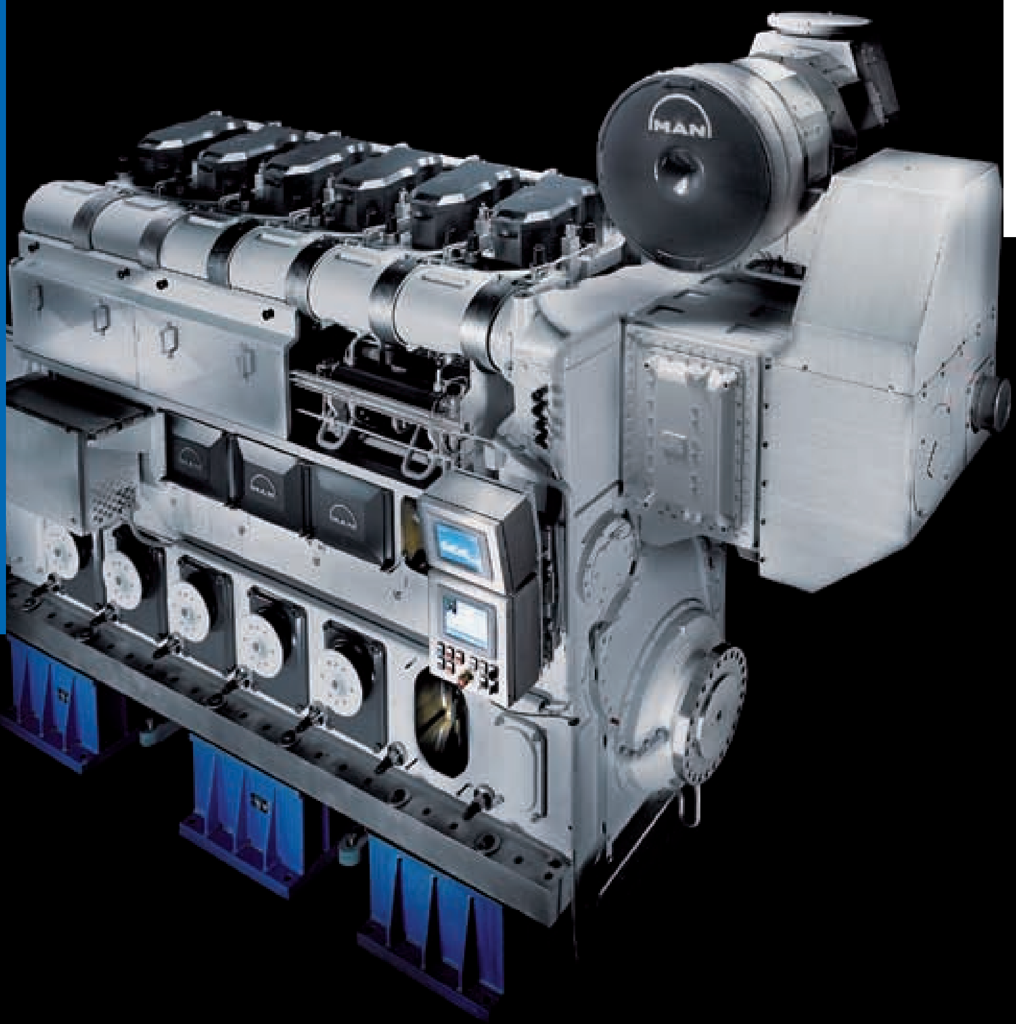

LARGE-BORE ENGINES CLEAN AND RELIABLE?

CONTENTS

COVER STORY

LARGE-BORE ENGINES CLEAN AND RELIABLE?

4, 12 I Unexpected damages to ship's engines can have fatal consequences. Hence, it is all the more important to predict the durability of large engines. One of the most highly strained component parts is the crank shaft. MAN describes a method to evaluate the operating safety of these assemblies. Equally challenging for manufacturers are upcoming emission regulations. Wärtsilä conceptualizes strategies to meet the emission standard IMO III.

COVER FIGURE MAN

ENGINES AND EMOTIONS

Dear Reader,

Driving a car is characterised by emotion. Anyone who has the slightest fascination for technology and does not see a car simply as a means of "getting from A to B" will agree. We see, smell and feel a car – and we hear it. Especially the engine. But lately, engine sound has increasingly been relegated into the background.

Depending on the type of engine involved, it is not a question of fewer decibels reaching the driver's ear. Diesel engines in particular suffer acoustically under the strict and necessary development objective of emitting less CO_2. High pressures may be efficient, but they are not quiet. The sound of a diesel engine at work makes only a minor contribution to the emotionality of a car. And there is little space available for technically feasible sound design with the aid of resonators.

The petrol engine has it somewhat easier. But even here, less emission is more important than more emotion. And in times of rising petrol prices, this is also directly in the interests of the consumer – not to mention the environment. Added to this is a change in social acceptance: where we used to enjoy the muscular sound of a V8 engine, we now think primarily of its fuel consumption.

But there are exceptions to the rule, and we occasionally experience them in our test cars. Currently in the form of a Ford Focus RS, which gives the impression that the (five-cylinder) engine is still allowed to be a real engine. It angrily consumes any thoughts about efficiency in the form of excess petrol at places that are not the first choice. And in doing so, it arouses emotions. And let us hope that one day, when the challenge of emissions has finally been satisfactorily overcome, we can return to this attractive side of an engine – without a bad conscience. We shall even be addressing this topic in the cover story of the next MTZ.

RUBEN DANISCH, Vice-Editor-in-Chief
Wiesbaden, 27 April 2010

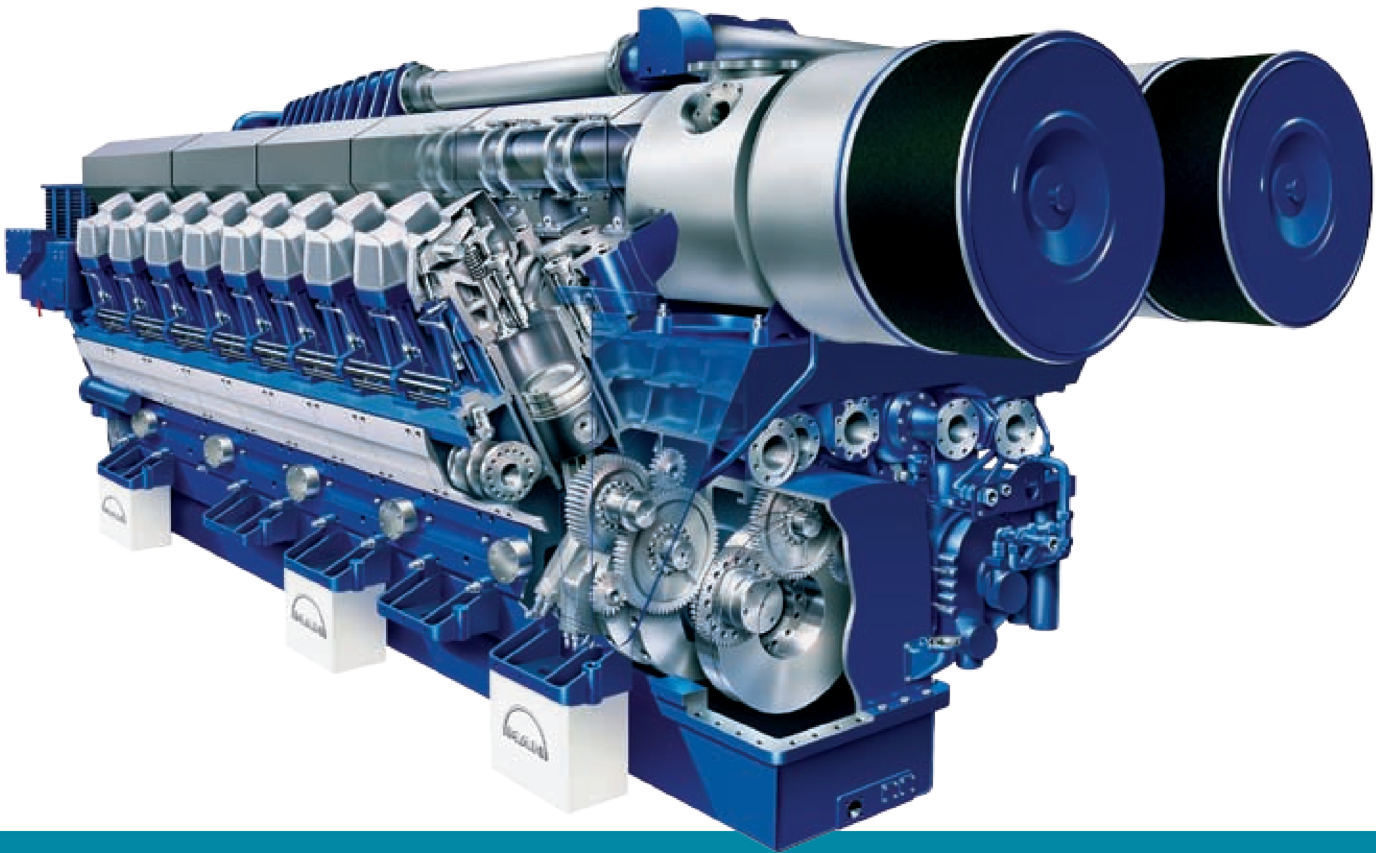

NUMERICAL FATIGUE STRENGTH ASSESSMENT FOR CRANKSHAFTS

Experimental assessment of the fatigue strength of crankshafts in large-bore four-stroke diesel engines is very expensive and time-consuming. Available theoretical methods are often based on analytical methods and simplified equivalent stress hypotheses, which can result in conservative designs. There are also limitations in determination of time-dependent stress distribution. In order to overcome these restrictions, the development and implementation of a numerical procedure at MAN Diesel & Turbo SE has been carried out for assessing operational reliability. Due to increasingly demanding performance specifications, this method is playing a crucial role in the design and rating process.

AUTHORS

DR.-ING. ROLAND KRIVACHY
is R&D Engineer in the Department Mechanics – Stress and Strength at MAN Diesel & Turbo SE in Augsburg (Germany).

DIPL.-ING. ANDREAS LINKE
is Senior Manager in the Department Mechanics – Stress and Strength at MAN Diesel & Turbo SE in Augsburg (Germany).

DIPL.-MATH. DIETMAR PINKERNELL
is Head of the Department Mechanics – Stress and Strength at MAN Diesel & Turbo SE in Augsburg (Germany).

DEMANDS ON CRANKSHAFT DESIGN

The crankshafts of large-bore four-stroke diesel engines can be more than 10 m long and weigh up to 30 t. As a result of these dimensions and its associated high manufacturing costs, it is nearly impossible to conduct fatigue strength tests on these components. For this reason, analytical and numerical approaches to the determination of mechanical stresses and providing assessment of operational reliability must be pursued.

According to the current state of the art, the crankshafts of large-bore diesel engines are rated and evaluated with regard to operational reliability by ship classification societies, based on IACS guideline UR M 53 [1]. Characterised by transparency and easy, inexpensive implementation, this analytical procedure has proven extremely useful in practice. However the disadvantage of the procedure is that it tends to comparatively high conservative results. In connection with the development of new engine designs, it becomes essential to develop components with higher performance or reduced mass. In order to reach this objective, it is absolutely necessary to attain a higher material loading without compromising operational reliability. Therefore, a deep knowledge of all available loading potential within the component are obligatory, which in turn requires intensive studies with a high grade of detail. In order to determine the time-dependent stress distribution, the numerical strength assessment presented here is carried out for the entire crankshaft giving special consideration to known high-stress areas (fillets: radius transitions between journal and web, oil drillings).

In order to be able to implement such a method efficiently, different approaches are selected and investigated with respect to time, cost and quality in its application. Parts of this article are based on a presentation given at a Femfat user meeting [2].

MULTI-BODY SIMULATION WITH FLEXIBLE BODIES

Multi-body simulation (MBS) offers the necessary basis for determining both the timing and the positioning of the mechanical stresses. The transient simulation is carried out under consideration of the general equation of motion and of rigid body kinematics. Non-linearities and gyroscopic effects are taken into account. Speeds, accelerations and displacements of the bodies are determined and, in addition, the forces or moments at the coupling points are determined. For a fatigue strength assessment, the component must be flexible and locally deformable. For this reason, finite element models with a fewer degrees of freedom are used in the multi-body simulation.

REDUCTION AND MODELLING

For the crankshaft with inner part of damper, a FE model with approximately 200,000 nodes is generated, ❶. The number of available degrees of freedom must be reduced considerably without changing the global rigidity characteristics or the basic dynamic properties of the body. To that end, both modal and static modes are measured. These are superimposed in the later simulation, in order to determine the deformation of the reduced body. Hence every change in geometry which affects rigidity necessitates a new reduction. The modes to be calculated must be selected carefully in order to achieve the lowest possible number of remaining degrees of freedom that are nonetheless necessary. For the global behaviour of the crankshaft, 50 to 100 modal modes are calculated. In addition, 200 to 250 static modes are determined at points where local force transmission occurs. After the reduction with the FE program Abaqus [3], the degrees of freedom of the crankshaft are reduced from approximately 600,000 to approximately 300.

❶ FE mesh of global overall crankshaft model

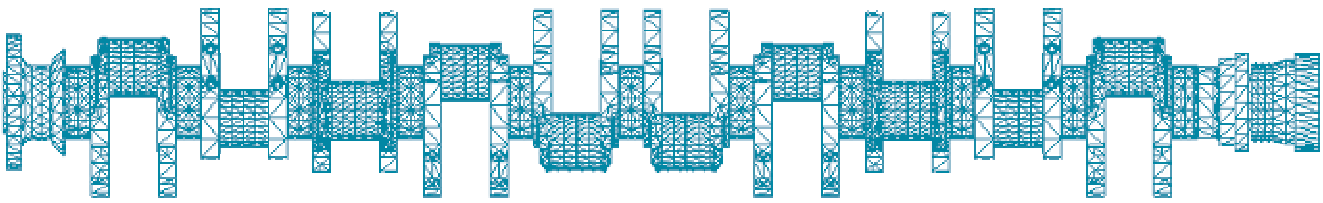

The reduced flexible bodies are entered into a MBS system (First/Tower [4]). In addition to the crankshaft, the cylinder crankcase, damper and flywheel are also taken into account as elastic bodies. The frame is mounted at the centre of gravity against rigid body movements. The crankshaft is incorporated into the frame via hydrodynamic radial and axial bearings. A characteristic map solution (impedance method) is used for calculation of the plain bearings. Parameters used to model the bearings include bearing diameter, width, clearance and viscosity. Clutch, flywheel and dampers are modelled with the corresponding rigidity and damping characteristics. In addition, gas pressure characteristic, ignition sequence and an analytical, rigid crank drive are incorporated into the simulation.

SIMULATION

The simulation is carried out with the solution of the general Newtonian equation of motion in the time domain. In doing so, the rigid body motions are integrated separately from the deformations. The gravitation and the hydrodynamic damping are incorporated together with structural damping of the components. A limit frequency prevents the integrator from taking very small steps. Above this frequency, the associated modes are still taken into account but the modal masses are increased virtually. It is possible to incorporate external forces, structure couplings or non-linear spring characteristics. The simulation is carried out for multiple working cycles. For numerical reasons (transient oscillation of the system), only the last working cycle is used to determine the results. These can then be evaluated by means of two different methods:

1. Method (Channel-Max):
In this simpler approach for the overall modelling of the structural dynamics, the results are used directly for the fatigue strength assessment.

2. Method (Trans-Max):
The disadvantage of this approach is that it requires an additional step with a finite element simulation, the results of which form the basis for the fatigue strength assessment. Its advantage is the more detailed conclusions which can be reached regard to local mechanical stresses.

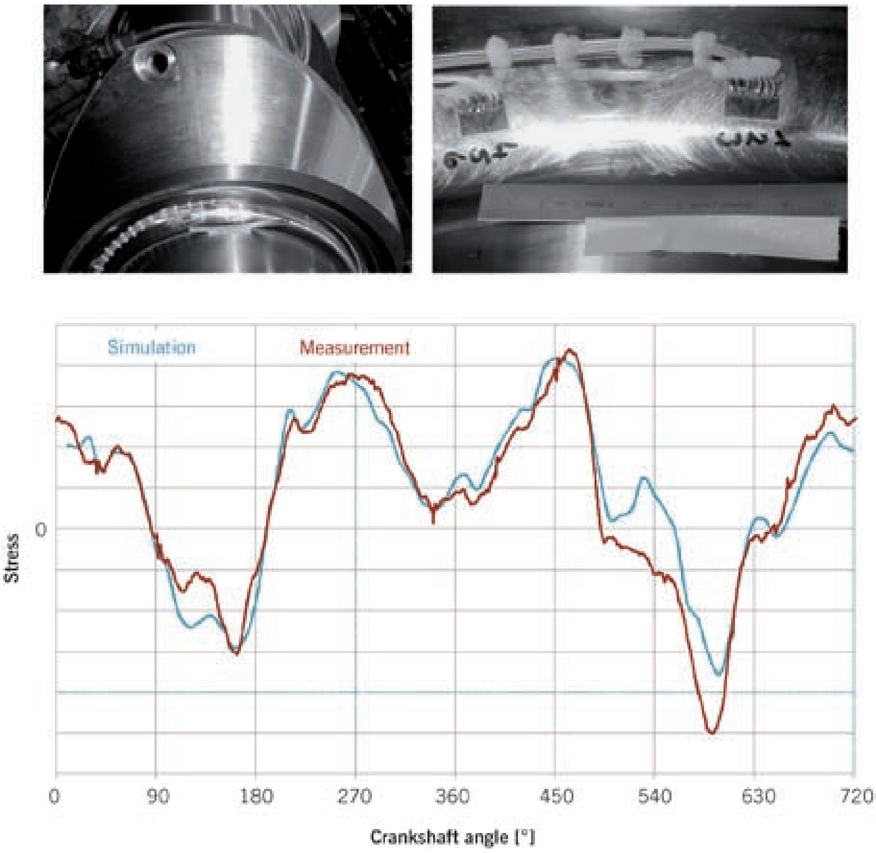

❷ Strain gauges in fillet of crankshaft (top); comparison between measurement and simulation of normal stresses at fillet (bottom)

A simulation according to the finite element method (FEM) can be useful in the stress analysis of complex components under multi-axial loads. A MBS analysis provides the elastic deformations for each node of the FE model. The deformations are exported as input data for the FE program Ansys [5] for a sufficient number of time steps and the resulting stresses are calculated.

CALCULATION / MEASUREMENT COMPARISON

A calculation/measurement comparison serves to verify the boundary conditions, correct model arrangement and that all relevant variables have been taken into account. It can be carried out via stress-strain comparison, for example, or also via a comparison of the torsional moments in the main bearings with other simulation methods.

The results from a transient First/Tower calculation are compared with the results of strain gauge measurements of the stresses present in a fillet of the crankshaft of a large-bore diesel engine. For the measurement, rosette strain gauges were applied for the determination of the multi-axial elastic strain, ❷ top. The strain curves measured were converted into normal stresses along the longitudinal axis of the engine (bending load). A comparison between the stresses determined in the simulation and those of the test shows that they correlate very well in terms of the amplitudes, mean stresses and the shape of the curve, ② bottom.

Another option to verify correct modelling is to compare the results with a simulation method in the frequency range. The in-house software Lidmoa (which has been used for many years now at MAN Diesel & Turbo SE) models the crankshaft with the crank drive, flywheel with clutch and torsional damper as an one-dimensional torsional vibration system around the torsional axis. Lidmoa determines the shear stress in the crankshaft at a specified system for different load points. The torsional moments calculated for the engine represented are compared with those from the MBS for modelling the global dynamics, ❸, and also exhibit a very good correlation.

FATIGUE STRENGTH ASSESSMENT

The fatigue strength assessment is carried out with Femfat software from ECS [6]. The complete stress information is evaluated and the critical plane approach is used to transform it to a scalar comparative stress. Here, the scaled normal stress hypothesis is applied and the corresponding mean and amplitude stresses are calculated. The local safety factor is given as the final result at the node. For this purpose, the two methods mentioned – Channel-Max and Trans-Max – can be used. These will be discussed in greater detail below, ❹.

FIRST METHOD: CHANNEL-MAX

If a component is subjected to time-dependent loads (which are otherwise constant in terms of position and direction) without non-linear effects, then operational fatigue strength can be calculated using channels (Channel-Max method). Here, the modes and the associated scaling factors are read into the system. Each channel can have its own variation in time. This method offers the following advantages:

: fully dynamic fatigue strength assessment without ignoring individual vibration components with all of the possibilities of non-linear MBS
: transient time curves of unrestricted length
: data volume comparable to that of an FE modal analysis
: easy implementation and rapid application
: no additional stress calculation with the FEM.

This method does have the disadvantage, that no further evaluation with a high degree of detail can be carried out for the component. Thus it is only suitable for the assessment of the overall dynamics.

SECOND METHOD: TRANS-MAX

As a result of the multi-body simulation, the local elastic deformations are first determined in a body fixed coordinate system.

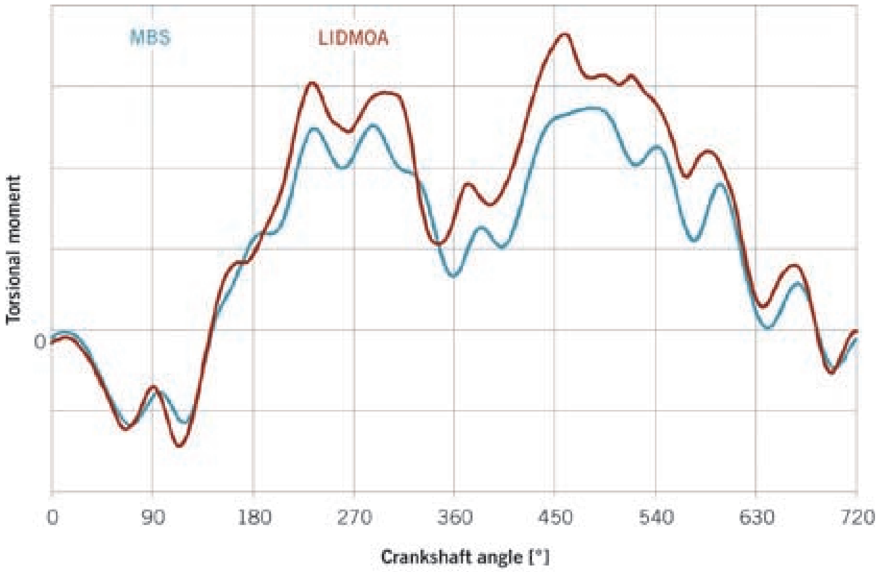

❸ Comparison between a method in frequency domain and MBS with flexible bodies in time domain

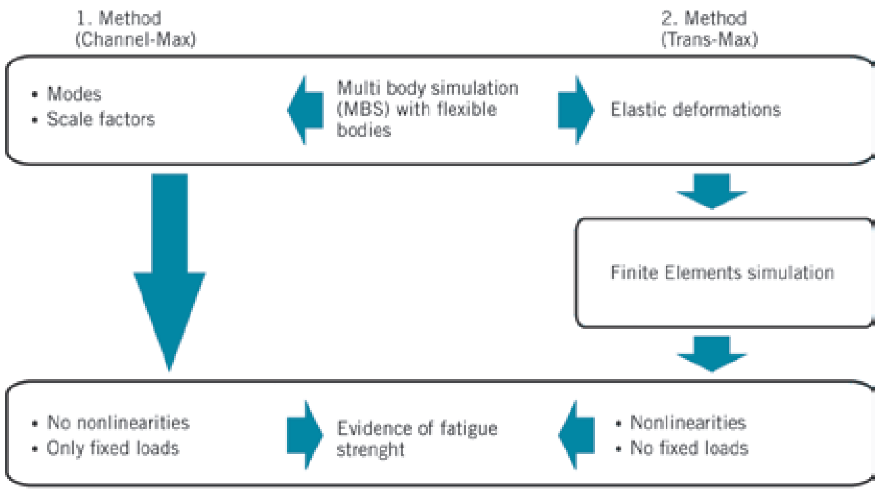

❹ Interdisciplinary procedure starting from a multi body simulation with flexible bodies to a fatigue assessment

These then serve as the boundary conditions for a finite element simulation, as for the fatigue strength assessment of a component subject to loading that changes position or direction and/or non-linear effects, FE stress data must be available at all times (Trans-Max method). The disadvantage of this method is that the stresses are simplified quasi-statically and a further, more complex step is required. Moreover, owing to the large number of load steps, the volume of data to be processed can be very large under certain circumstances. The advantage of this method, however, is that after calculation of the FEM for any number of areas of the component, FE submodel calculations and subsequent evaluation can be carried out with a much greater degree of detail.

RESULTS

A comparison of the two mentioned methods shows results which correlate well [2]. As the elastic deformation in the MBS is determined from the linear superposition of the modes calculated in the reduction, the ability to take non-linear effects into account with the second method has no impact. A more detailed submodel calculation and subsequent evaluation can be used for this purpose. This is necessary for a more precise examination of points subjected to maximum

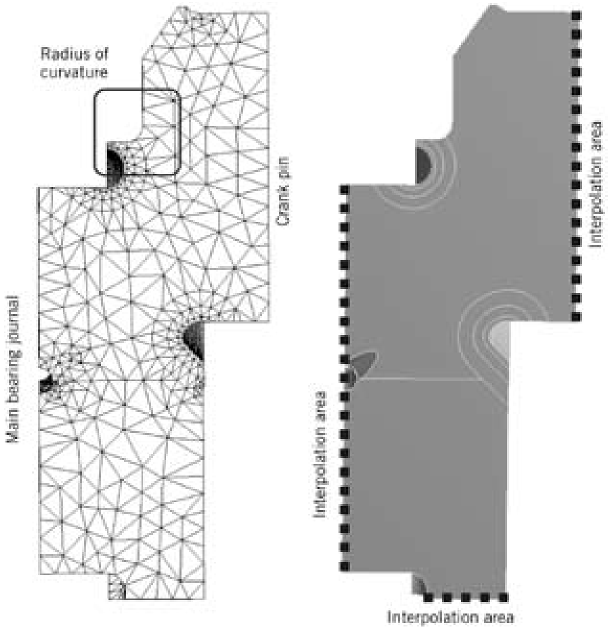

❺ Cross section of crankshaft web with main bearing journal and crank pin: meshing of fillets (fine sub model) (left); interpolation area of elastic deformation from global overall model to fine sub model (dotted line) (right)

local stresses (e.g. fillets or oil drillings). Owing to its finer mesh possibilities in the submodel calculations and the resulting greater conclusiveness of all results, use of the second method is particularly favoured in the design process for the crankshaft of modern large-bore diesel engines.

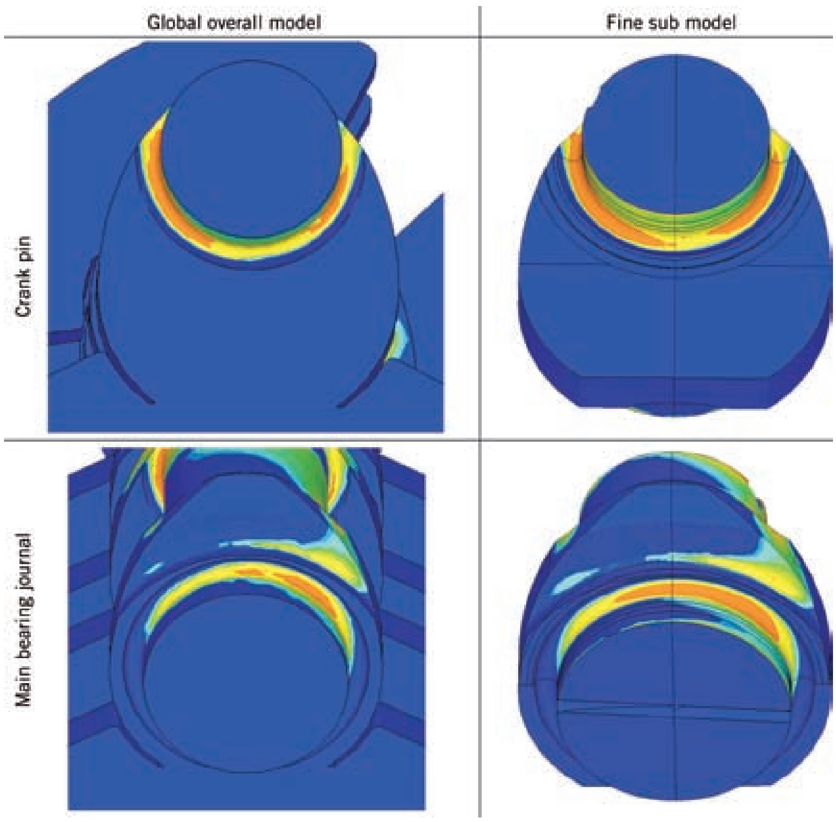

❻ Comparison of fillet fatigue results of global overall and fine sub model at the area of main bearing journal and crank pin, respectively

STRENGTH ASSESSMENT WITH SUBMODELS

The overall model used up until now represents primarily the global dynamics of the system. However, if from a strength perspective it is necessary to determine the local mechanical stresses in greater detail, more geometrically exact submodels of the fillets and oil drillings of the crank pin are required. Therefore the 2nd method Trans-Max is generally used for both. The fillets are subjected to multiaxial stresses due to both torsional and bending loads. The strength assessment is carried out numerically by means of Femfat software. The oil drilling, on the other hand, involves a nearly single-axial stress state. In addition to the known Femfat evaluation, an analytical strength assessment is also possible, e.g. based on the FKM-guideline [7].

FILLETS – MULTI-AXIAL STRESS STATE

The fillets are meshed in the area of the radii according to the CIMAC guidelines of the ship classification societies [8], ❺ (left). At the interface (interpolation area), the elastic deformations are exported from the global overall model to the fine submodel for each load step. As displacements for each load step of the submodel computation, these elastic deformations are then taken into account as boundary conditions, ⑤ (right).

Comparison of the fatigue strength results of the fine submodel with the global overall model provides a very good correlation between the two evaluations, ❻. In the submodel, the safety factors against fatigue fracture are slightly lower than those of the overall model. In the crank pin, there is a good correlation between the respective stress distributions. The distribution and positioning of the highest mechanical stress among the main bearing journal fillets are nearly identical. In this example the influence of mesh quality on calculated mechanical stresses is relatively low. Because this is not assured generally at different crank-

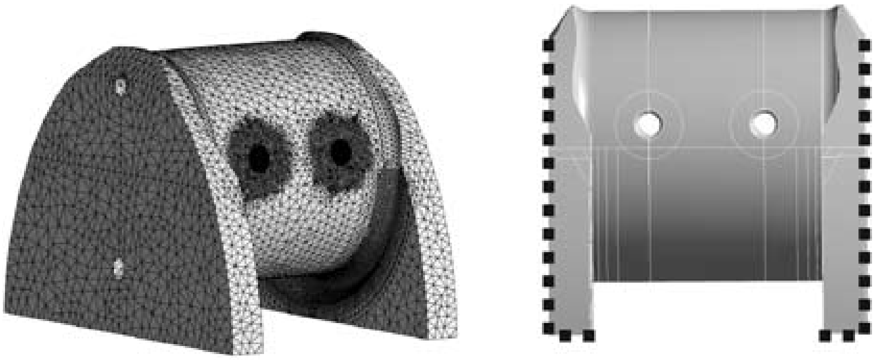

❼ Sub model oil drilling mesh arrangement (left); interpolation area of elastic deformation at fine sub model (dotted line) (right)

shaft geometries (e.g. due to different stiffness behaviour) the application of submodel technique is recommended.

OIL DRILLING – NEARLY SINGLE-AXIAL STRESS STATE

The outlet areas of the oil drillings in the crank pin are very finely meshed. In a process similar to the one described above, the deformations for each load step are exported at the marked interface, ❼. The forces of the crank drive are applied as a boundary condition in the submodel. In order to prevent any influence on the area around the oil drilling, interior nodes are applied at 2/3 of the crank pin diameter. In addition, the rotational speed ω is taken into account.

In comparing the results of the fatigue strength analysis, basic agreement between the overall model (left) and the submodel (right) is once again apparent, ❽. At the top of the image there is an area of low load (blue area), which transitions into higher loads (gradient from green to yellow). In the lower area of the image, the torsional band with higher loading in the crank pin is clearly evident in both models. For reasons of efficiency, the oil drillings cannot be taken into account in the overall model. High stress gradients are likely in this area, which would occur as a result of a local deviation of the safety factors between an overall and a fine mesh. Consequently a higher degree of detail in the mesh arrangement is necessary for fatigue strength assessment at the oil drillings. According to this, the 2nd method with the fine submodel is used.

The area of the oil drillings is subject to a nearly single-axial, tangential load. ❾ clearly shows the distribution of the safety factors in detail, whereby the lowest factor occurs in the right oil drilling.

For this point, the system gives the scalar comparative stress curve calculated by the Femfat software and the tangential stresses according to the FEM over one working cycle, ❿. In the Femfat graph below both the amplitude and the shape of the curve match very well with the tangential stresses in the y-direction from the FEM. For the nearly single-axial stress state, both the static and the dynamic strength assessment are carried out according to the FKM guideline. The dynamic safety factor is equivalent to the results of the lowest safety factor from the Femfat software [2].

CONCLUSION

In addition to the analytical methods used up to now, the design process of a modern large-bore diesel engine crankshaft requires a numerical fatigue strength assessment that determines the time-dependent distribution of mechanical stresses. This ensures that the demand for higher material load-

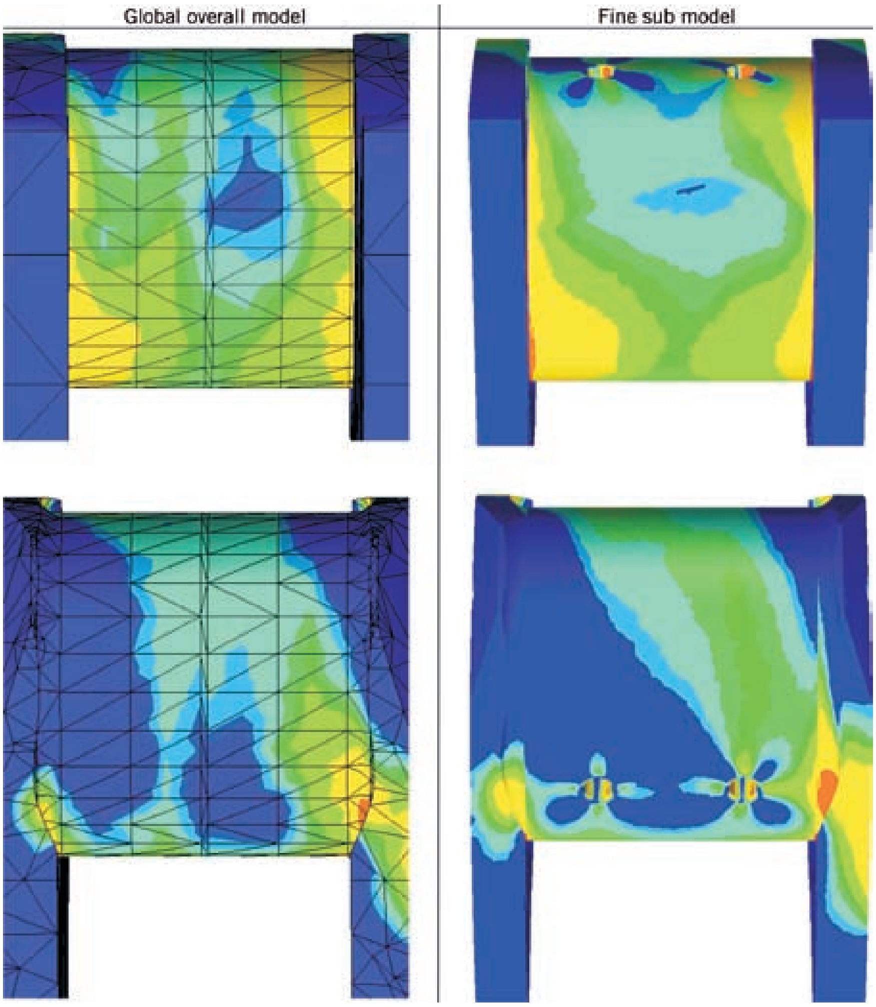

❽ Comparison of fatigue strength assessment of global overall model with sub model at crank pin

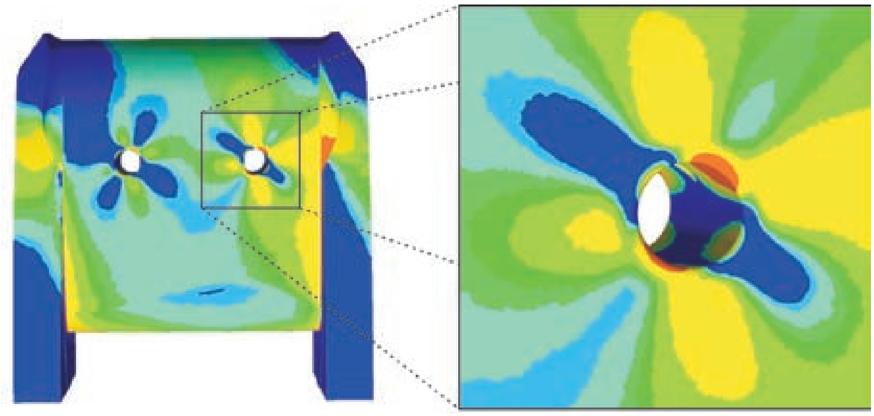

❾ Loading in area of oil drilling. In this image the highest loading is at the oil drilling on the right

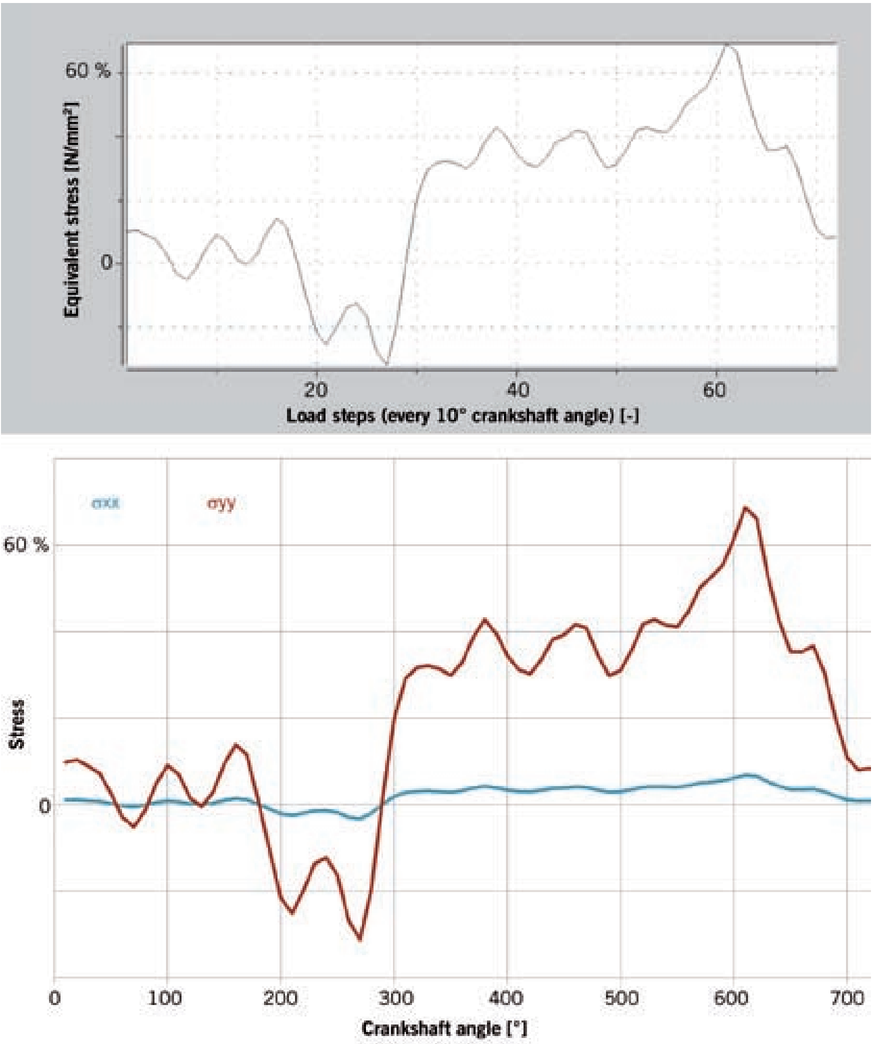

❿ Comparison between distribution of equivalent stress calculated by FEMFAT (top) and stresses in a local coordinate system at oil drilling of FE-simulation (bottom)

ing through lightweight design and higher performance does not compromise operational reliability. For this reason, MAN Diesel & Turbo SE is using the interdisciplinary approach presented here. This makes it possible to efficiently determine the maximum of loading in a component and to realise its improvement potential. It has been shown that a comparison between the two methods, Channel-Max and Trans-Max, referring to fatigue strength assessment delivers comparable results. The Channel-Max method is based on a global FE mesh and a structural dynamics simulation with the MBS. Therefore it offers an overall optimisation. A detailed optimisation with evaluation of local mechanical stresses requires the Trans-Max method. In this case, an additional FE simulation is necessary. For fillets and oil drillings, which are particularly relevant to fatigue, submodels are generally used. The distribution of the safety factors determined numerically corresponds well here to the overall model. Due to the local stress gradients, however, the fatigue strength of the oil drillings can only be assessed by means of a submodel technique. An analytical assessment according to the widely used FKM-guideline also shows very good agreement for this uni-axially stressed area.

REFERENCES

[1] International Association of Classification Societies: Requirements concerning Machinery Installations: UR M 53 – Calculation of Crankshafts for I.C. Engines, 2004
[2] Krivachy, R. et al.: Durability calculation of crankshafts in large-bore diesel engines, Femfat-User-Meeting 2009
[3] N.N.: Abaqus/Standard, Version 6.5, Abaqus, Inc., 2004
[4] N.N.: First/Tower, Version 6.2, ist GmbH, 2003
[5] N.N.: Ansys, Version 11, Ansys, Inc., 2007
[6] N.N.: Femfat, Version 4.7b, ECS GmbH & Co KG, 2008
[7] Hänel, B. et al.: Rechnerischer Festigkeitsnachweis für Maschinenbauteile (Analytical strength assessment of components in mechanical engineering) 4th edition; Frankfurt: VDMA, 2002
[8] International Association of Classification Societies: Requirements concerning Machinery Installations: UR M 53 – Calculation of Crankshafts for I.C. Engines, Proposal for Appendix III, 2009

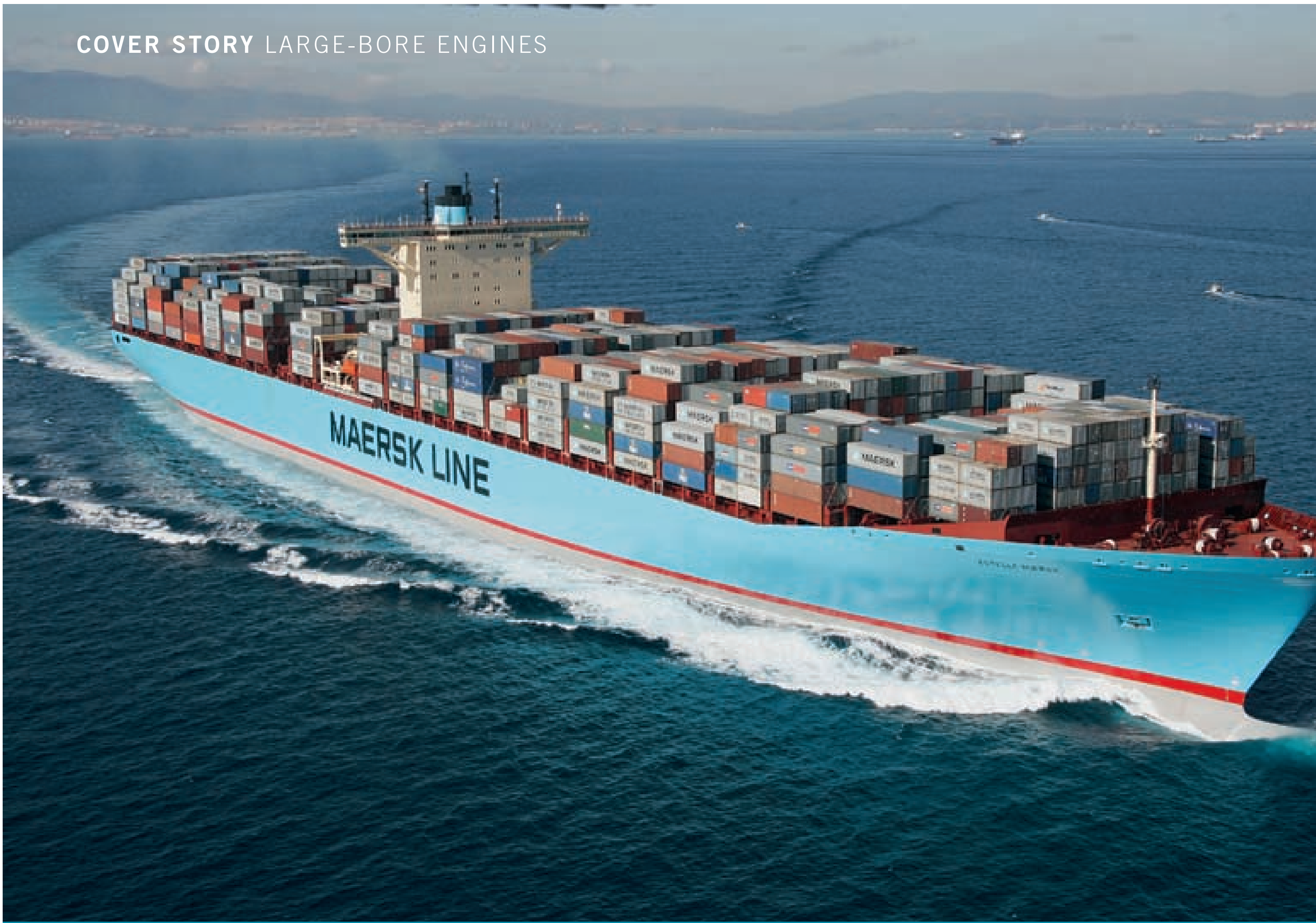

TIER III EMISSION ROADMAP FOR MARINE ENGINE APPLICATION

The Upcoming IMO Tier III emission legislation in 2016 is at the moment the strongest driver for the marine engine applications development. NO_x (Nitrogen Oxide) reduction in the range of 80 % compared to the present level clearly implies the need for a technology leap in the products. Furthermore the future coexistence of IMO Tier II and IMO Tier III emission areas will boost the demand for engine operation flexibility. Wärtsilä gives an insight into the most promising emission reduction technologies tested and developed by showing the potential in terms of NO_x reduction.

AUTHORS

MIKAEL TROBERG
is Director Testing & Performance,
Global R&D at Wärtsilä
in Trieste (Italy).

DIEGO DELNERI
is Manager Product Performance,
Global R&D at Wärtsilä
in Vaasa (Finland).

INITIAL SITUATION

Shipping is the most cost effective way of goods' transportation. Lifetime and overhaul intervals are important for optimizing lifecycle costs. Some ship installations operate above 7 000 hours per year and make a dry dock every third year. Ideally for a ship owner the engines would have maintenance only during ship dry docking which would result in up to 22.000 running hours between overhaul. Comparing this to the automotive industry the target can be considered extremely challenging. The ship owners are becoming more global by the day and they are expecting to operate their ships without limitations due to local emission restrictions or fuel availability. The trend of measuring the carbon emission on consumer products will result in a further focus on CO_2 emissions from shipping.

Conventional technologies for emissions reduction used in other industries such as Exhaust Gas Recirculation (EGR) and catalysers are creating challenges due to the vast variety of fuels in the shipping industry. Liquid fuels starting from automotive fuels up to fuels with sulphur content of 3,5 % and viscosity's to 800 cSt (centiStroke) creates challenges in terms of material choices and design solutions. In normal operating conditions the exhaust gas temperatures after turbo chargers are around 340 °C which is on the lower limit for a functional SCR catalyst.

The high content of sulphur in fuel in combination with ash and vanadium content creates fouling and wear of engine components which in combination with high exhaust gas temperatures (before turbo charger) > 550 °C results in reduced component lifetime and deterioration of engine performance. Already a 1 % loss in engine efficiency has an impact as a ships fuel cost is calculated in millions of Euros.

The future legislation will promote higher grade fuels which opens the possibility to utilize technologies like EGR on medium and slow speed engines.

Since emissions requirements are becoming more stringent, gas (methane) as energy source for shipping has become an alternative. Gas is a clean fuel with low emissions. Gas engines with a unit output up to 17.1 MW (18V50DF) are available, ❶, as usually smaller (12V50DF/6L50DF) units for redundancy is preferred. The first installations with large gas engines came quite naturally through gas carriers as the trend is now moving towards more traditional ships like ferries. The DF (dual fuel) technology is based on having a liquid fuel (heavy or marine diesel oil) as backup fuel which might be needed if there is an interruption in gas availability. In locations where the gas availability is secured the SG (spark ignited gas engine) is considered an option.

This paper provides an overview of the emission reduction technologies developed by Wärtsilä and highlights the potential in terms of NO_x reduction. Candidate IMO Tier III solutions for four-stroke medium speed engine application are as well presented and assessed according to their impact on the product lifecycle cost.

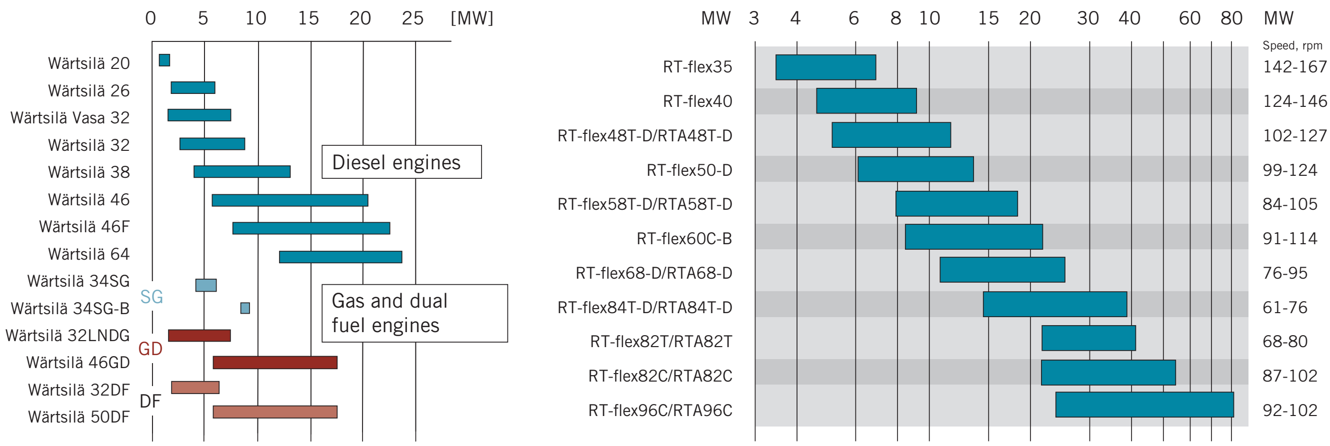

❶ Wärtsilä engine portfolio (left: four-stroke, right: two-stroke)

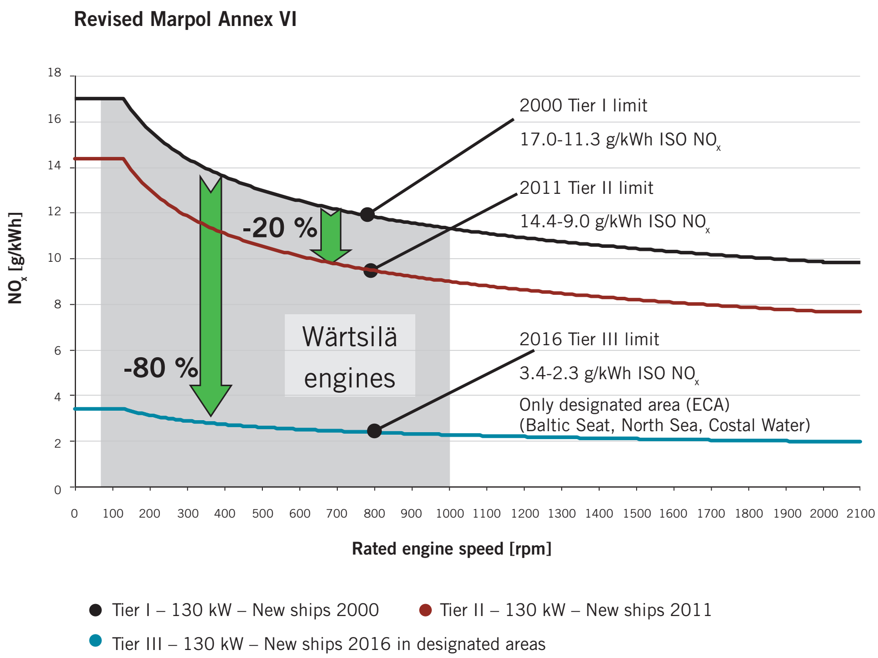

❷ Upcoming NO_x emission limitation

UPCOMING EMISSION LEGISLATION

The IMO Tier II (Marpol Annex VI) standard for marine engine application will come into force in January 2011, ❷. The NO_x limit reduction from the present IMO Tier I level is in the range of 15 % for the low speed engine (two-stroke application) up to 20 % for the medium speed engine (four-stroke application).

IMO Tier III standard will come into force in 2016, and will be applied only in designated emission control areas (ECA). Expected areas where IMO Tier III will be applied are for instance the Baltic Sea, the North Sea as well as the US and Canada costal water. IMO Tier III standard will introduce a drastic reduction on the cycle average NO_x emission limit equal to 80 % of the current standard. Furthermore the new standard will require that the measured emission level in each point of the emission cycle must not exceed 1.5 times the cycle average limit, with the exception of the 10 % load point. This new limitation is very challenging for the low load optimization, where normally higher NO_x emissions are accepted in order to reduce the particulate and smoke formation. IMO Tier III and IMO Tier II will be coexisting standards from 2016 onwards, and most of the ships will move frequently from a Tier II to a Tier III area. This implies that engine must be flexible in handling different emission limits with the best possible operating efficiency.

Coexistence of IMO Tier II and IMO Tier III areas after 2016 will additionally demand more flexibility in the engine tuning; customized solutions might be thus needed according to the specific application and customer needs in order to achieve the best possible operating cost and keep the market competiveness.

The fuel sulphur content limit, ❸, in the Sulphur Emission Control Area (SECA) was 1.5 % and has been reduced to 1.0 % from 1 January 2010. Controlling the fuel quality is a way to reduce not only the SO_x (Sulphur Oxide) but also the particulate emission, strongly linked to the fuel sulphur content. In the SECA area the "High Sulphur" operation will be allowed if an exhaust scrubber is used.

Fuel quality requirement has as a clear impact on the ship operating costs since the Low Sulphur Fuel (LSF) price can be twice that of current residual fuels (HFO).

In 2015 the fuel sulphur cup in the ECA will be reduced to 0.1 % implying that IMO Tier III will be operated either with LSF or alternatively with exhaust scrubber.

NO_x REDUCTION TECHNOLOGIES

In order to reduce the emissions at the exhaust stack it is possible to work on the following options:
: engine technology
: after treatment technology
: fuel type and quality.

In developing the new concepts to meet the IMO Tier III emission level Wärtsilä is focusing on all the above mentioned aspects. Different technologies for NO_x reduction have been explored, and some of them are already implemented on Wärtsilä engines. A brief overview of the available technologies is presented below.

HIGH PRESSURE CHARGE AIR SYSTEM

This technology is based on the effect of the Miller Cycle (early inlet valve closure,

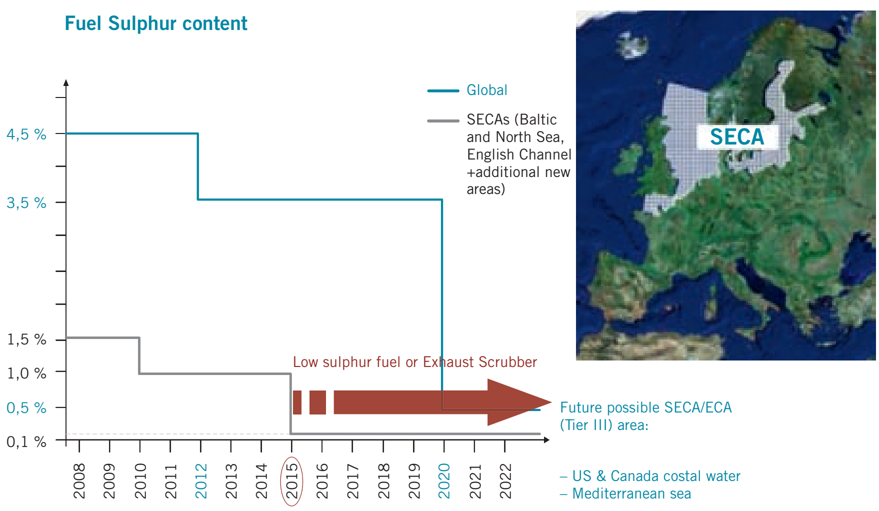

❸ IMO fuel sulphur cap

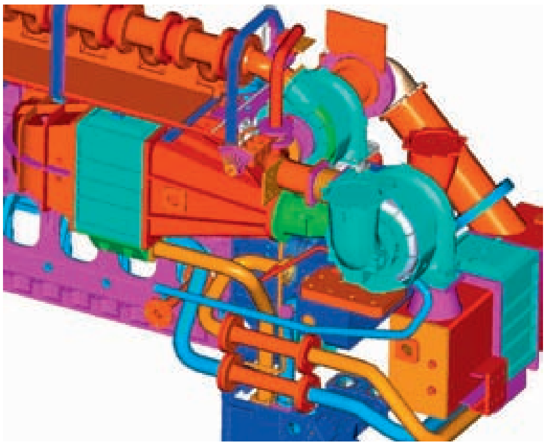

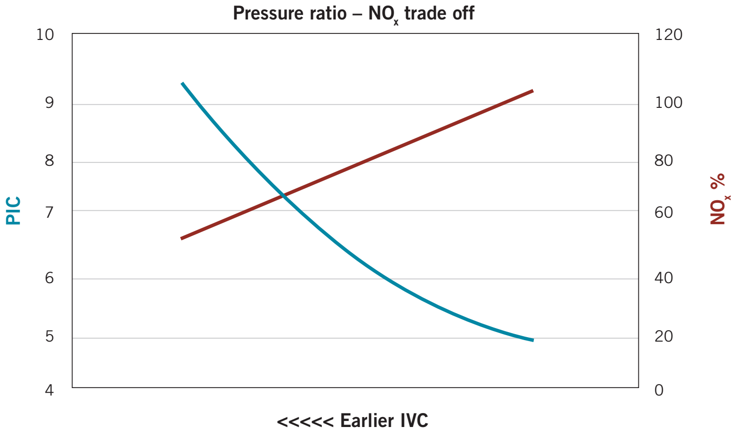

❹ Wärtsilä 20 prototype two-stage system

IVC, before bottom dead centre) on the combustion temperature. By anticipating the inlet valve closure the effective compression ratio is reduced leading to a lower temperature in the compression and expansion phase. Since NO_x formation is thermally activated, the Miller cycle has a remarkable potential in terms of NO_x reduction. To keep the same air-to-fuel ratio (thermal load), higher boost level is needed to compensate the reduction of the effective displacement during the intake stroke.

Consequently the biggest limiting factor in applying the Miller Cycle is the pressure ratio demand from the turbo charger (TC). Based on the test results, the boost pressure needed to maximize the gain in terms of NO_x reduction is clearly beyond the single stage turbo charging system potential, as a consequence the two-stage TC system is the preferred solution for such technology.

The two-stage TC system has been tested on a Wärtsilä 20 medium speed engine, ❹, where a NO_x reduction of 40 % was achieved with overall compressor pressure ratio of 9 [1].

Other benefits of the two-stage system are the superior TC efficiency (about 10 % higher than the single stage) resulting in improved engine fuel consumption and the possibility to increase the engine output (brake mean effective pressure) thanks to the boost pressure availability.

The main drawback of the two-stage system is the part load behaviour where the combination of the TC system characteristic (sharp drop in boost at low engine load) and the Miller timing leads to generally poor performance (steady state and transient). To cope with this problem Wärtsilä has developed the VIC system (Variable Inlet valve Closure) that enables the Miller timing tuning at different loads. This system is already in production on the Wärtsilä 32 D in combination with a high pressure single stage charger and Miller timing.

Similar effect of the four-stroke Miller cycle is obtainable on Wärtsilä two-stroke engines by closing the exhaust valve later and compensating again for the lower effective compression ratio by increasing the scavenging pressure. Such tuning gives similar benefit in terms of NO_x reduction as on the four-stroke engines.

LOW NO_x COMBUSTION TUNING

The Low NO_x combustion tuning, ❺, is achieved by increasing the compression ratio as close as possible to maximum firing pressure and, at the same time, by slowing the injection rate in order to minimize the pressure increase rate in the combustion chamber. The target is to get close to the constant pressure combustion (theoretical Diesel Cycle) resulting in a lower combustion peak temperature and consequently lower NO_x emissions. Piston top design and injector lay-out are optimized accordingly. The emission reduction potential is the range of 10 to 15 % with limited fuel consumption penalty.The penalty in fuel efficiency has been minimized by increasing in-cylinder pressures up to 230 bar.

By utilizing the flexibility of the electronic fuel injection equipment it is possible to tune the combustion for low NO_x emission along the whole engine operative field. For this reason, common rail technology is part of the concept as well.

EXHAUST GAS RECIRCULATION SYSTEM

Exhaust Gas Recirculation (EGR) is a technology largely applied in the automotive industry. By recirculating cooled exhaust gases in the combustion chamber the effective lambda (air-to-fuel ratio) is reduced without impacting the engine thermal load. As a result of the lower air to fuel ratio and consequently of the lower oxygen concentration, a remarkable reduction on NO_x emission can be achieved (-60 %). Main drawback of this technology for the marine application is the incompatibility with High Sulphur Fuel (HSF).

Use of EGR requires further development of the fuel injection equipment in order to cope with the particulate emissions and soot. Injection pressures need to be further increased from today's 1800 bar and post injection will become a standard.

WETPAC TECHNOLOGY

Water can be used as a mean to reduce the NO_x emission. Water vapour acts as a temperature damper and dilutes the oxygen concentration in the combustion air, reducing the NO_x formation rate. If water is directly injected in the combustion chamber it has the additional affect of cooling the combustion process directly (energy is required for heating up and evaporating).

Different Wetpac technologies have been developed by Wärtsilä to control the

NO_x emission: Wetpac H, Wetpac E, Wetpac DWI.

In the Wetpac H (Humidification) concept the combustion air is saturated with water immediately after the compressor. By increasing the air temperature after the compressor cooler it is possible to reach Water to Fuel (W/F) ratio up to 1.3, resulting in NO_x reduction of 40 % [2].

In the Wetpac E (Emulsion) concept fuel is mixed with water before injection. Achievable water fuel ratio is related to the injection system capacity, and normally it is possible up to 0.3 with a resulting NO_x reduction of 20 % [2].

In the Wetpac DWI (Direct Water Injection) water is directly injected in the combustion chamber. 50 % NO_x reduction is achievable with a W/F ratio of 0.6 [2].

Main concerns in using wet technologies are linked to high water consumption, its availability on board and the cost to treat it.

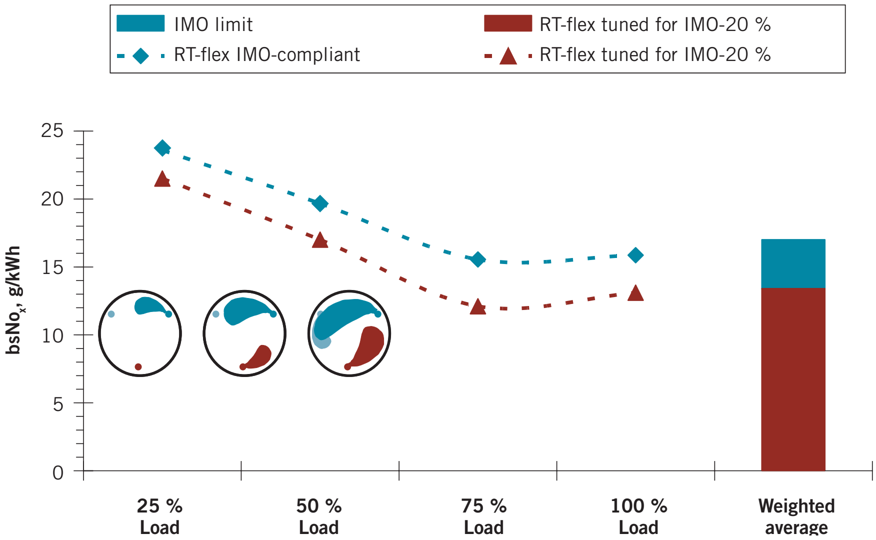

❺ RT-flex58T-B sequential injection for low NO_x tuning

NITROGEN OXIDE REDUCER

Selective catalytic reduction is one of the most effective ways of reducing NO_x emissions. Urea injected in the exhaust pipe evaporate to form ammonia (NH_3) that reacts on the catalytic substrate, reducing NO_x to N_2 (Molecular Azoth).

Test results on the Wärtsilä Nitrogen Oxide Reducers (NOR) prototype installed on the Wärtsilä 26 laboratory engine, ❻, have shown NO_x reduction rates up to 90 %. Total hydrocarbon (THC) and particulate emissions are also positively affected. Since the NOR technology allows to meet the IMO Tier III level, Wärtsilä has started the design and the production of a modular NOR family to cover the engine portfolio.

Biggest challenge for the application of NOR is the engine integration. NOR requires a specific operating temperature range as a function of the fuel quality (sulphur content) and this has to be matched with the overall engine performance (exhaust gas temperature). The integration is more challenging on two-stroke engines where NOR has to be installed before the turbocharger for temperature reasons.

DUAL FUEL AND GAS TECHNOLOGY

Wärtsilä offers different gas engine technologies in its portfolio: SG (Spark ignited gas), DF (Dual Fuel), GD (Gas Diesel). Differently from the GD concept where the gas is directly injected in the combustion chamber, the gas is injected at low pressure into the intake port in the DF and SG engines. The combustion mode is homogenously premixed and lean (air-to-fuel ratio close to two) resulting in a lower and even combustion temperature, leading to very low NO_x emission levels (more than 85 % reduction versus IMO Tier I).

❻ Wärtsilä NOR system overview

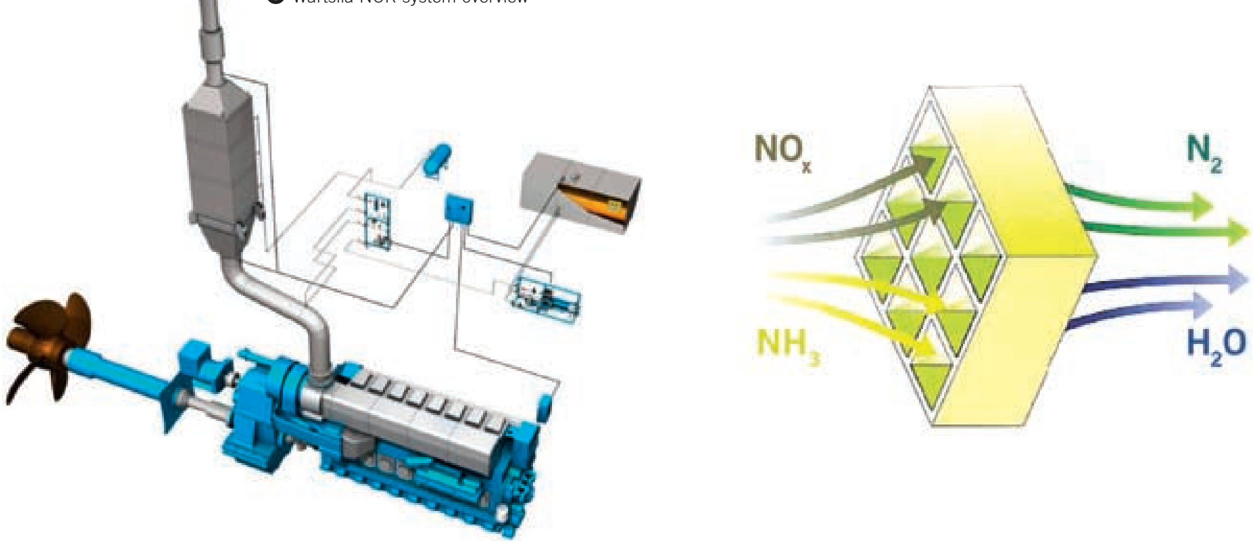

In particular the DF engine is currently very attractive for some specific Marine market segments (e. g. LNG carrier) because of the possibility of running on different fuel (LFO, HFO, “low pressure” GAS). In future this concept will be even more interesting since it has the potential to be IMO Tier III compliant in gas mode (ECA area) and IMO Tier II compliant in liquid fuel mode (non ECA area).

EVALUATION OF CANDIDATE TECHNICAL SOLUTIONS

Most of the technologies for NO_x reduction are not sufficient to achieve the IMO Tier III emission level. Only with the Nitrogen Oxide Reducer and Gas engine technology, it is possible to hit the future Tier III emission target, ❼.

Potential combinations of different technologies can be used to reach the limit. At this point in time it is crucial to test the compatibility of the different technologies, to evaluate the technical risks and to understand the implications on the total cost of ownership. For this purpose, various candidate Tier III solutions, which were derived from combinations of compatible individual technologies, have been analyzed from a lifecycle cost point of view, thereby considering specific engines from the Wärtsilä portfolio. In this context, various typical scenarios regarding operational characteristics and fuel quality requirements have been taken into consideration. In the determination of first and operating cost effects, current market data have been used, supplemented by estimates on the basis of prototype installations as necessary.

For the four-stroke engines, we can conclude that there are various options which are largely similar in terms of their lifecycle cost effect. However, the combination of two-stage turbo charging technology and SCR seems to be particularly interesting. The analysis also clearly indicates that the cost increase related to the use of Low-Sulphur Fuel in ECA Area represents the dominant factor of the cost calculation. This study hence suggests that the exhaust scrubber technology, enabling the operation with residual fuel also in the ECA area, would have a relevant impact on the ship operating cost.

Anyhow, due to the uncertainties on the future fuels and urea market prices, it is difficult at this stage to take a final decision on the best Tier III technology and other promising combinations such as the Wetpac and EGR plus two-stage TC system deserve further evaluation.

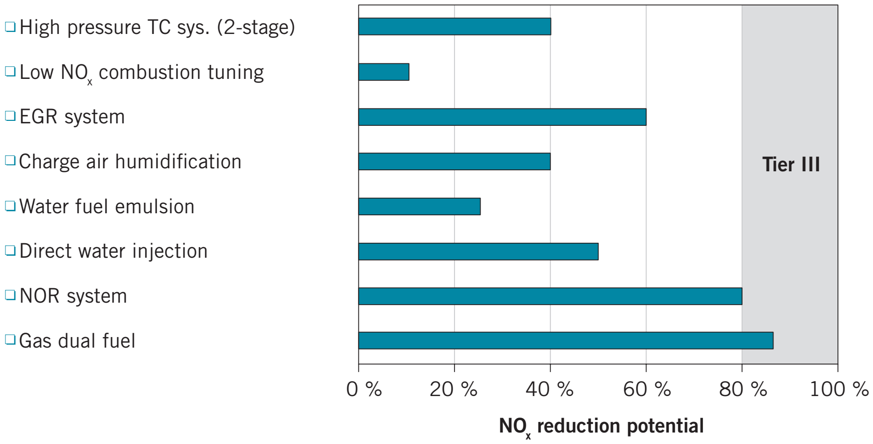

❼ NO_x reduction technology potential

IMO TIER II AND TIER III EMISSION ROADMAP

Within 2009 the Wärtsilä product portfolio will be IMO Tier II compliant with limited penalty in terms of efficiency and/or output compared to the Tier I concepts. At the same time, improved Tier II solutions mainly utilizing the new turbo charger generation, flexible valve timing, and updated engine design for higher firing pressure are under development.

The development of Tier III concepts with after treatment is currently ongoing. Engines will be tuned for low specific fuel consumption and high exhaust gas temperature (340 to 360 °C) to enable SCR operation with high sulphur residual fuel. This concept will be optimized for waste heat recovery as well.

Tier III concept based on internal engine methods will be by far the strongest focus in next four years. In this timeframe the most promising technical solutions will be tested and developed into a product. High pressure turbocharging combined with Miller Cycle and increased valve timing flexibility will be the base for the concept development.

Gas engine Tier III concept development will be run in parallel. Main focus will be on Dual Fuel engine and in particular on liquid fuel mode performance. Efficient HFO operation is needed in order to improve the operating cost in the non ECA area where the engine could run on liquid fuel according the IMO Tier II emission limit. At the same time Tier III multiple engine solutions (pure gas for ECA area and Tier II Diesel for non ECA) will be investigated. Final goal for Wärtsilä is to be prepared for the 2016+ market with competitive technical solutions fulfilling at best the need coming from different customers.

CONCLUSIONS

The upcoming IMO Tier III emission limit is very challenging. Based on current knowledge, high pressure turbocharging, multi fuels operation and after treatment (NOR) seem to be the key technologies for the future.

Operating flexibility between different emission areas will be a key success factor for the future engine concepts. Required fuel quality (LSF) in the ECA areas might affect significantly the lifecycle cost for the ship operators. Scrubber technology could be a key factor to tackle this challenge.

In the coming years Wärtsilä will continue exploring and testing different technology combinations for NO_x emission reduction aiming to develop the best possible Tier III solutions based on engine internal methods, after treatment and gas technology.

REFERENCES

[1] C. Wik, B. Hallbäck: Utilization of two-stage turbo charging as an emission reduction means on a Wärtsilä four-stroke medium-speed diesel engine. Paper no. 101, 25th CIMAC Congress, Vienna 2007

[2] J. Hupli, D. Paro: Humidification methods for reduction of NO_x emissions. Paper no. 112, 24th CIMAC Congress, Kyoto 2004

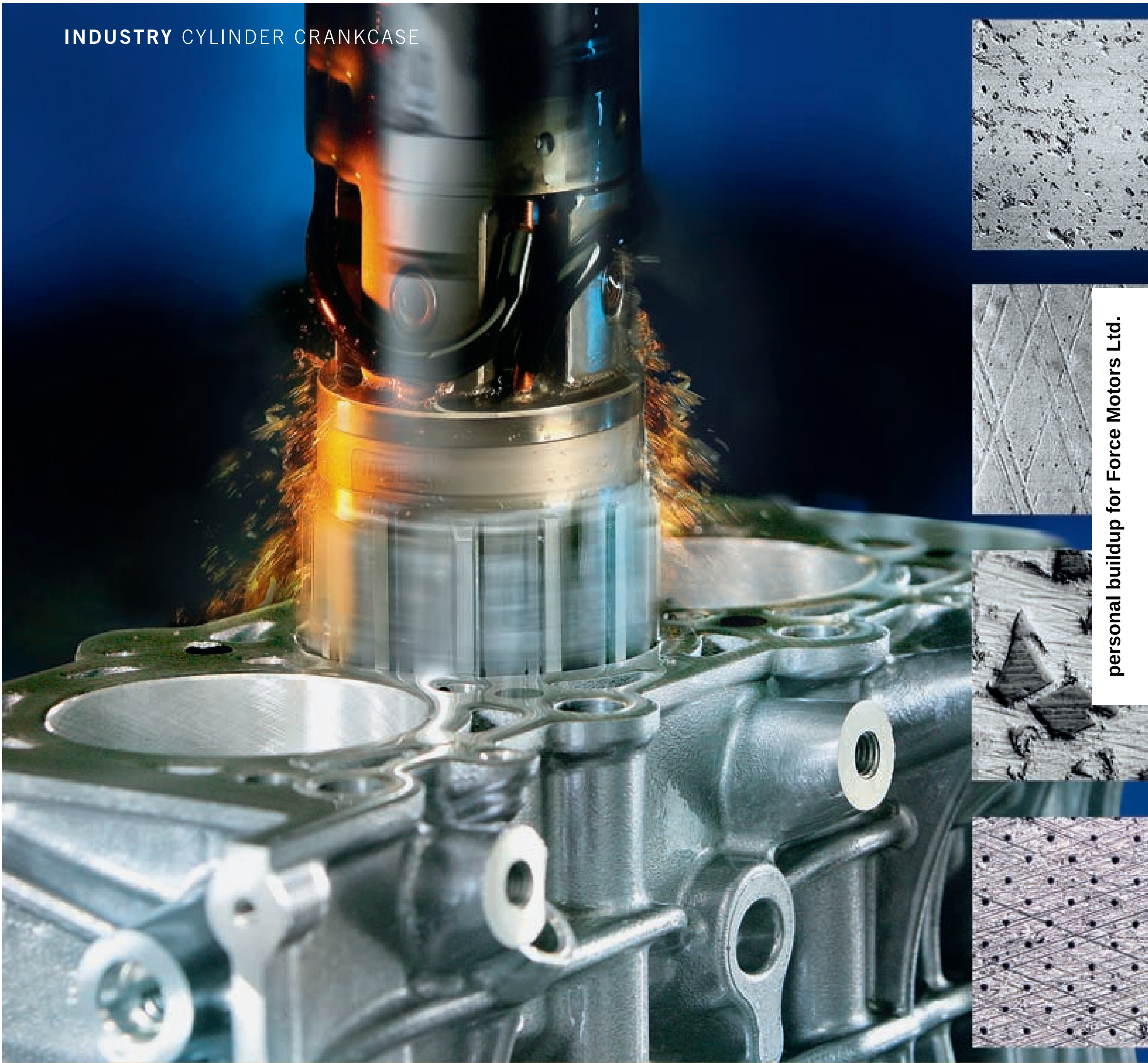

FRICTION OPTIMIZATION OF CYLINDER SURFACES FROM THE PERSPECTIVE OF PRODUCTION TECHNOLOGY

A study by the company Nagel shows the possibilities offered by fine finishing processes for the further reduction of friction and wear on cylinder running surfaces. Based on the current honing process, future developments are presented and their potentials are analysed.



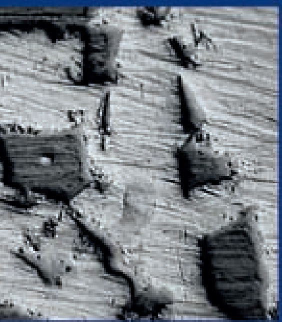
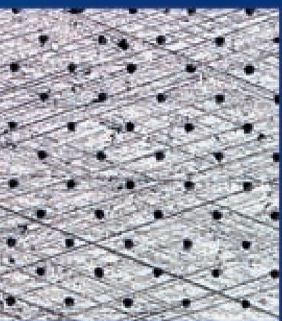

AUTHOR

JOSEF SCHMID
is Manager R&D Process and Abrasives Development at Nagel Maschinen- und Werkzeugfabrik GmbH in Nürtingen (Germany).

HONING SIGNIFICANTLY REDUCES FRICTION

In the past few decades, continuous improvement to the finishing process (honing) of engine cylinder bores has led to a considerable reduction in engine friction, wear, and oil consumption via modifications to the surface topology. Further process optimizations, such as helical slide honing, have been integrated into production through developments to the honing machine, hone tooling, and hone process. In addition to improving the surface structure, honing, as a quality-determining finishing process, could also contribute to a further reduction in frictional losses by compensating for bore distortions; e.g. torque plate honing (honing under tension to simulate cylinder head bolt-up distortion). In some cases, the material or surface optimization potential (in the case of great distortion) has only been recognized as a result of this.

HONING TECHNOLOGY DEVELOPMENT AS A SOURCE OF INNOVATION

Machinery suppliers alone cannot take all the credit for these advancements. Honing machine manufacturers, who are responsible for the finishing process, depend on the cooperation of engine development engineers and related component suppliers. In order to exploit even more potential, the development of honing technology must not be considered to be more than one single measure. Today, this is considered to be both a source of inspiration as well as a reactive measure to a complex interaction of many variable individual factors, ❶. Here, this finishing process has different requirements to meet, both from the development side, as well as from the production per-

❶ The honing process, taking the constraints of the engine into account

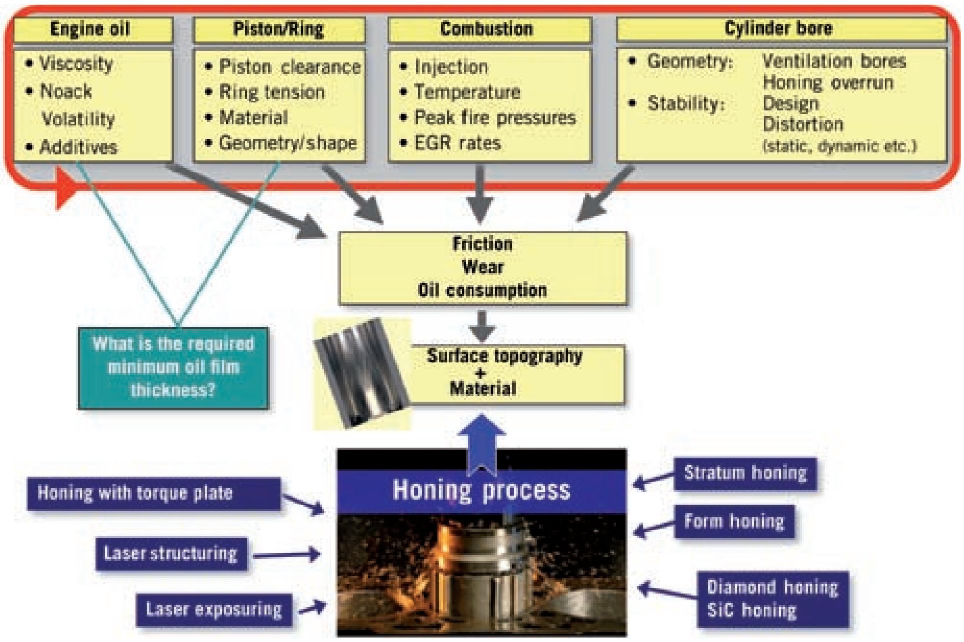

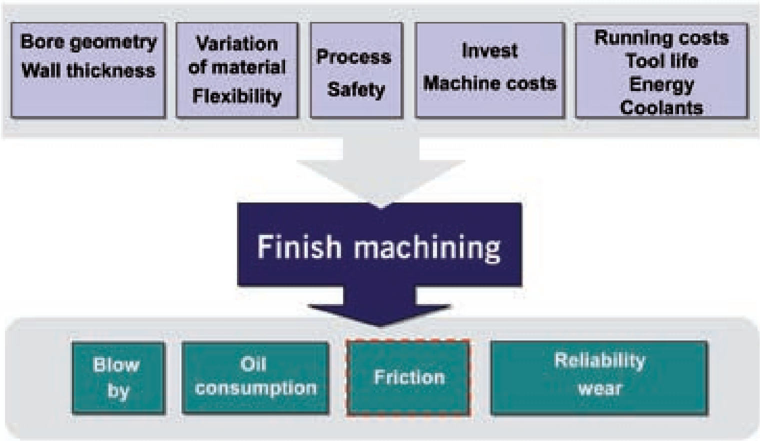

❷ The honing process, taking the production conditions into account

spective of the customer, ❷. The tribological process present in an operating combustion engine is very complex and to date, only some of these processes have been researched. A lack of knowledge has led to a wide variety of honing theories, and therefore to numerous honing variants employed throughout the industry.

UNECONOMICAL VARIETY OF PROCESSES

These many variations in the finishing process for the basic combustion engine employed by engine manufacturers are not desirable; for cost and quality reasons and for logistical reasons. In addition, further developments and/or release procedures are required for every combination of surface variant and corresponding piston ring. Therefore, the machinery supplier and engine manufacturer responsible for final the production process must critically scrutinize all "honing theories" to dispel prevalent misconceptions relating to the hone process.

STUDIES CONTRADICT THEORIES

For example showed an analysis of the long held theory "oil pumping", whereby engine oil can be pumped by the piston ring with every stroke through the numerous honing valleys in the combustion chamber and is supposedly the primary cause for oil consumption, that it cannot be true. If this were true, the oil consumption of "normally" honed engines would lie in the range of the fuel consumption [1]. It also can be shown that "isolated micro-pressure chambers" do not exist. As soon as a hydrodynamic lubricating film builds up, which is actually self-evident, this system is then a communicating system. The direct contribution of the graphite ("open graphite for self-lubrication") to the tribology of the combustion chamber surface is extremely questionable, since these are recessed after a short time due to cavitations, ❸. Further proof against this theory is the widespread use of diamond honing (which increases the imbrications in the graphite lamellas) has prevailed as the most common reliable and economic production process.

The assumption that a relatively rough honed surface is required for compensation of bore distortion in order to "seat" the piston ring to the cylinder wall is also incorrect. The correction potential of a rough honed surface is 1 to 2 µm, whereas the static distortion due to cylinder head mounting is in the range of 20 to 40 µm. Therefore, it makes more sense to hone to a finer surface finish, minimizing friction, than honing a rougher finish for the purpose of high run-in wear.

SLIDE HONING

One of the most important measures when developing a production process is analyzing the run-in surface of the finished cylinder. As a result, slide honing (i.e. the generation of a pseudo "run-in" surface topography via the honing process) has been developed and has been implemented in more than forty production applications worldwide in just a relatively short time span. Production implementation in a wide range, from compressor applications to passenger car engines and truck engines (gasoline and diesel) has been so quickly realized because the development of the abrasive was integrated with the hone process development at the machinery supplier. This allowed for quick, individual reaction to the respective component and material differences.

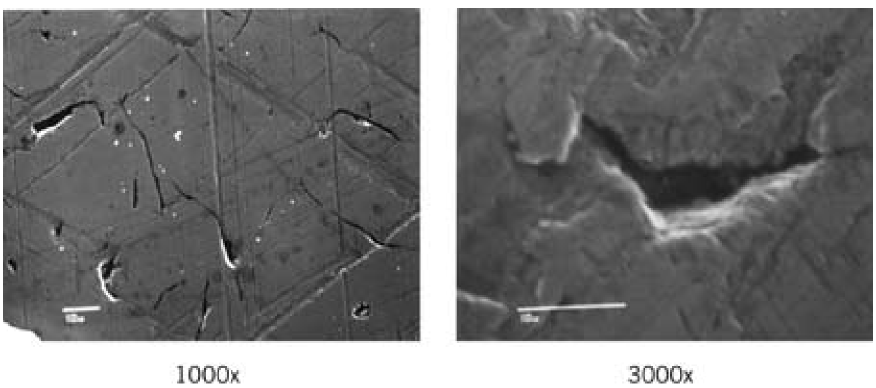

❸ Recessed graphite lamellas on a run cylinder surface

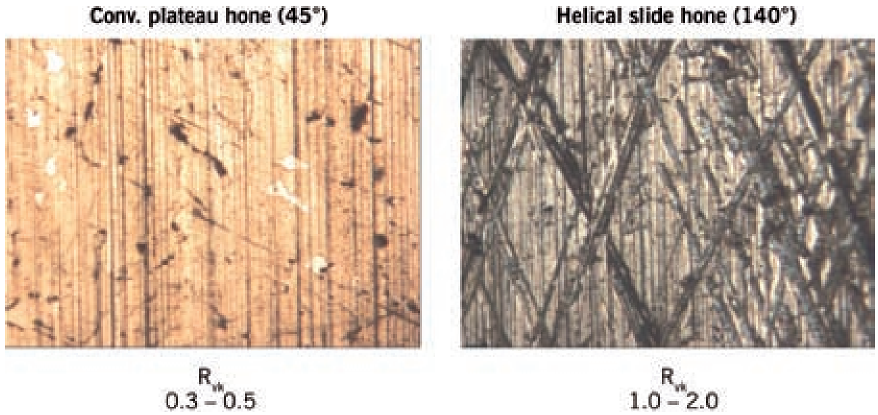

❹ Cylinder microscope image passenger car engine after 1200 h test run

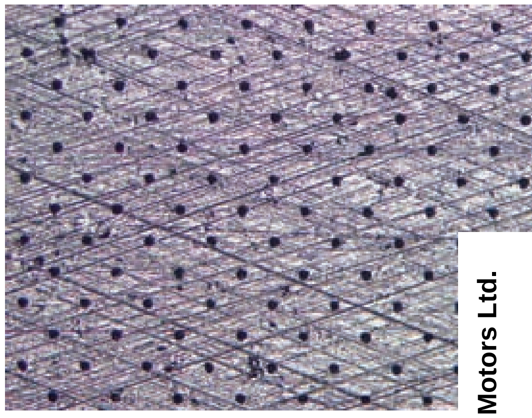

❺ Further developed, finer laser structure

HELICAL SLIDE HONING PROCESS

This experience in the non-automotive area (compressor applications) has led to re-evaluation of the honing angle and its function, especially in the reversal areas. For the O.D. honing of piston rods, the inclusion of axial honing valleys for reducing friction and wear has been prevalent. Due to their slow stroke speed, these do not run in the hydrodynamic range. These areas also exist for piston power machines at the reversal points and are subject to the highest wear. It was therefore logical to investigate whether this was transferable to the combustion engine. Here, it was shown that during the I.D. honing of cylinder bores, the optimum honing angle lies in the range of 140°, taking the production machinery as well as product functionality into account.

Together with a reduction in the honing valley width, a wear resistance, unreachable before, was achieved due to the topography produced by the helical slide honing process, while simultaneously reducing oil consumption in production engines [2]. For the same range of Rvk values, there is an improved surface stability as compared to a standard plateau honed surface. Increasing with run-time, there is lower wear and friction, ❹, especially in the reversal areas. The reduced friction values were confirmed within the scope of the EU project "Oil-free powertrain" on an unfired test bench [3]. An advantage of this honing method is its wide range of applications. Production applications reach from industrial engines to utility vehicles to gasoline passenger car engines. With material-related adaptations, helical slide honing is now also used in production applications of aluminium cylinder surfaces. Especially in the case of the aluminium application, the cooperation of all areas of expertise, from engine development, machine manufacturers and piston ring and material suppliers, has contributed to its success. The implementation of the helical slide hone process now allows the focus of alloy development to be directed towards strength rather than by silicon crystals determined tribological functionality. The latter is now determined by the honing.

ALTERNATIVES TO SURFACE STRUCTURING

Further development of the finished cylinder surface includes varying methods of "structuring" the bore surface. Sometimes referred to as „laser honing", structuring of the cylinder surface employing a laser has been in production since 2000. As opposed to the valleys of a helical slide honed surface, relatively wide structures from 50 to 80 µm are typical of the laser structured surface.

Another application of this laser technology in production is laser exposuring. As opposed to structuring, not only is the topography changed, but also the material properties in the area near the surface. Special cylinder bore pre-machining methods are employed in the production implementation of this process. Currently, finer laser structures (< 40 µm) are being investigated with regard to their production applicability, ❺.

Advances in machine technologies; control systems and tooling allow the generation of new surface structures, even with diamond honing, e.g. with different characteristics in the axial direction, ❻.

❻ Variable honing structures in the axial direction

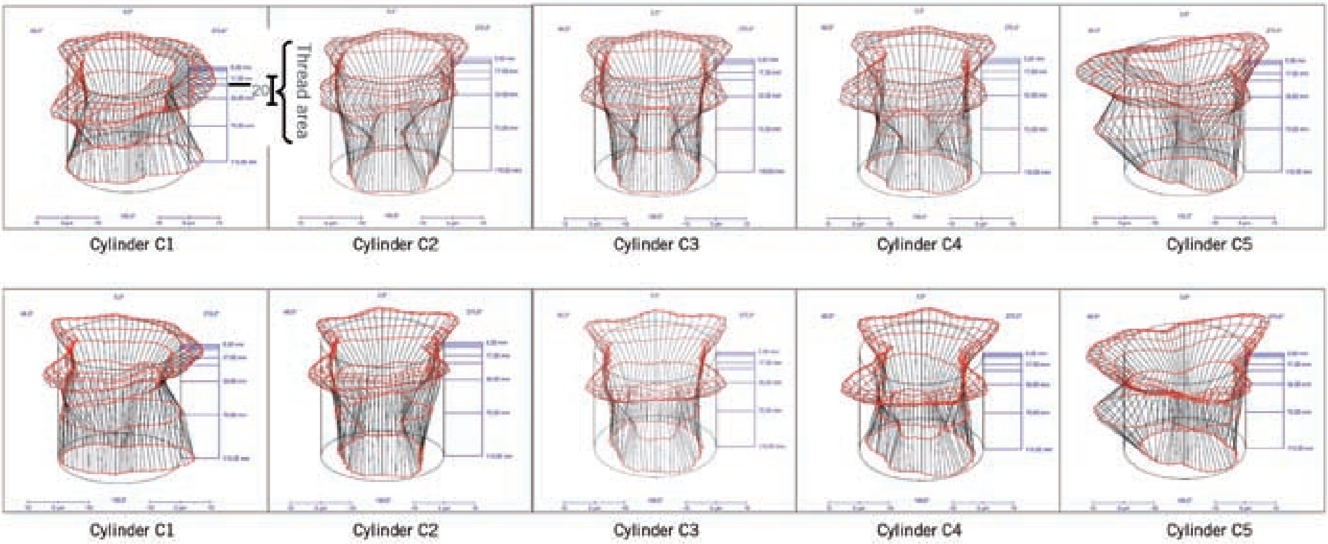

❼ Simulated deformation of piston bores by the assembly of a cylinder dummy head

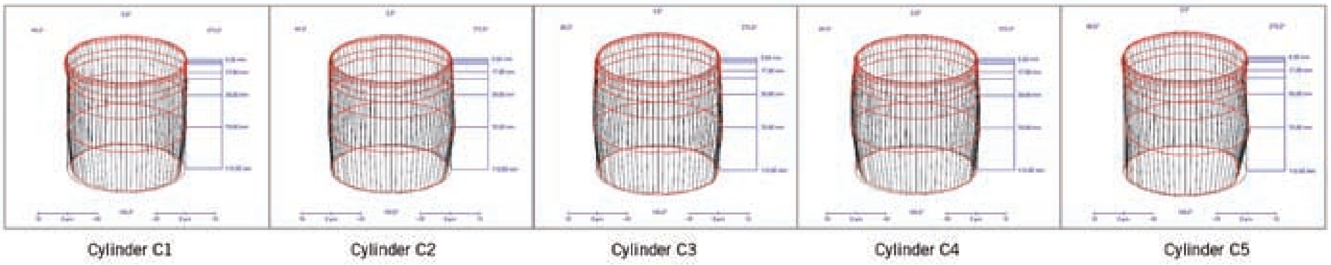

CYLINDER	C1	C2	C3	C4	C5	
CYLINDRICITY						
	3.2	3.8	3.4	3.6	5.1	µm
ROUNDNESS						
Level 1 (5.00 mm)	1.9	1.5	1.4	1.8	1.6	µm
Level 2 (7.00 mm)	1.8	1.5	1.5	1.7	1.5	µm
Level 3 (9.00 mm)	1.8	1.6	1.5	1.7	1.3	µm
Level 4 (17.00 mm)	1.5	2.0	1.8	1.9	1.1	µm
Level 5 (24.00 mm)	1.7	2.3	2.1	2.5	1.1	µm
Level 6 (39.00 mm)	2.4	2.7	2.6	2.9	2.1	µm
Level 7 (70.00 mm)	2.5	1.9	1.8	2.0	3.1	µm
Level 8 (110.00 mm)	2.8	1.9	2.0	1.9	3.1	µm
STRAIGHTNESS						
Angle 1 (0.0°)	1.7	1.3	1.5	1.4	1.3	µm
Angle 2 (90.0°)	1.0	1.5	1.9	2.3	1.1	µm
Angle 3 (180.0°)	1.9	2.1	1.6	1.5	2.7	µm
Angle 4 (270.0°)	1.2	2.7	2.0	1.7	2.8	µm
PARALLELISM						
Angle 1 (0.0° / 180.0°)	1.9	2.1	2.1	1.7	2.8	µm
Angle 2 (90.0° / 270.0°)	4.3	3.0	2.4	2.7	4.4	µm

❽ Cylindricity after honing with a torque plate and the corresponding shape values

LOW-FRICTION MATERIALS AND COATINGS

Another field of activity for production development is the fine machining of frictionally favourable materials; e.g. coatings. Plasma coatings have long been established for race applications, as these engines practically have no run-in phase. Especially high demands are put on the honing quality of cylinder bores for racing applications. Even high volume production, a similar porous surface without protrusions is indispensable for reliable function.

The range of alternative materials for which honing methods have already been pre-developed is very broad and ranges from ceramic layers to metal/ceramic layers all the way to multiphase metal layers, which can be applied as powder or wire, using a flame, arc or plasma. An advantage of a porous sprayed layer is that the surface topography remains practically constant over the entire service life of the engine, regardless of wear.

AVOID BORE DISTORTION

One potential factor for reducing friction, which cannot be underestimated, is the minimization of bore distortion. However, this fundamentally must come from the component design. There are many causes for cylinder distortion, which cannot be completely remedied by "form-correcting" honing.

But also in the case of constructive measures, e.g. monoblocks or stronger materials, cooperating with the development department of the engine builder is required for providing the right tools and/or abrasives, for example.

Honing with a torque plate is a proven way of compensating for the static distortion seen during cylinder head assembly. This static distortion is simulated when the torque plate is bolted on prior to fine boring and honing, ❼ and ❽. This technology has been standard in racing for a long time, and is commonly used in the production of many diesel and some gasoline engines. From a production standpoint, this method is more expensive, but it allows the ring tension (especially the oil scraper ring) to be greatly reduced, which contributes to an overall reduction in engine friction. This is especially evident when an optimized honing process, such as helical slide honing, is employed and is already used in series production.

FREE-FORM HONING

As an alternative to torque plate honing, and theoretically, "free-form" honing offers more freedoms in engine block design. There are two approaches to this, first the position-dependent piloting of (short) honing ledges. A non-round, non-straight bore is generated directly with the goal of reproducing a negative form of the assembled distortion. Distortion direction and magnitude varies by bore and location within the block, so each bore must be corrected individually. Wall thickness variation and other form deviations due to core shift when the blocks are cast, cannot realistically be taken into consideration. Whether or not "free-form" honing will be employed in a production process depends, in no small part, on how the problems regarding in-process measurement, surface consistency, machining times, and tool wear are solved.

Second, an alternative method is to hone using tension, which is generated by applying an external force in the vertical and horizontal directions.

Even though only simple deformations of low order can be generated this way, this method could be implemented in a reasonable time frame on existing machinery. Currently, investigations are ongoing as to whether the theoretical potential of this process can be achieved, in combination with a friction-optimized surface, and at a non-prohibitive cost [4].

Other advantages for this process include:

: a round bore is still machined the target form is only created after relaxation of the tension forces, as is the case with torque plate honing, all existing in-process measuring and process correction options can be utilized
: the position of the bore (perpendicularity, parallelism, straightness) can still be maintained (using long honing ledges)
: the effect of casting core shift is taken into consideration.

Fundamentally, the future potential of form honing cannot be overestimated, since it cannot reasonably compensate for the non-static deformation (or only to a very limited degree), which arises during real motor operation. Possible causes for cylinder deformation are:

: static distortion due to assembly (e.g. cylinder head, additional units)
: dynamic distortion (ignition pressure)
: thermal distortion (in general and additionally in material compounds, e.g. Fe-Al)
: distortion due to aging processes
: distortion due to piston movement (friction, buckling).

Furthermore, when form honing, remember that because piston clearance keeps getting smaller, this method has limits for piston assembly, respectively the crankcase might have to be retensioned. Thus, form honing can only support constructive measures, but cannot replace them.

CONCLUSION

For each application case, check which measures from the areas of construction, materials and honing technology result in the optimal cost/benefit ratio to reduce friction, wear and oil consumption.

REFERENCES

[1] Schmid, J.: Optimiertes Honverfahren für Gusseisen-Laufflächen, VDI-Bericht 1906 (2006)
[2] Hoen, T.; Schmid, J.; Stumpf, W.: Weniger Verschleiß und Ölverbrauch durch Spiralgleithonung bei Deutz-Motoren. In: MTZ 70 (2009), Nr. 4
[3] EU-Projekt Oil-Free-Powertrain Projekt Nr. IPS 2001-80006 Final Report 7/2005
[4] Karrar, E.: Potentiale zur Reibungsreduktion in der Kolbengruppe. ATZ/MTZ-Konferenz „Reibungsminimierung im Antriebsstrang", Esslingen 2009

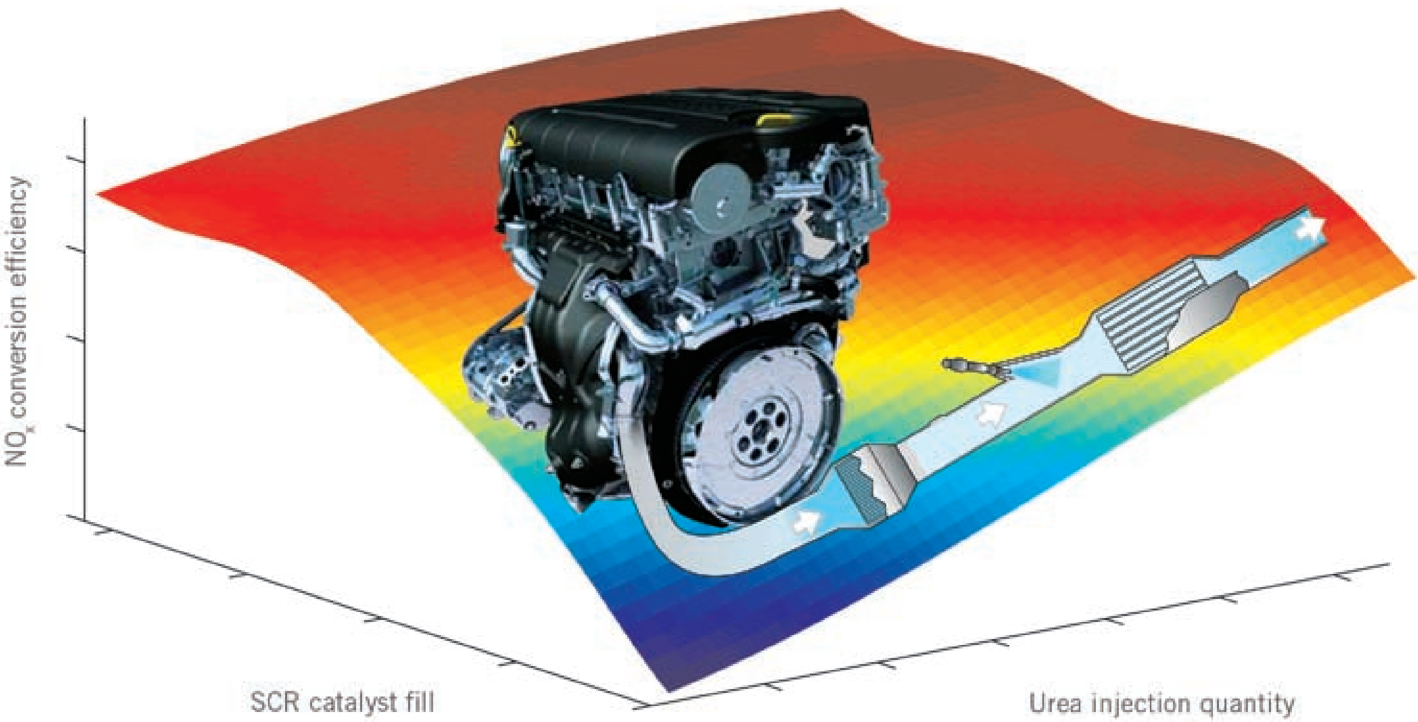

SCR CALIBRATION USING DESIGN OF EXPERIMENTS

NO_x catalysts play a key role in reducing oxides of nitrogen. Further degrees of freedom are introduced into the calibration process when a selective catalytic reduction (SCR) system is incorporated. Ricardo and General Motors have developed an advanced calibration process which counters the increasing complexity of powertrain calibration by using Design of Experiments (DoE). A reduction in development outlay can be achieved despite increased system complexity.

AUTHORS

DR. JUSTIN SEABROOK
is Technical Specialist in Calibration Process at Ricardo UK Ltd. in Shoreham-by-Sea (Great Britain).

MARTIN REBHAN
is Development Engineer in the Performance and Calibration Department for Ricardo Deutschland GmbH in Schwäbisch Gmünd (Germany).

DR. YONGSHENG HE
is Staff Researcher at GM Global Research & Development in Warren (USA).

PAUL A. BATTISTON
is Senior Staff Engineer in the Advanced Engineering Department at GM Powertrain in Warren (USA).

DR. XIN HE
is Senior Researcher at CIDI Engine Group of GM Powertrain Systems Research Lab in Warren (USA).

ENGINE AND SCR SYSTEM OPTIMISED IN PARALLEL

In the relevant emissions regulations for diesel engines due in the coming years the reduction of oxides of nitrogen (NO_x) in exhaust gas is of great importance. Experience shows that the successive optimisation of engine and selective catalytic reduction (SCR) systems does not necessarily lead to optimal powertrain calibration. Engine calibration strategies, like exhaust temperature management, are necessary and these should ideally be calibrated in parallel with the SCR system but, for practical reasons, are often done before SCR calibration. Therefore, time intensive and costly development cycles may result from SCR calibration.

The authors like to present an alternative calibration methodology for the calibration of an engine and SCR system. For this purpose the method set out here involves design of experiments (DoE). The advantage of this method lies in the combination of an engine model and an exhaust system model. In the case of the engine, as with other conventional applications of DoE, the model is created from test data. A unique characteristic of the presented procedure is that a DoE model of the exhaust and aftertreatment system is employed in conjunction with the engine model. This makes it possible to simulate and optimise the system as a whole for a desired drive cycle. The goal is to calibrate the ECU to give the lowest fuel and urea consumption with allowance for the applicable emissions legislation. Through simultaneous rather than successive optimisation, a reduction of the development cycle for the calibration of an SCR exhaust system can be achieved. The paper is based on a collaboration work for the DEPE consortium [1, 2].

APPROACH

For the described development programme, a turbocharged diesel engine of approximately 2 litre capacity with common rail fuel injection system was used. A diesel oxidation catalyst (DOC) was fitted in the exhaust system. After the DOC, the NO_x catalyst was located with the necessary dosing unit for the urea. The SCR system consisted of two bricks with copper zeolite coated cordierite substrate (cyclosilicate). ❶ shows the principal exhaust-gas system layout with the measurement points.

The calibration process can be broken down into two phases. In the first phase the DoE model for the engine and the exhaust system are set up. In the creation of the DoE models for the engine the standard control unit variables were taken into account, namely injection timing, injection mass, EGR rate, rail pressure and boost pressure. Differing from the normal calibration process the exhaust system is represented by a model capable of predicting instantaneous NO_x conversion efficiency. Both DoE models are combined and used together during optimisation to generate a base engine calibration and an initial urea injection map.

In the second phase the engine calibration is optimised. Therefore, a DoE test is carried out utilising the real SCR system

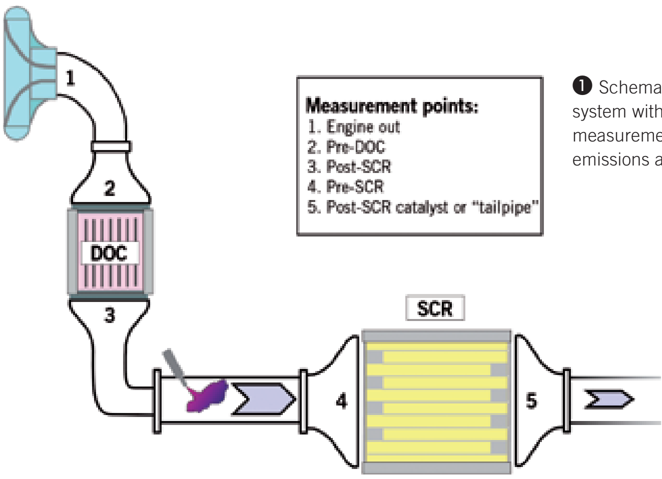

❶ Schematic of the exhaust-gas system with five components and measurement points for temperature, emissions and mass flow

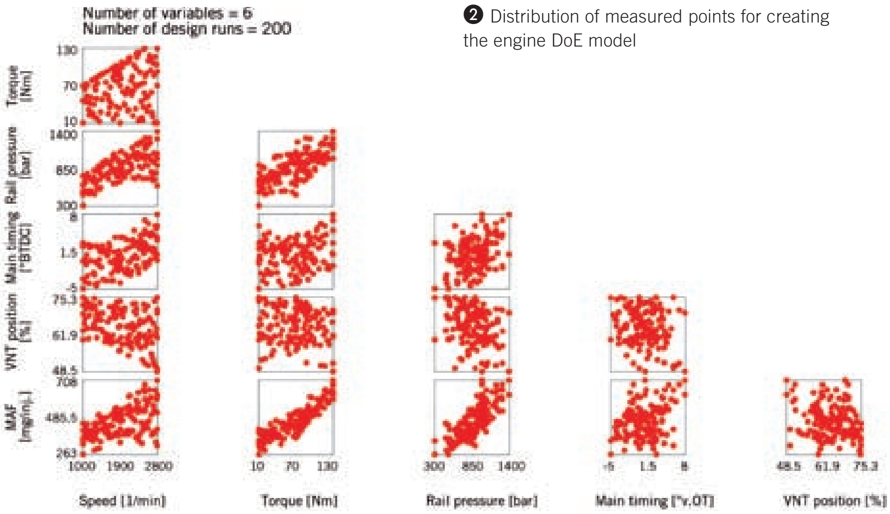

❷ Distribution of measured points for creating the engine DoE model

NAMES	UNIT	NAMES	UNIT
Fuel	kg/h	Turbine out temperature	°C
CO	g/h	DOC inlet temperature	°C
HC	g/h	DOC outlet temperature	°C
NO	g/h	SCR catalyst inlet temperature	°C
NO_2	g/h	SCR catalyst outlet temperature	°C
NO_x	g/h	ECU fuel demand	mg/cycle
Soot	g/h	Boost pressure	hPa
Particulate matter (PM, estimated)	g/h	Exhaust-gas mass flow rate	kg/h
Combustion noise	dB(A)		

❸ Modelled measurements

on a test bed. The goal is to optimise urea dosing quantity depending on speed and load.

PHASE 1: CREATION OF DOE MODELS FOR THE ENGINE

A global DoE model was developed for the engine. In the global approach, which produces very substantial reduction in testing compared to conventional key point methods, engine speed and load are input variables in the DoE design. With additional consideration of SCR behaviour, it is possible to carry out the final optimisation of the engine map based on the global engine model for any given drive cycle.

In ❷ the design space for the engine DoE model can be seen. It is possible to see the asymmetric distribution of test points which results from the use of 3D design constraints. These constraints avoid variable combinations where the engine is not able to run. The test plan was carried out on a fully automated testbed with a total duration of 25 hours for 200 test points. The DoE models, which characterise the behaviour of the engine, are shown in ❸.

The modelling of the given measurements in ③ required less than a day to complete. The applied modelling approach is based on stochastic process models (SPMs) [3]. A key advantage of SPMs, compared to other advanced methods, is that an expert user is not required to get good results. The generated models for compressor out temperature, combustion noise, soot, NO_2 and NO are shown in ❹.

CONSIDERING THE THERMAL INERTIA OF EXHAUST SYSTEM

As all measurements were steady state the models developed from the measured data only give information about the engine behaviour in steady state conditions. When temperature SPMs are used for a later drive cycle optimisation, the resulting temperature variations, caused by the thermal inertia of the exhaust system, must be considered. For this reason, a phenomenological temperature model of the exhaust system upstream of the SCR was applied to predict pre-SCR temperature from the modelled turbine out temperature. The phenomenological model was a simple heat loss model for a pipe and DOC.

GENERATION OF A DOE MODEL OF THE SCR SYSTEM

As the last step in phase 1, a DoE model for the SCR system was created. As is

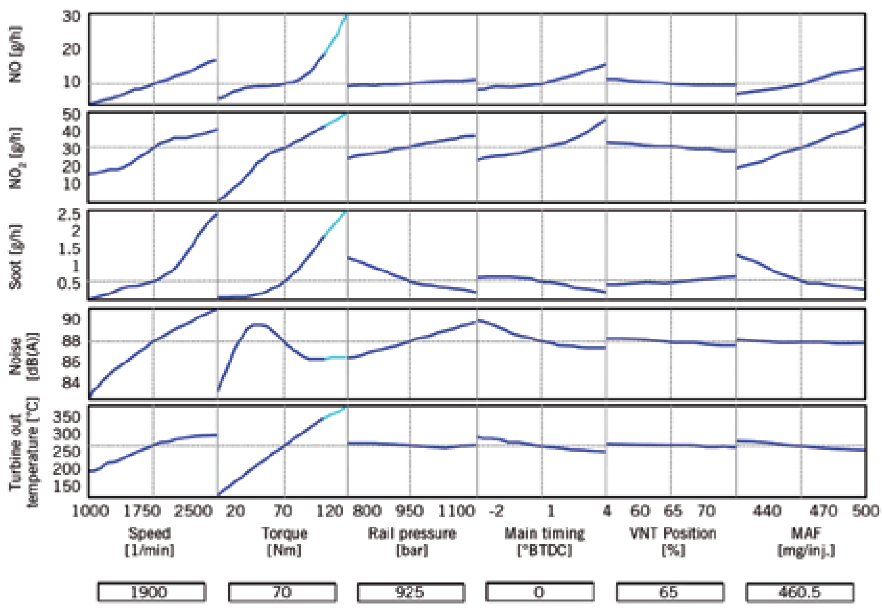

❹ Engine model – visualisation of chosen stochastic process models (SPMs)

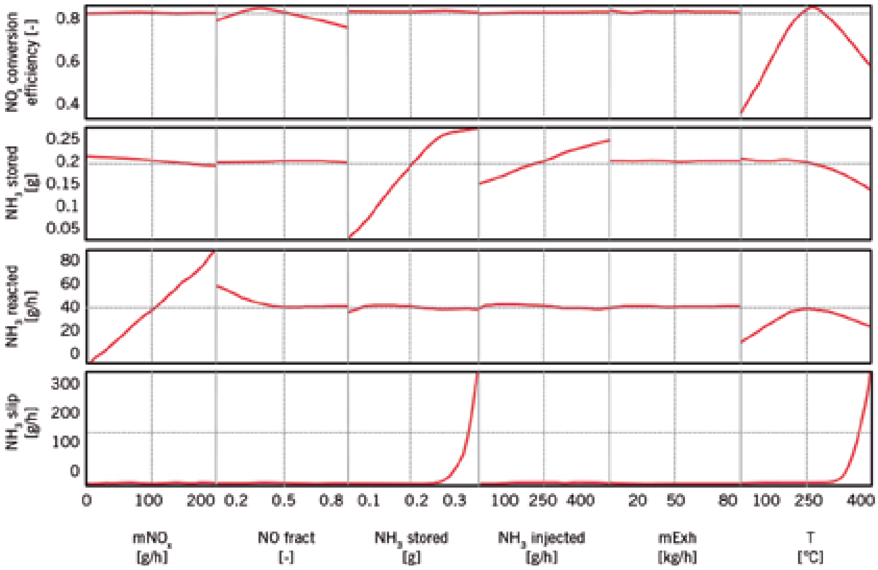

❺ Graph of SCR model created by DoE

shown in ① the SCR system involved a urea injection system. The phenomenological model of the SCR catalyst was created in Matlab/Simulink. The computer model incorporates the urea-based NO_x conversion chemical reactions and also the reaction kinematics which are dependent on the concentration of reactants.

In real SCR systems it can be seen that when exhaust NO/NO_x ratio is 0.5 the conversion performance at low exhaust temperatures is considerably increased. This fact can be used, for drive cycle based calibration optimisation. Due to the complexity of the Simulink model the simulation of drive cycles takes a long time. Therefore, it is advantageous to "translate" such a physical model into a SPM to realise the benefit of fast calculation of system response. Thus the engine and SCR calibration is able to utilise fully computer based optimisation, which typically runs through hundreds of thousands of optimisation situations. The SPMs of the SCR system created by Simulink are shown in ❺.

The SCR model shown in ⑤ gives the behaviour of the SCR system on a second by second basis. For drive cycle simulations the SCR model is calculated time-based to take the continually changing NH_3 amount into account which is stored in the SCR system. This is necessary as the NH_3 catalyst fill level has an impact on NO_x conversation efficiency. It can be seen that the NH_3 slip increases sharply as soon as the amount of stored ammonia reaches the saturation ("NH_3 stored"). The presented SCR model can be linked to the engine model in ④.

CLOSED-LOOP OPTIMISATION OF ENGINE AND SCR CALIBRATION

The Phase 1 DoE models are used to generate the engine calibration and the initial urea injection quantity map. The optimisation objective applied is the lowest "total fuel plus urea cost" over the NEDC. The main constraints taken into account were NO_x and soot emission targets. The steps in the process, which were carried out during the time-based drive cycle optimisation, are shown in ❻.

In a first step the NO and NO_2 emissions, the exhaust mass flow and the exhaust temperature of the engine were calculated. Then the temperature at SCR inlet was found with the dynamic temperature SPM. The amount of ammonia available to the SCR was calculated from the virtual urea map, which characteristics are object of the processed optimisation.

Based on an original virtual engine calibration, the maps of engine ECU and injected urea solution are calculated. This sequence was repeated until a solution was found where the optimisation criteria were achieved. The cells in every operating map were interpreted by the optimisation tool as independent variables which could be individually changed. To illustrate the magnitude of the interaction

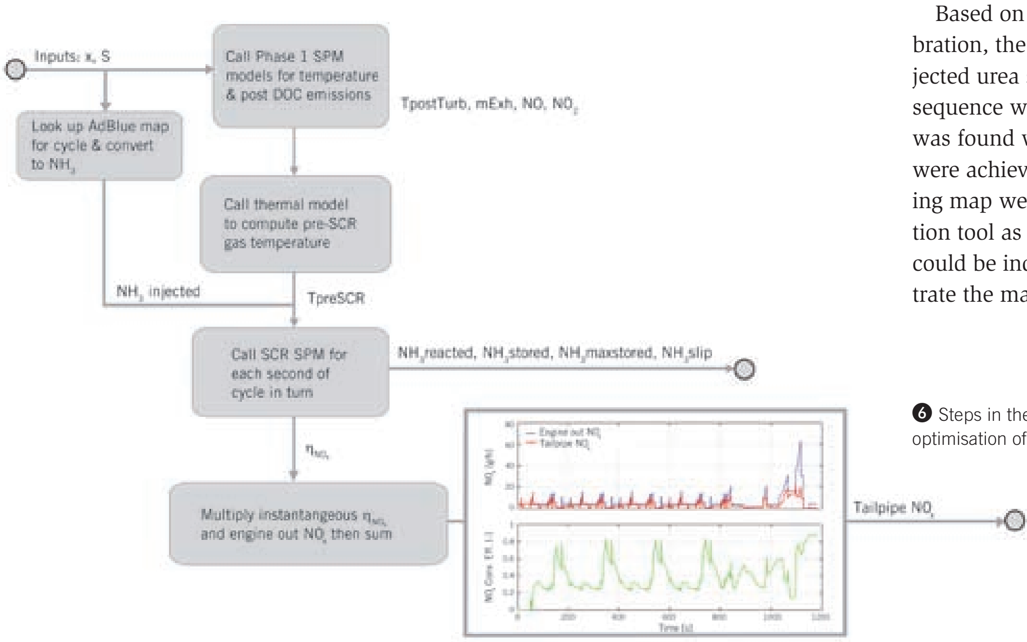

❻ Steps in the process for the combined optimisation of engine and SCR calibration

	OBJECTIVES AND CONSTRAINTS	OPTIMISATION VARIABLES	NEDC RESULT NO_x
1	Minimise engine out NO_x (subject to constraints on other emissions and fuel economy); no urea injection	Engine calibration only	190 mg/km
2	Minimise tailpipe NO_x (using fixed engine calibration from 1)	Urea dose calibration only	108 mg/km
3	Minimise tailpipe NO_x	Engine and urea dose calibrations together	38 mg/km

❼ Comparison of individual calibration phases

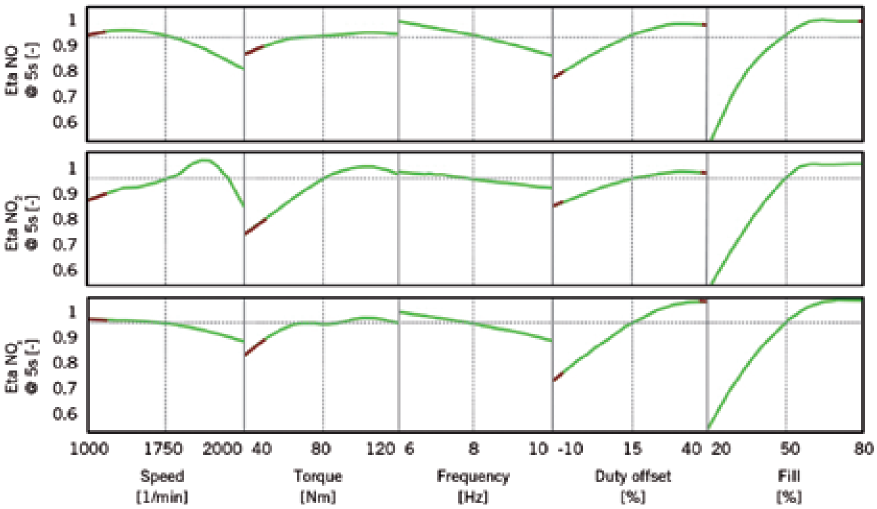

❽ Models for NO and NO_2 conversion efficiency of the real SCR catalyst

between base engine calibration and urea dosing calibration, optimisation results are presented in ❼.

Reviewing these results, it is clear that optimising the base engine and urea dose calibrations simultaneously, rather than in series, leads to a significantly better result: 80 % less NO_x emissions are achievable for the calibration methodology presented here. The impact of the introduced NO_x emission reduction approach will vary between the used SCR hardware. But this difference is representative of cycles where significant base calibration changes are required to put the SCR catalyst in the correct temperature window.

PHASE 2: DOE BASED CALIBRATION OF THE SCR SYSTEM

In the second test phase, the objective is to optimise the urea solution quantity and injection pulse rate for each speed and load. A DoE test was carried out based on perturbing the quantity of urea solution either side of the values in the optimisation maps generated during Phase 1. The behaviour of a SCR catalyst depends on the amount of ammonia stored. For that reason, the fill level of the SCR catalyst must be a DoE variable. A procedure was developed that was able to achieve a pre-determined level of NO_x storage in the SCR catalyst.

DOE TESTING AND FINAL OPTIMISATION

The design used for the DoE test had 30 cases. Low speed and torque combination have been excluded from the test matrix as the NO_x conversion at those load conditions is not possible. ❽ shows the DoE models for NO and NO_2 conversion efficiency of the real SCR catalyst. It can be seen that the SCR catalyst fill of NO_x has a great influence on the conversion behaviour.

The Phase 2 NO_x conversion efficiency models are now used with an optimiser to determine the dose and injection frequency that maximises conversion efficiency or achieves a target value. For Euro 6 and other cycles of equivalent NO_x stringency, it is necessary to maximise NO_x conversion efficiency whether or not the particular operating point has an active heating strategy. Additionally, the models can be used to verify the accuracy of the Phase 1 SCR catalyst model.

CONCLUSIONS

The optimisation results for Phase 1 demonstrate the importance of optimising base engine calibration and dosing in a single coherent process. In Phase 2, both urea quantity and frequency were significant variables. By using DoE, the behaviour of complex systems can be modelled and visualised. Optimisation of the DoE models can be performed on PC with advantages in time effort and cost. Overall, compared to a conventional SCR calibration process, the total test duration is reduced

The high testing requirement for conventional SCR calibration is partly explained by the need to put the SCR catalyst into the correct temperature region; without negatively affecting the fuel consumption characteristics. The temperatures are difficult to achieve due to the low engine load of the driving cycles. This time intensive and costly project phase is, in this concept, reduced by more extensive use of computer simulation. In conclusion, it can be established that, in comparison to conventional SCR calibration, a reduction in total test time in combination with better overall optimisation is achieved.

REFERENCES

[1] http://www.ricardo.com/depe
[2] Seabrook, J.; He, Y.; Battiston, P. A.; He, X: Application of DoE to the Optimisation of Engines with Selective Catalytic Reduction (SCR) Systems. Design of Experiments (DoE) in Engine Development Conference, Berlin, 2009
[3] Seabrook, J.; Salamon, T.; Edwards, S; Noell, I.: A Comparison of Neural Networks, Stochastic Process Methods and Radial Basis Functions for the Optimisation of Engine Control Parameters. Tagung, Haus der Technik, Design of Experiments in Engine Development, Berlin, 2003

READ THE FUTURE

NUMBER 1 IN AUTOMOTIVE ENGINEERING SINCE 1898

Source: Daimler AG

We offer the leading automotive engineering trade media for the entire sector – complete with the newest results from international research, development and manufacturing, as well as fascinating contributions from chosen experts. And because it is all about progress here, we have gone one step further: Thanks to their new design, the ATZ media are now even easier to read, even more clearly structured, and even more attractive. **emagazine.ATZonline.com**

ATZ

YES, I WOULD LIKE TO TRY ATZ! Please send me the next two issues of ATZ – Automobiltechnische Zeitschrift. In order to continue to receive the eMagazine, I need do nothing further. I will receive the eMagazine at the price of only **€ 269.00**. I can cancel my subscription at any time after receiving any issue. Any fees I paid for issues that were not delivered to me will be reimbursed.

CANCELLATION GUARANTEE: I can cancel this agreement in writing within 14 days. The postmark date shall be proof of timely dispatch to Springer Automotive Media, Leserservice PF 18, Abraham-Lincoln-Str. 46, 65189 Wiesbaden, Germany.

COMPANY	CITY / POSTCODE
FIRST / LAST NAME	COUNTRY
POSITION	Please send me your free ATZonline-newsletter periodically:
DEPARTMENT	E-MAIL ADDRESS
STREET ADDRESS	DATE / SIGNATURE

Simply fill out this voucher and fax it to **+49 (0)611.7878-407**
or order online at **emagazine.ATZonline.com**

○ I will also receive 6 issues/year of the FISITA magazine **ATZ autotechnology** in printed form – **at no extra cost!**

NEW FLOW BENCH
FOR CYLINDER HEADS, INDUCTION AND EXHAUST SYSTEMS

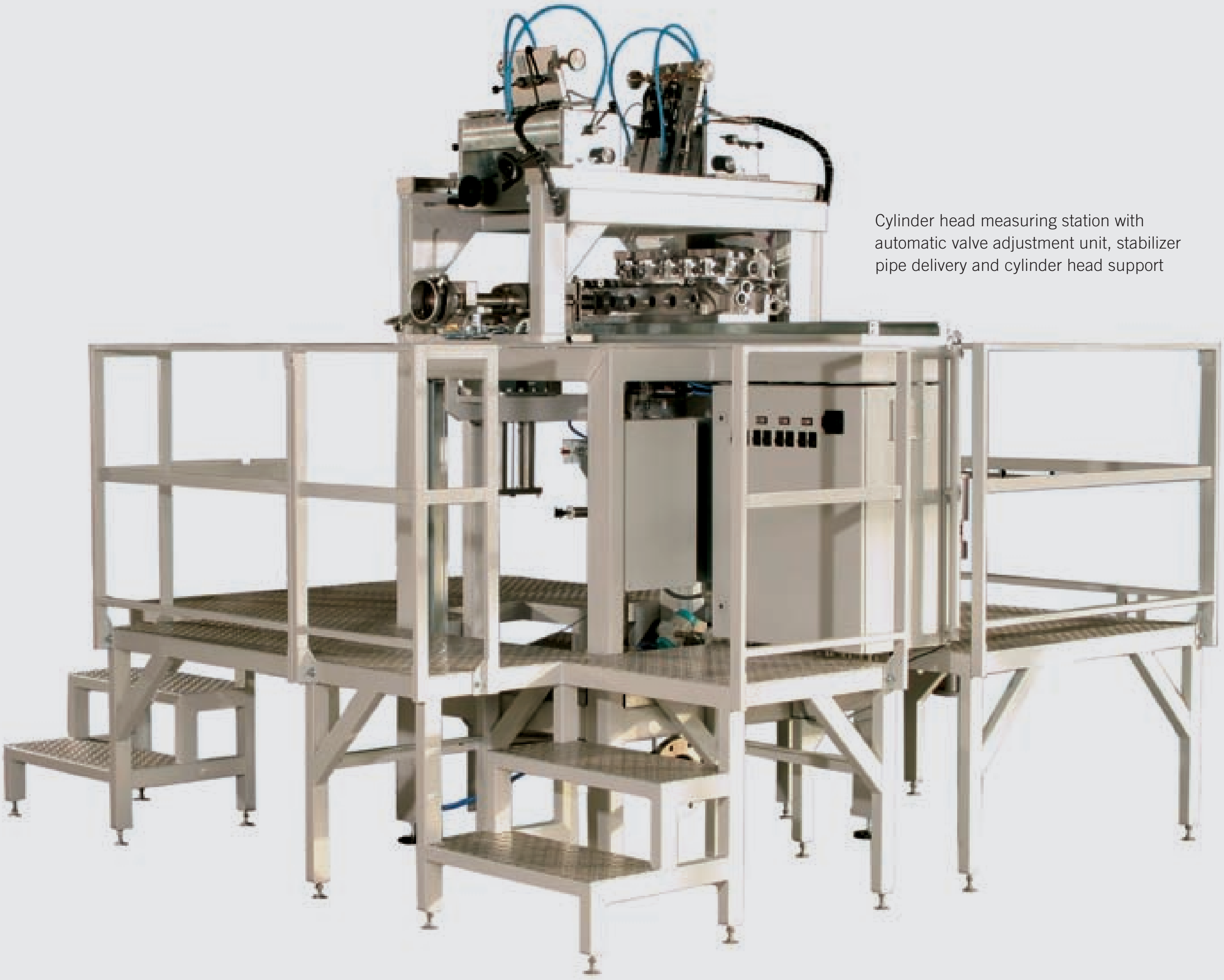

Cylinder head measuring station with automatic valve adjustment unit, stabilizer pipe delivery and cylinder head support

In 2008/2009, the BMW Group in Munich completed a section of its Test Equipment Centre, outfitting it with numerous test stations for engines, drive trains and aggregates. The continuous improvements being made in modern combustion engines and the resulting demands on test stand technology also called for a new flow bench for cylinder heads, induction and exhaust systems in Munich. Edag Test Systems in Recklinghausen, Germany, handled this task for the BMW Group.

AUTHORS

DIPL.-ING. ROBERT STANG
is Project Manager at Edag GmbH & CO. KGaA, Department Test Systems in Recklinghausen (Germany).

DIPL.-ING. PETER D.A. BREITBACH
works at the Department Research Drive of the BMW Group in Munich (Germany).

TASK

The cylinder head is the assembly that plays a decisive role in defining the performance, fuel consumption and exhaust emission characteristics of a combustion engine. For some considerable time now, BMW has been determining and optimising the flow characteristics of cylinder heads and other components in the intake and exhaust tract of combustion engines that are relevant to the gas exchange cycle on suitable test stands.

When the new Test Equipment Centre was being constructed, some thought was given to the idea of modifying an existing test stand and moving it from the old premises in the Riesenfeldstraße into the new building.

However, after briefly considering and observing the many additional functions it would offer, it was decided that a new test stand would be the better option. This decision offered the opportunity of operating the old test system without interruption until the new test stand was started up.

The new flow bench has a surface area of approximately 170 m² in three rooms in the Research and Innovation Center (FIZ) of the BMW Group in Munich. The system, ❶, comprises two measuring stations, one for cylinder heads and the other for general measuring purposes, each of which is located in a separate room and operable independently of the other. There is also a machine room housing two large screw-type compressors, a vacuum vessel, a pressurised vessel and various control circuits. There is a control room from which the system is monitored and operated.

The test stand, developed and supplied by Edag as a turnkey system, was put into operation in 2009.

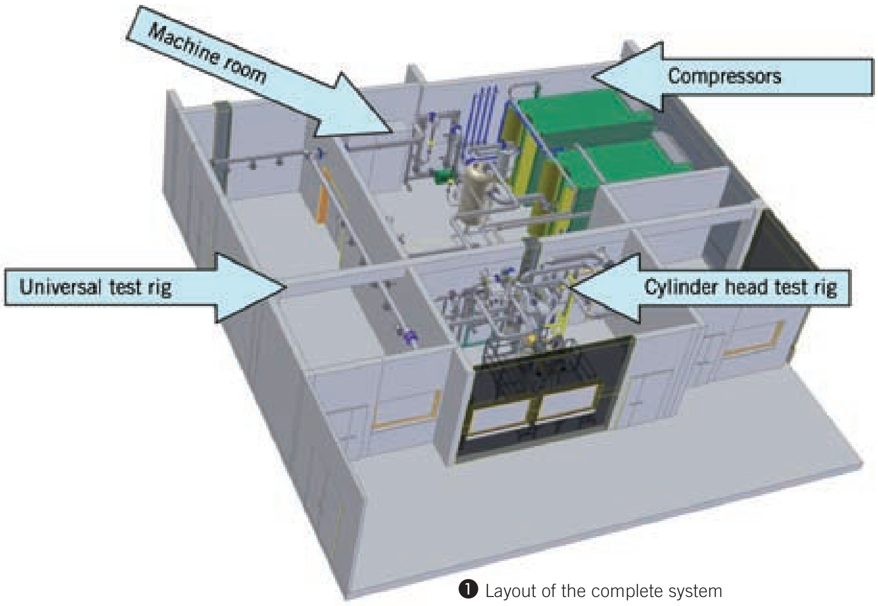

❶ Layout of the complete system

FUNCTIONAL EXTENSIONS

The idea behind the planning and the design of the new test stand is to enable the functions of the previous tests to be extended. In this way, the measuring and control range for mass flow and pressure were enlarged in order to have sufficient reserves for future engine concepts even in the upper performance range. The equipment concept was designed for either open or, if preferred, closed operation to make it possible for the test object to intake air freely from the atmosphere, but also to set variable degrees of low pressure or overpressure as well as differential pressures. Intended to provide pressure and suction modes relating to the test object connection, the concept, in conjunction with a wide variety of flow path change-over options on the cylinder head measuring station, covers virtually any flow instance imaginable. Due to the extended, fully automatic functioning of the valve adjustment of the cylinder head measuring station, it should be possible to record the performance data of all the cylinders in a cylinder head in sequence without the operator having to intervene or to make adjustments. It should be feasible to run both test stations concurrently in order to ensure the most economical use.

GENERATION AND CONDITIONING OF COMPRESSED AIR

Two absolutely oil-free, water-cooled screw-type compressors are used for the generation of compressed air. These are located in the machine room and supply both flow benches with pressurised air, the „cylinder head measuring station with valve adjustment“ and the „general measuring station“. The screw-type compressors are speed-controlled in sequence. The asymmetrical design of the compressors permits infinite adjustment of the mass flow between 500 und 4000 kg/h by controlling the speed of the drive systems and applying a suitable switch-on/switch-off concept. Two compressed air reservoirs are used to disconnect the compressor station and the test stand as well as to stabilise the pressure on the pressure and inlet sides.

At both compressors, intercoolers and aftercoolers pre-cool the air to approximately 30 °C. In the following pressure pipes, the air is intermittently heavily restricted. For this reason, there is a further heat exchange device before each test station by means of which the air temperature can be adjusted to 20 °C +/- 1 °C. This means that, as measuring is always carried out at a standard temperature, there is no need to correct the results in this respect.

Starting from the vacuum and pressurised vessels, the cylinder head measuring station and the general measuring station have independent pipe networks with their own measuring and control engineering. Volumetric flow is measured by means of a measuring cascade consisting of several laminar flow elements and a venturi tube. The evaluation of measuring data, the internal comparison of the measuring stages for "infinitely variable measuring" and the calculation of the mass flow with further measured variables are all performed by a flow computer. This means that measuring accuracy across the entire measuring range is better than 1 %. A cascade in the inlet and return pipes, comprising of one control valve and one needle valve, controls admission pressure, differential pressure or mass flow. The control elements were designed by Edag. The integration of a bypass pipe between the inlet and the pressure tanks with a high-resolution needle valve enables even very small mass flows to be set at the test stations.

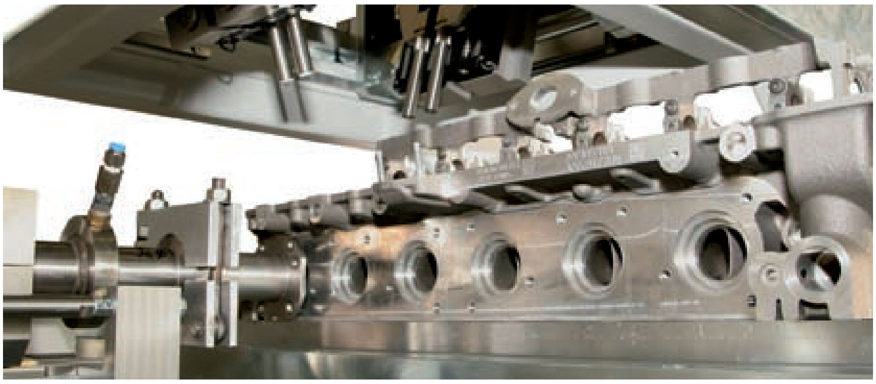

❷ Cylinder head at the valve adjustment unit

The concept described permits a very wide spread of measuring and control ranges for pressure and mass flow which is further increased in the volumetric flow.

CYLINDER HEAD MEASURING STATION

In this measuring station, ❷, cylinder heads of engine blocks with a maximum of six cylinders undergo fully automatic measuring. At the heart of the station is a device which sets each cylinder head on a component-specific adapter plate. The inlet port, the outlet port and the combustion chamber of the test object are adapted to the flow path by means of stabilizer pipes. Working continuously and independently of each other, four position-controlled servo-motors operate the inlet and discharge valves, positioning them with a precision better than +/- 0.05 mm. Piezoelectric force sensors are used to find the zero point of the valve lift. There are a variety of different settings with linear and angular adjustment helping to fit the various cylinder head geometries on the test stand.

The infeed of the cylinder head from cylinder to cylinder, the stabilizer pipe carrying to the port on the flow path and the valve operation on the cylinder head all occur fully automatically. Tests on the individual cylinders are carried out one after another without any additional adjustments, overnight for instance.

The pipe system is fitted with numerous switching valves so that air can be passed through the cylinder head in the closed system (pressure mode, six flow instances) in each direction of flow between the inlet, outlet and combustion chamber. For overlap testing between the intake port and exhaust

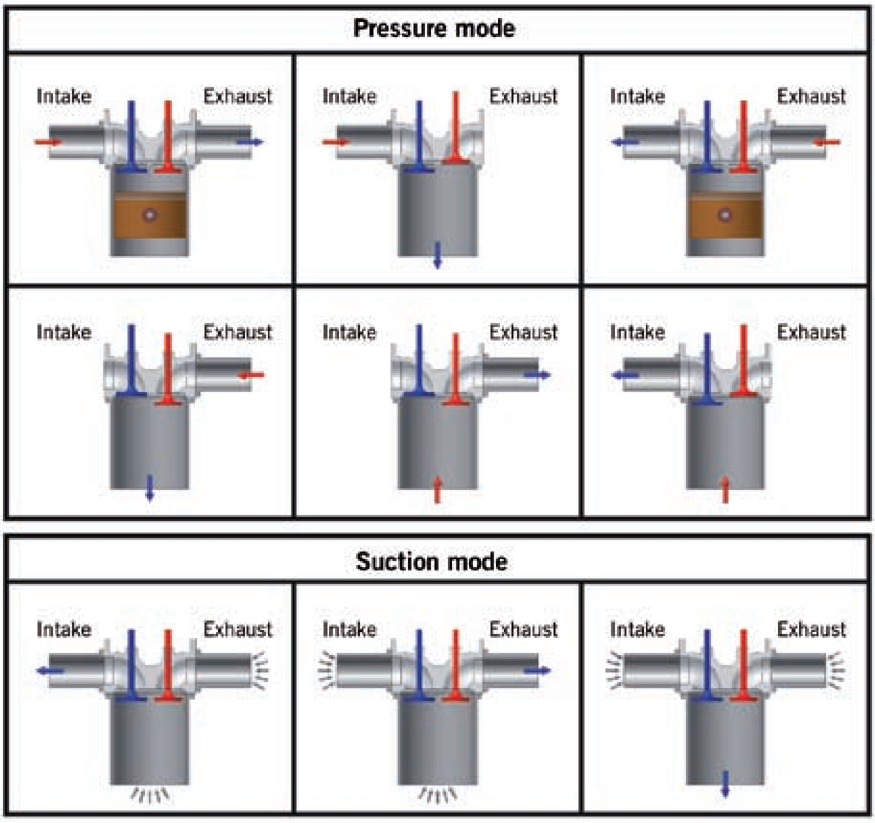

❸ Flow instances at the cylinder head measuring station port, a dummy piston can be inserted into the adaptation in order to simulate a realistic reconstruction of flow conditions.

In another operating mode (suction mode, three flow instances), there is the option of adapting the inlet duct, the outlet duct or the cylinder to the test stand's suction line. Then, inflow is via the other two ports which remain open during these tests. A swirl and tumble measuring device applied below the cylinder head provides data on flow turbulence in the combustion chamber on two axes. In closed operating mode, either the mass flow, differential pressure or pressure ratio can be controlled. In free intake operating mode (alternative mode), only the intake pressure behind the test object can be adjusted within the limits of -0.05 to -0.3 bar as differential pressure to the atmosphere. In this operating mode, the mass flow adapts itself to the specific test object.

Virtually any flow path, ❸, occurring at the cylinder head in real life can be reproduced with the concept described here. The acquired performance data with various valve lifts serve to evaluate and optimise the design and production of the cylinder head.

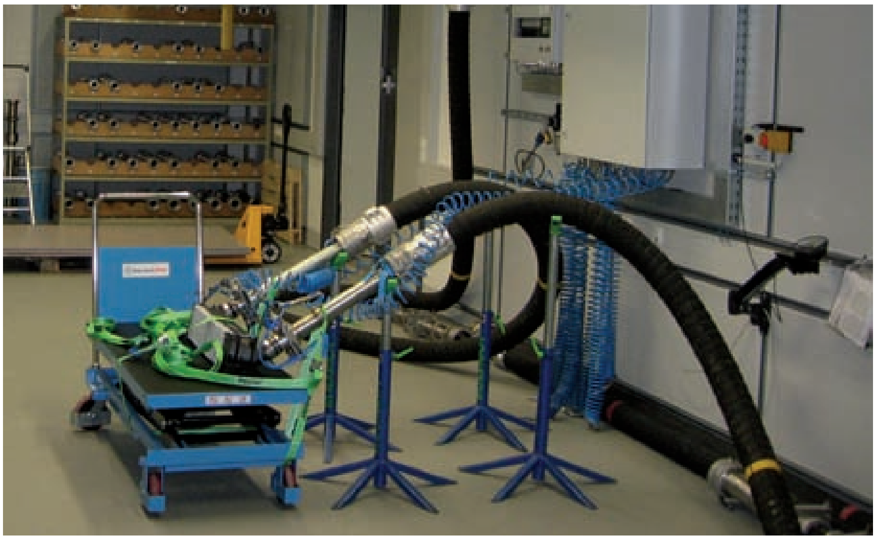

❹ General measuring station with a charge air cooler as test object

GENERAL TEST STATION

Air flow directing components such as exhaust systems, throttle valves, air mass sensors, etc. can be examined in the general test station, ❹. To this end, the measuring station has one rotating suction line and one rotating pressure line. Each has a variety of contact points to which the test objects can be adapted to pressure and temperature measuring points by means of quick-acting couplings, tubes and stabilizer pipes.

In closed operating mode, this test station also offers the choice of mass flow, differential pressure or pressure ratio control.

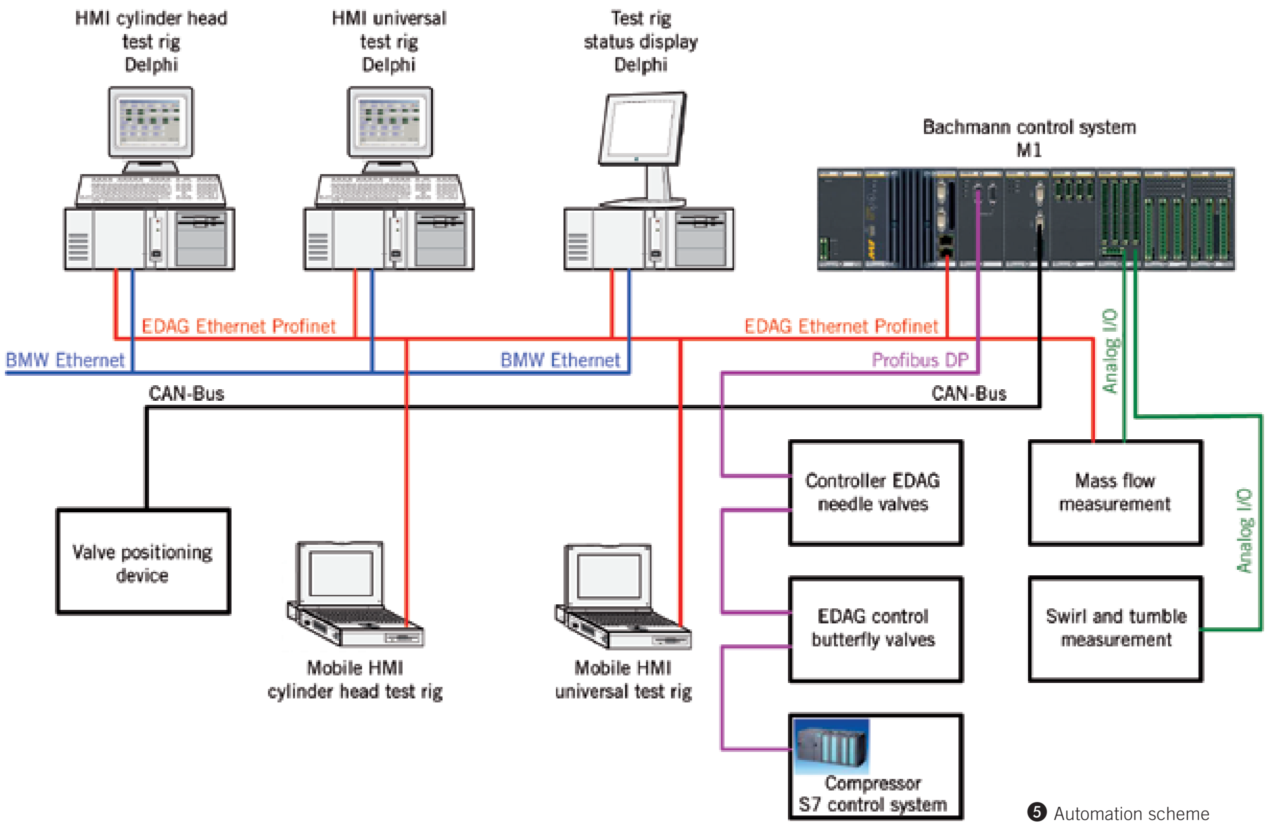

❺ Automation scheme

In free intake operating mode, the intake pressure behind the test object can be adjusted within the limits of -0.05 to -0.3 bar as differential pressure to the atmosphere. In this mode, the mass flow, as a dependent value, adjusts itself.

Further, the measuring of exhaust systems calls for a clear blow-out mode. Here, the pressure is adjusted in front of the test object and the component-specific mass flow results.

The characteristic lines and resulting flow parameters – mass flow, loss of pressure and temperature – are recorded throughout the tests. An I/O interface permits further sensors to be linked to the test object. In this way, temperature and pressure curves for complex exhaust systems can be recorded or air mass flow sensors on the system gauged.

AUTOMATION

An intelligent MSR system, type Bachmann M1, which communicates with the subordinate sub-systems via Profibus, CAN-Bus, Ethernet and an analogous interface is used for the automation, ❺, of the test stand. The Bachmann system takes over all measuring, controlling and regulating functions performed by the software as well as most of the online calculations. It is programmed in Structured Text in accordance with IEC 61131.

In the control room, one industrial PC per test station is used as the central interface to the operator. A comprehensive Delphi application installed on this computer carries out all superordinate control applications as well as data acquisition and storage. A further observation PC in the control centre shows all states and conditions throughout the entire system and can in addition be used for maintenance purposes.

The test parameters and results recorded on the two test stations are stored in an Access database where they can undergo further processing. Measurement files can also be converted into either an Excel or MDF format and exported. This means that they are also available for external evaluation.

SCREW-TYPE COMPRESSORS				
DESCRIPTION	**COMPRESSOR 1**		**COMPRESSOR 2**	
Rated intake volume flow	380 to 1300 m³/h		970 to 1920 m³/h	
Mass flow	480 to 1680 kg/h		1280 to 2500 kg/h	
Min. input pressure (absolute)	0.5 bar		0.5 bar	
Max. output pressure (absolute)	6 bar		6 bar	
Compressor speed	634 to 1800/min		900 to 1655/min	
Engine power	250 kW		315 kW	
CYLINDER HEAD MEASURING STATION				
DESCRIPTION	**MEASURING RANGE**		**ACCURACY**	
Air-mass flow	3 – 2000 kg/h		≤ 1 % from reading	
Primary pressure (relative) at specimen	max. 4 bar		≤ 1 % from reading	
Differential pressure via specimen	0.05 to 4 bar		1 % from reading respectively 5 mbar	
VALVE POSITIONING DEVICE				
DESCRIPTION	**START**	**END**	**TOLERANCE**	**UNIT**
Number of cylinder in-line	1	6	–	–
Travel servomotor valve positioning device	0	approx. 200	± 0.05	mm
Valve travel	0	20	± 0.05	mm
Force per valve	–	max. 1000	–	N
Number of synchronous operated valves	1	4	–	unit
Cylinder head travel	0	max. 940	≤ 0.1	mm
GENERAL MEASURING STATION				
DESCRIPTION	**MEASURING RANGE**		**ACCURACY**	
Air-mass flow	50 – 4000 kg/h		≤ 1 % from reading	
Primary pressure (relative) at specimen	max. 4 bar		≤ 1 % from reading	
Differential pressure via specimen	0.05 to 4 bar		1 % from reading respectively 5 mbar	

❻ Technical data of the flow bench

SUMMARY

In terms of energy efficiency and performance yield, BMW has taken a leading position at international level. The Group's engine range goes from four-cylinder mid-capacity brackets through to large-volume V12 engines. Increasing stringent legislation on exhaust emissions and limited raw material resources have led, among other things, to the development of supercharged engines with small to mid-range engine capacities. In the last few years, BMW has significantly reduced the fuel consumption and pollutant emissions of its fleet in Europe. That environmentally friendly fuel saving technologies in no way diminish the pleasure of driving is the philosophy behind the award-winning “BMW Efficient Dynamics” technology package. The enhancement of existing engine concepts and the development of new ones call for extensive testing. The new test stand which shows the following technical data, ❻, contributes to this with its significantly improved functionality, increased performance data and higher degree of automation.

IMPRINT

MTZ

WORLDWIDE

www.MTZonline.com

Founded 1939 by Prof. Dr.-Ing. E. h. Heinrich Buschmann and Dr.-Ing. E. h. Prosper L'Orange

Organ of the Fachverband Motoren und Systeme im VDMA, Verband Deutscher Maschinen- und Anlagenbau e.V., Frankfurt/Main, for the areas combustion engines and gas turbines
Organ of the Forschungsvereinigung Verbrennungskraftmaschinen e.V. (FVV)
Organ of the Wissenschaftliche Gesellschaft für Kraftfahrzeug- und Motorentechnik e.V. (WKM)
Organ of the Österreichischer Verein für Kraftfahrzeugtechnik (ÖVK)
Cooperation with the STG, Schiffbautechnische Gesellschaft e.V., Hamburg, in the area of ship drives by combustion engine

06 I 2010 _ June 2010 _ Volume 71
Springer Automotive Media I Springer Fachmedien Wiesbaden GmbH
P. O. Box 15 46 · 65173 Wiesbaden · Germany I Abraham-Lincoln-Straße 46 · 65189 Wiesbaden · Germany
Amtsgericht Wiesbaden, HRB 9754, USt-IdNr. DE811148419

Managing Directors Dr. Ralf Birkelbach (Chairman), Armin Gross, Albrecht Schirmacher I **Senior Advertising** Armin Gross I **Senior Marketing** Rolf-Günther Hobbeling
Senior Production Christian Staral I **Sales Director** Gabriel Göttlinger

EDITORS-IN-CHARGE
Dr.-Ing. E. h. Richard van Basshuysen
Wolfgang Siebenpfeiffer

EDITORIAL STAFF

EDITOR-IN-CHIEF
Johannes Winterhagen (win)
phone +49 611 7878-342 · fax +49 611 7878-78462
johannes.winterhagen@springer.com

VICE-EDITOR-IN-CHIEF
Ruben Danisch (rd)
phone +49 611 7878-393 · fax +49 611 7878-78462
ruben.danisch@springer.com

CHIEF-ON-DUTY
Kirsten Beckmann M. A. (kb)
phone +49 611 7878-343 · fax +49 611 7878-78462
kirsten.beckmann@springer.com

SECTIONS
Electrics, Electronics
Markus Schöttle (scho)
phone +49 611 7878-257 · fax +49 611 7878-78462
markus.schoettle@springer.com
Engine
Ruben Danisch (rd)
phone +49 611 7878-393 · fax +49 611 7878-78462
ruben.danisch@springer.com
Online
Katrin Pudenz M. A. (pu)
phone +49 6172 301-288 · fax +49 6172 301-299
redaktion@kpz-publishing.com
Production, Materials
Stefan Schlott (hlo)
phone +49 8191 70845 · fax +49 8191 66002
Redaktion_Schlott@gmx.net
Research
Dipl.-Ing. (FH) Moritz-York von Hohenthal (mvh)
phone +49 611 7878-278 · fax +49 611 7878-78462
moritz.von.hohenthal@springer.com
Service, Event Calendar
Martina Schraad (mas)
phone +49 611 7878-276 · fax +49 611 7878-78462
martina.schraad@springer.com
Transmission
Dipl.-Ing. Michael Reichenbach (rei)
phone +49 611 7878-341 · fax +49 611 7878-78462
michael.reichenbach@springer.com

PERMANENT CONTRIBUTORS
Richard Backhaus (rb), Christian Bartsch (cb), Dipl.-Reg.-Wiss. Caroline Behle (beh), Prof. Dr.-Ing. Peter Boy (bo), Prof. Dr.-Ing. Stefan Breuer (sb), Jörg Christoffel (jc), Jürgen Grandel (gl), Ulrich Knorra (kno), Prof. Dr.-Ing. Fred Schäfer (fs), Roland Schedel (rs), Bettina Seehawer (bs)

ENGLISH LANGUAGE CONSULTANT
Paul Willin (pw)

ADDRESS
P. O. Box 15 46, 65173 Wiesbaden, Germany
redaktion@ATZonline.de

MARKETING I OFFPRINTS

PRODUCT MANAGEMENT AUTOMOTIVE MEDIA
Sabrina Brokopp
phone +49 611 7878-192 · fax +49 611 7878-78407
sabrina.brokopp@springer.com

OFFPRINTS
Martin Leopold
phone +49 2642 9075-96 · fax +49 2642 9075-97
leopold@medien-kontor.de

ADVERTISING

AD MANAGER
Britta Dolch
phone +49 611 7878-323 · fax +49 611 7878-78140
britta.dolch@gwv-media.de

KEY ACCOUNT MANAGEMENT
Elisabeth Maßfeller
phone +49 611 7878-399 · fax +49 611 7878-78140
elisabeth.massfeller@gwv-media.de

AD SALES MANAGER
Sabine Röck
phone +49 611 7878-269 · fax +49 611 7878-78140
sabine.roeck@gwv-media.de

AD SALES
Frank Nagel
phone +49 611 7878-395 · fax +49 611 7878-78140
frank.nagel@gwv-media.de

DISPLAY AD MANAGER
Petra Steffen-Munsberg
tel +49 611 7878-164 · fax +49 611 7878-443
petra.steffen-munsberg@gwv-media.de

AD PRICES
Price List No. 53 (10/2009)

PRODUCTION I LAYOUT
Heiko Köllner
phone +49 611 7878-177 · fax +49 611 7878-78464
heiko.koellner@springer.com

SUBSCRIPTIONS
VVA-Zeitschriftenservice, Abt. D6 F6, MTZ
P. O. Box 77 77, 33310 Gütersloh, Germany
Renate Vies
phone +49 5241 80-1692 · fax +49 5241 80-9620
SpringerAutomotive@abo-service.info

YOUR HOTLINE TO MTZ
Editorial Staff
☎ +49 611 7878-393
Reader's Service
☎ +49 611 7878-151
Advertising
☎ +49 611 7878-395

SUBSCRIPTION CONDITIONS
The eMagazine appears 11 times a year at an annual subscription rate of 269 €. Special rate for students on proof of status in the form of current registration certificate 124 €. Special rate for VDI/ÖVK/VKS members on proof of status in the form of current member certificate 208 €. Special rate for studying VDI members on proof of status in the form of current registration and member certificate 89 €. The subscription can be cancelled in written form at any time with effect from the next available issue.

HINTS FOR AUTHORS
All manuscripts should be sent directly to the editors. By submitting photographs and drawings the sender releases the publishers from claims by third parties. Only works not yet published in Germany or abroad can generally be accepted for publication. The manuscripts must not be offered for publication to other journals simultaneously. In accepting the manuscript the publisher acquires the right to produce royalty-free offprints. The journal and all articles and figures are protected by copyright. Any utilisation beyond the strict limits of the copyright law without permission of the publisher is illegal. This applies particularly to duplications, translations, microfilming and storage and processing in electronic systems.

Springer Automotive Media is a brand of Springer Fachmedien. Springer Fachmedien is part of the specialist publishing group Springer Science+Business Media.

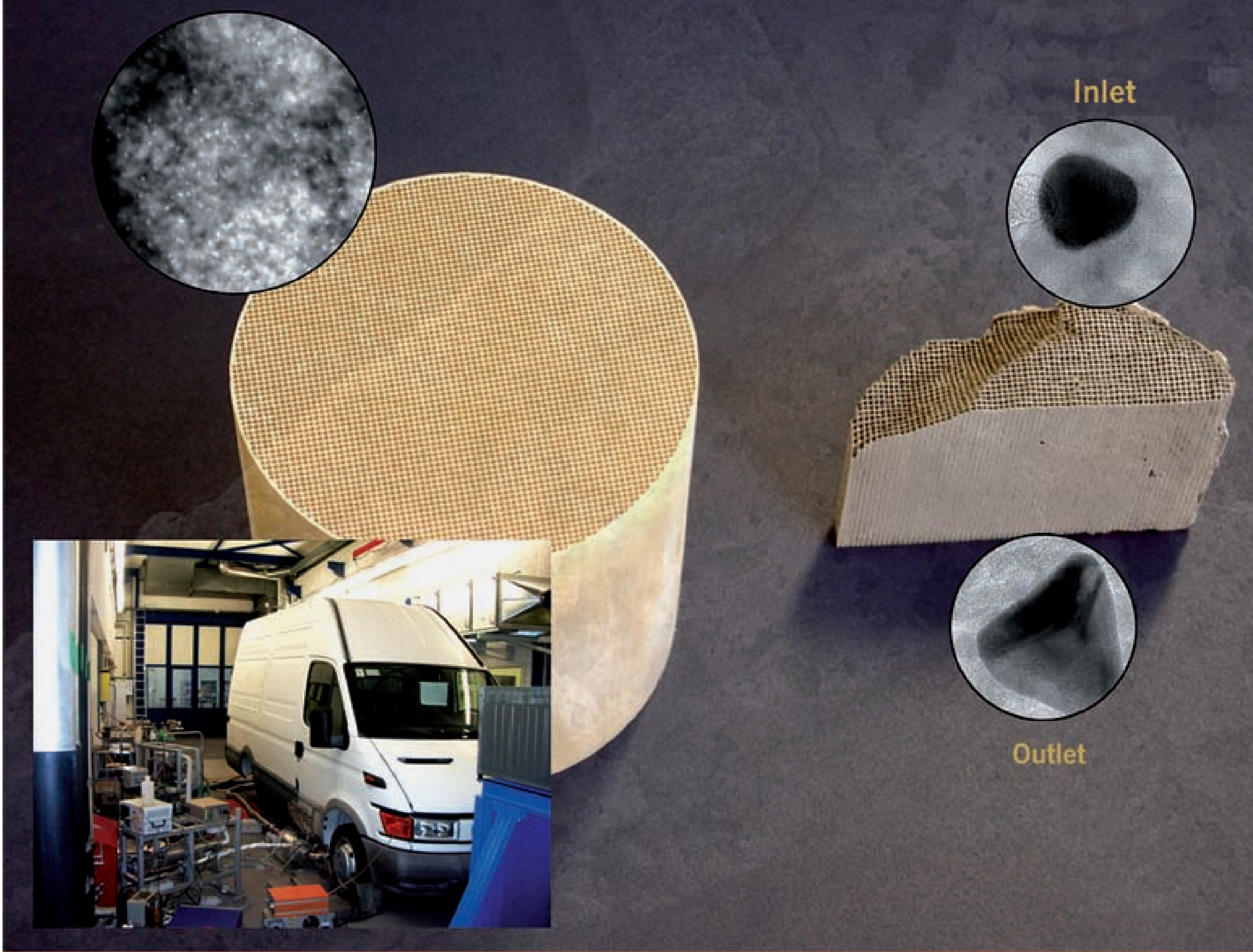

ANALYSIS TECHNIQUES FOR DIESEL OXIDATION CATALYST AGING PHENOMENA

Increasingly stringent emission regulations in combination with high durability demands for the exhaust aftertreatment systems require detailed knowledge of the related aging phenomena. In this paper by Empa, Swiss Federal Laboratories for Materials Testing and Research, contemporary analysis methods are implemented in order to demonstrate chemical and thermal aging on a Diesel Oxidation Catalyst (DOC).

AUTHORS

DR. RER. NAT. ALEXANDER WINKLER
leads the Catalyst Aging Project at Empa in Duebendorf (Switzerland).

DR. SC. NAT. DAVIDE FERRI
leads the Heterogeneous Catalysis Group at Empa in Duebendorf (Switzerland).

DR. SC. TECHN. ETH PANAYOTIS DIMOPOULOS EGGENSCHWILER
leads the Exhaust Aftertreatment Group at Empa in Duebendorf (Switzerland).

DR. RER. NAT. MYRIAM AGUIRRE
leads the Specialist Area Microanalysis at Empa in Duebendorf (Switzerland).

MOTIVATION

The upcoming Euro-6 emission legislation poses high demands on the performance and the long term durability of the exhaust aftertreatment systems of passenger cars and trucks. Especially the long term durability can be severely limited due to aging phenomena, ultimately resulting in not fulfilling the required emission limits. An additional problem, attributed to the increased complexity of exhaust aftertreatment systems, is the impact of aged components on other aftertreatment devices. The continuous passive regeneration of Diesel Particulate Filters (DPF), for example, requires high upstream NO_2 concentration. Therefore the oxidation of the engine-out NO has to occur in the upstream DOC. Increased DOC aging results in reduced NO_2 supply thus increasing active regeneration requirements. Active regeneration on the other hand occurs with the thermal assistance of the combustion of excess, deliberately generated hydrocarbons within the DOC, thus increasing its thermal load [1, 2].

DOC activity is restricted by chemical as well as thermal aging [3, 4, 5]. While the former can be traced to additives in the lubricating oil blocking the diffusion of the pollutant molecules to the active sites, the latter occurs with high thermal loads and results in the sintering of the catalytically active precious metal particles.

Results regarding different aging phenomena on a used DOC of a small truck are reported within this paper.

ANALYSIS METHODS

Scanning Electron Microscopy (SEM) provides micrographs of structural changes and deposits on the catalyst surface. In combination with Energy Dispersive X-ray (EDX) analysis element composition as well as associated spatial distributions can be determined.

With High Resolution Transmission Electron Microscopy (HR-TEM) structures at the nanometer scale (e.g. catalytically active platinum particles) can be resolved.

Contrast based imaging of heavy precious metals (Pt in this study) suspended in a matrix of lighter elements (here Al_2O_3) can be achieved by HAADF-STEM (High Angle Annular Dark Field – Scanning TEM). Both the precious metal distribution in the wash coat and the agglomeration advancement can be quantified.

X-ray Photoelectron Spectroscopy (XPS) enables the identification as well as quantification of elements on surfaces.

Diffuse Reflectance Infrared Fourier Transform Spectroscopy (DRIFTS) of carbon

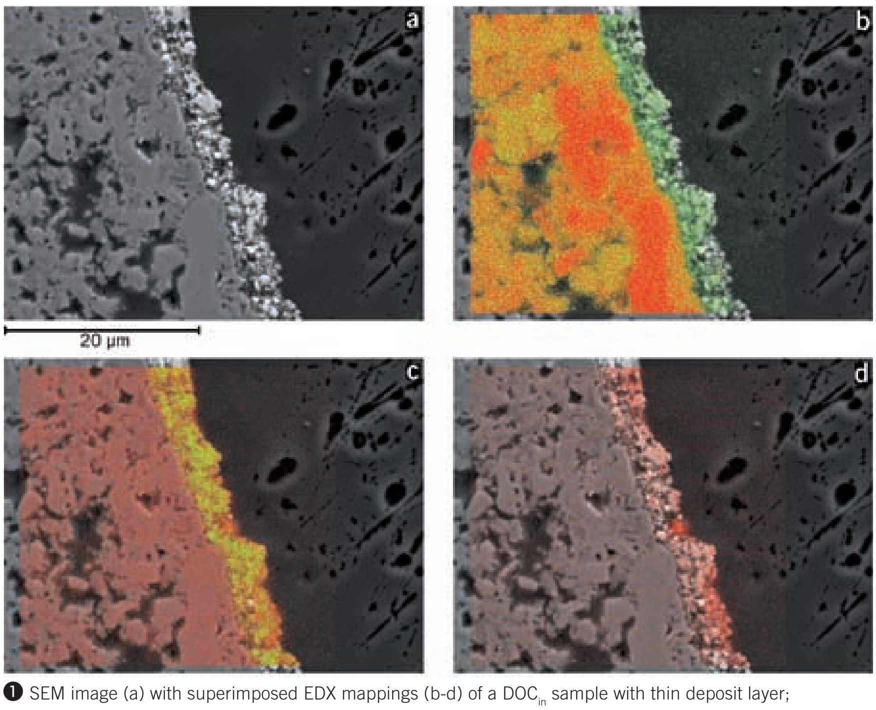

❶ SEM image (a) with superimposed EDX mappings (b-d) of a DOC_{in} sample with thin deposit layer; colour code: (b) red: Al, green: Si; (c) red: P, green: Zn; (d) red: Mg monoxide (CO) adsorption on Pt can be used to investigate the structure of the catalytically active platinum particles. The vibration frequency of CO strongly depends on the different Pt sites on which it adsorbs.

The oxidation state of Pt particles is decisive for their catalytic activity and can be determined using X-ray Absorption Near Edge Structure (XANES) spectroscopy. The height of the platinum absorption signal (whiteline) is determined for the sample and compared to reference materials like metallic Pt and PtO_2.

The catalytic activity of the DOC with regard to a certain exhaust gas species is determined in a plug flow reactor using precisely defined feed-gas compositions.

CHEMICAL AGING

The identification as well as the distribution of aging components were determined by SEM/EDX and is displayed in ❶. ① a shows the wash coat from the upstream gas entrance section (DOC_{in}) of the examined DOC. Clearly discernible is the wash coat (grey colour, on the left) as well as an approximately 5 µm thick deposit layer (light grey) on top of it. The right area of ① a shows a part of the empty catalyst channel. ① b to ① d show the distribution of different elements in the wash coat and/or the deposit layer. The coloured pigments inside the empty channel (right area in each image) originate from signal noise. In ① b, red corresponds to aluminium confirming the high Al content of the wash coat; no Al exists in the deposit layer. An additional wash coat component identified is Si, originating from SiO_2 or zeolites. Nevertheless Si has also been identified in the deposit layer, possibly originating from fuel based foaming inhibitors.

① c shows the distribution of phosphorus (P, red) and zinc (Zn, green); both ingredients of lube oil additives. While zinc was only identified in the deposit layer, phosphorus accumulates in the deposit layer as well in the wash coat. Yellow areas in ① c correspond to simultaneous Zn and P detection suggesting the formation of zinc phosphate species.

① d shows the distribution of magnesium, a further constituent of the lube oil additives, which contributes in form of e.g. magnesium phosphates to the deposit layer. Minor amounts of calcium have also

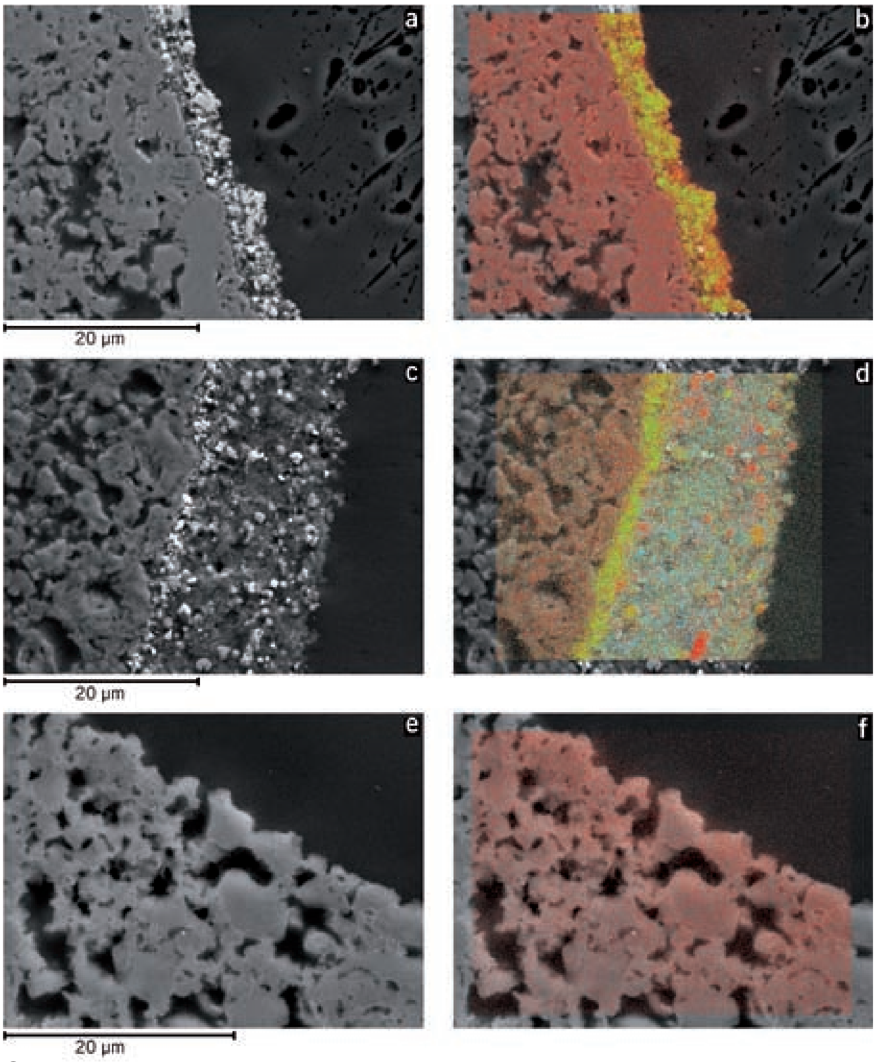

❷ SEM images (left) with superimposed EDX mappings (right) of a DOC_{in} sample with thin (a, b) and thick deposit layer (c, d) and of a DOC_{out} sample (e, f); colour code: (b) red: P, green: Zn; (d) red: P, green: Zn, blue: S; (f) red: P

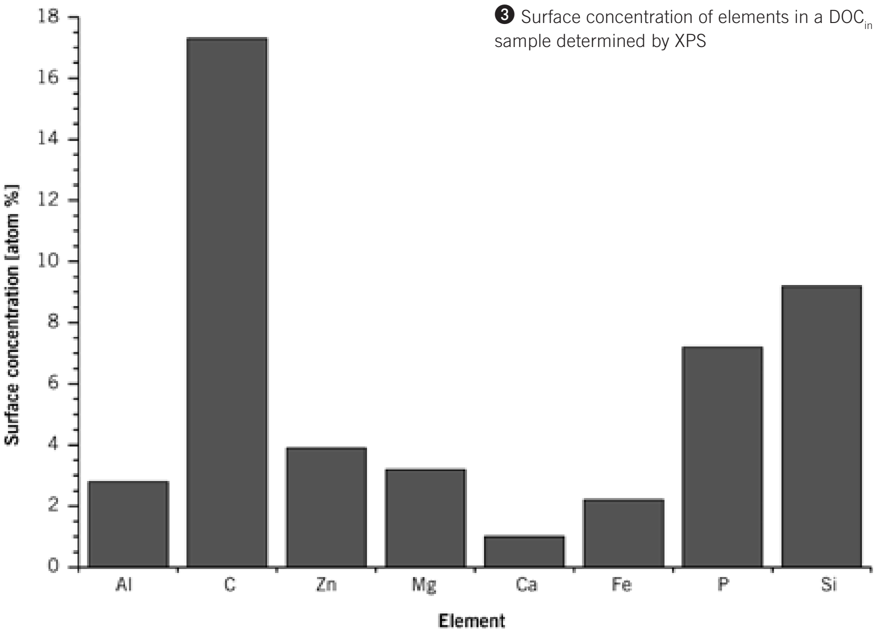

❸ Surface concentration of elements in a DOC_{in} sample determined by XPS been detected (not shown in ①). Phosphorus however is the only lube oil additive constituent with high diffusion into the wash coat. Zn, Mg and Ca only accumulate in the deposit layer.

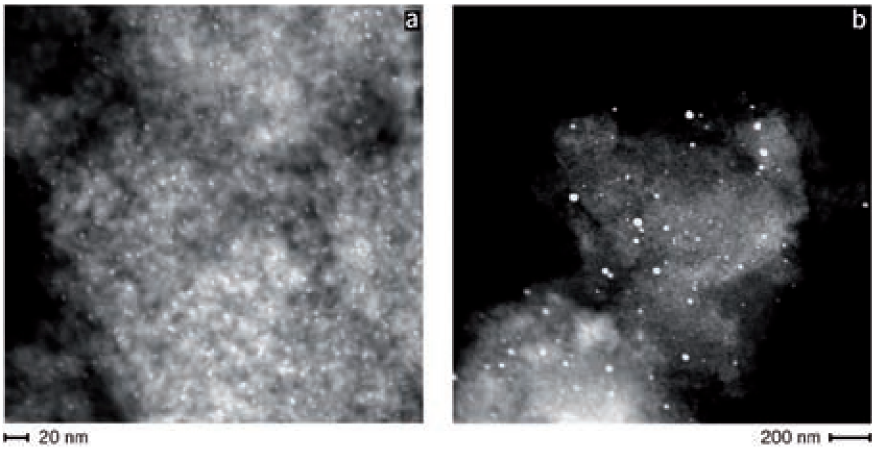

❹ HAADF-STEM wash coat images of a DOC_{new} (a) and DOC_{in} sample (b); white dots: Platinum particles

❷ displays SEM/EDX images from various locations of the aged DOC. ② a and ② c show two representative areas of DOC_{in}, while ② e shows a representative area of the DOC outlet (DOC_{out}). ② b, ② d and ② f display the corresponding EDX element mappings.

The SEM images in ② a and ② c show two characteristic structures of the deposit layer in DOC_{in}. The layer in ② c is approximately 15 µm thick and noticeably thicker than the 5 µm thick deposit layer in ② a. Two distinct areas can be identified in the deposit layer of ② c. The first 2 to 3 µm thick inner layer on top of the wash coat mainly consists of phosphorus (red) and zinc (green) compounds ② d. The composition of this inner layer is similar to the composition of the thin layer in ② b. The second substantially thicker layer (approximately 13 µm, ② c) mainly consists of sulphur (light blue, ② d) originating from the lube oil and the fuel. Sulphur could not be detected within the wash coat.

An SEM image of DOC_{out} is displayed in ② e. Interestingly no deposit layer could be identified. Phosphorus signal intensity in the wash coat is very similar to the noise intensity indicating very weak, if any, phosphorus deposition. Since no deposit layer could be observed in DOC_{out}, consequently no Zn, Mg, Ca, or S compounds could be identified. Thus, chemical aging is concentrated in the DOC_{in}.

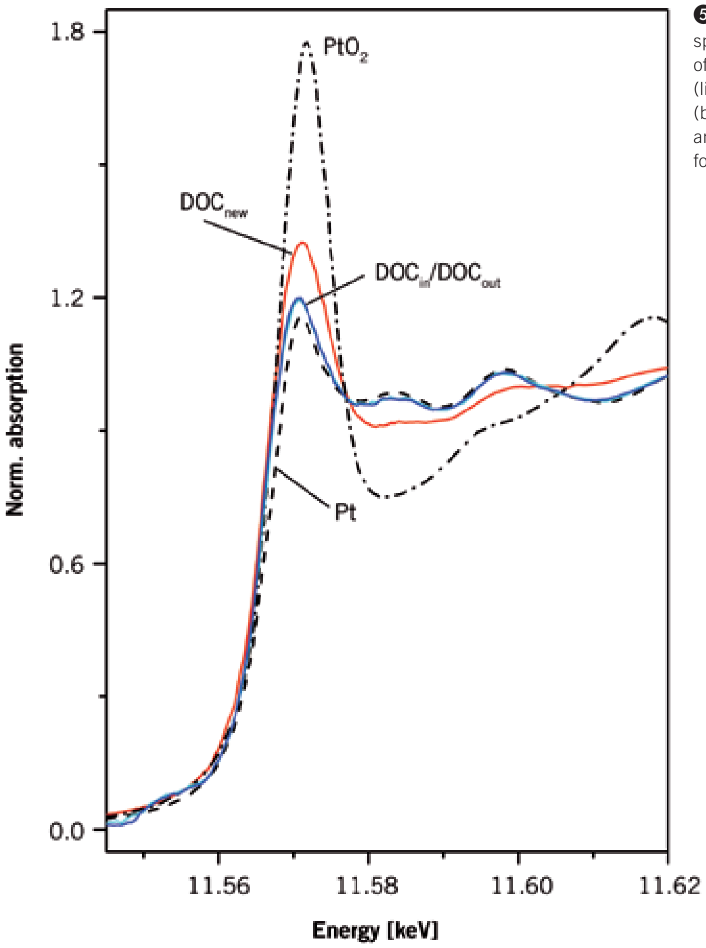

❺ Normalized XANES spectra (Pt L_{III} edge) of DOC_{new} (red), DOC_{in} (light blue) and DOC_{out} (blue); spectra of Pt and PtO_2 are shown for reference

XPS delivers quantitative information of the deposition elements in the first nanometres of the surface. ❸ exemplifies on a 100 µm analysis spot the quantitative element composition of DOC_{in}. Zinc, magnesium, phosphorus and calcium originate from lube oil additives. Ferrites originate from engine wear. In general, all XPS probes exposed to ambient air feature a carbon (C) signal originating from adsorbed airborne hydrocarbons. The resulting carbon signal intensity usually amounts to 6 to 9 atom %. The substantially higher values of approximately 17 atom % observed in these samples hint to soot deposition. Aluminium detection by the highly surface sensitive XPS demonstrates the irregular distribution of the deposit layer. Certain areas must be free of deposits for the wash coat based aluminium to be detected. High Si signal intensities originate from the wash coat as well as from deposits.

THERMAL AGING

Exhaust gas temperatures of diesels do not exceed 550 °C, at least upstream of the DOC. During phases of active DPF regeneration large amounts of unburned hydrocarbons are oxidized in the DOC.

Even then, the temperatures reached are not high enough to cause significant wash coat sintering. However, sintering of platinum particles can still be promoted. ❹ a shows HAADF-STEM images of the wash coat of a new DOC (DOC_{new}), while ④ b depicts the wash coat of the aged DOC. White points corresponding to the Pt particles have an average diameter of approximately 4 nm in the new DOC, ④ a. Pt particles in the aged DOC are approximately four times larger (average diameter of 20 nm). Isolated, significantly larger Pt particles have also been identified.

A further thermal induced effect is the alteration of the oxidation state of Pt in the aged DOC. This can be recognized from the whiteline of the XANES spectrum of the samples recorded at the Pt L_{III}-edge, ❺. The spectrum of DOC_{new} reflects the presence of both reduced and oxidized Pt. The attenuation of the whiteline from DOC_{new} to DOC_{in} (light blue)/DOC_{out} (blue) and the comparison with reference metallic Pt and oxidic PtO_2 reveal that the engine-aged DOC features metallic Pt as a result of particle growth.

COMBINED IMPACT OF CHEMICAL AND THERMAL AGING

❻ displays high resolution TEM images of individual Pt particles from DOC_{in}, ⑥ a, as well as DOC_{out}, ⑥ b, ⑥ c. For a direct comparison Pt particles of DOC_{new} are displayed in ⑥ d. The differences in morphology and size are striking. Pt particles of DOC_{in} are round and smaller than Pt particles of DOC_{out}, which, in addition, are polyhedric. Comparison of the DRIFTS spectra of adsorbed carbon monoxide (CO) on DOC_{in} and DOC_{out}, ❼, confirms the structural changes along the monolith. Adsorbed CO on even surfaces (blue signal, 2092 cm^{-1}) is significantly lower in DOC_{out} in comparison to the fraction of CO adsorbed on the edges (red, 2080 cm^{-1} and green, 2055 cm^{-1} signal in ⑦) of the Pt particles. This is in agreement with the morphological changes observed with the HR-TEM. While the sintering of the Pt particles is temperature induced, the morphological changes are determined by the environment. In the phosphorus abundant DOC_{in} Pt sintering leads to round particles. In DOC_{out} only negligible amounts of phosphorus were detected and sintering leads to the formation of polyhedric particles [6].

CATALYTIC ACTIVITY

The catalytic activity of all examined parts of the aged DOC is lower than the one of the new DOC, ❽ a only NO conversion is shown. A comparison of the catalytic activity of DOC_{in} and DOC_{out} shows no significant differences in NO, CO and HC conversion. A significant difference concerns the NO_2 selectivity, ⑧ b, of DOC_{in} and DOC_{out}. NO_2 formation begins at about 275 °C in all examined aged DOCs. Nevertheless, the NO_2 amounts formed in DOC_{out} are significantly larger than the amounts formed within DOC_{in}. The differences correlate with the different morphology of the Pt particles.

CONCLUSION

Chemical and thermal aging phenomena on DOCs have been characterised with a variety of analysis techniques. The spatial distribution as well as the elemental composition of deposits have been studied using SEM/EDX. On upstream parts of the DOC (DOC_{in}) two different types of deposit layers with different thickness and elemental composition were identified. Downstream parts of the DOC (DOC_{out}) were practically deposit free. Both types of deposit layers are consisting of lube oil and fuel additive based elements like Zn, Mg, Ca, S and P. Phosphorus was the only element identified inside the wash coat. Surface concentrations of the elements have been determined using XPS.

Thermal induced sintering of the catalytically active Pt particles has been identified using HAADF-STEM. While the average particle size in a new DOC was about 4 nm, the average Pt particle size was approximately 20 nm in the aged DOC. According to the HR-TEM images, the sintered Pt particles found within DOC_{in} had a round structure whereas the Pt particles found within DOC_{out} possessed a polyhedric structure.

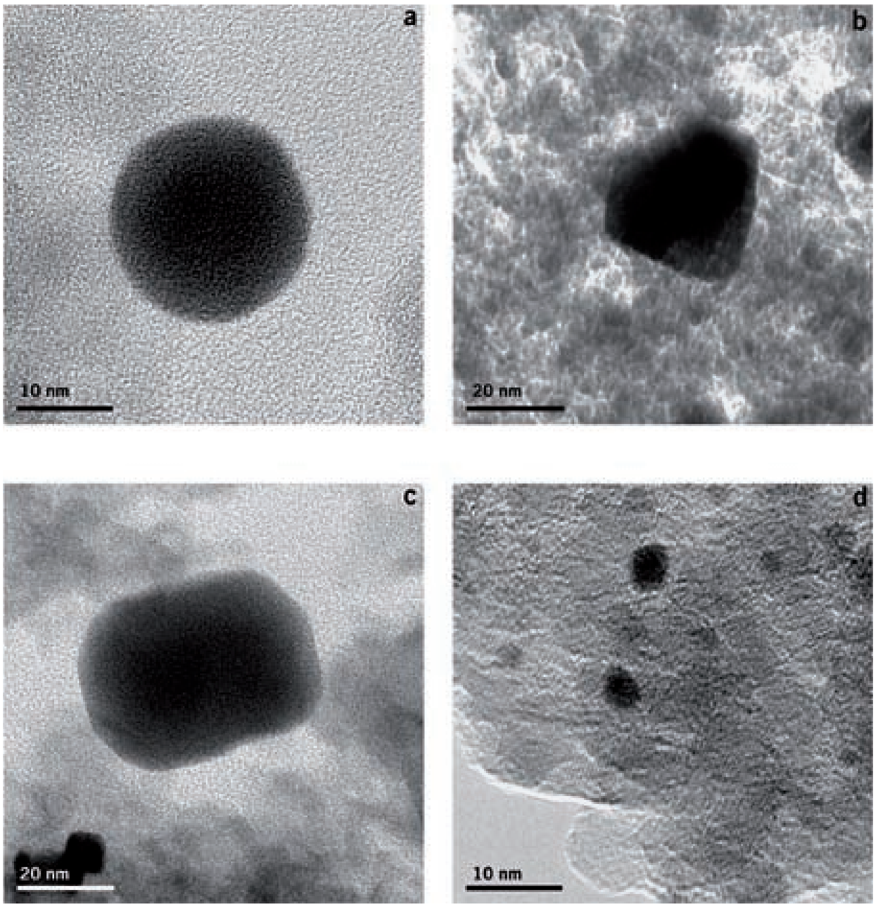

❻ HR-TEM images of Pt particles from DOC_{in} (a), DOC_{out} (b, c) and DOC_{new} (d)

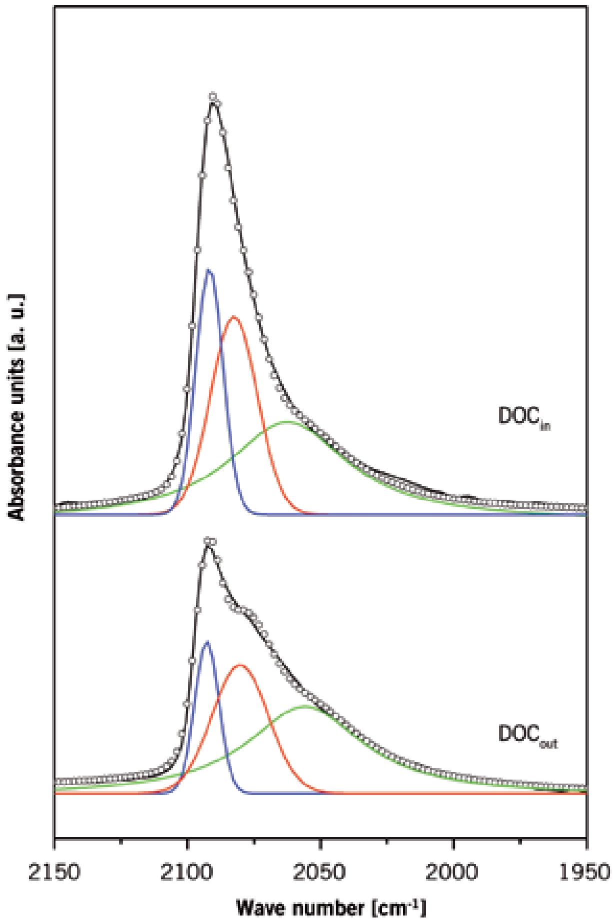

❼ DRIFTS spectra of adsorbed CO on Pt particles of DOC$_{in}$ (upper diagram) and DOC$_{out}$ (lower diagram) with corresponding signal deconvolution (blue, red, green) – the various signals represent Pt-CO species adsorbed on different Pt sites

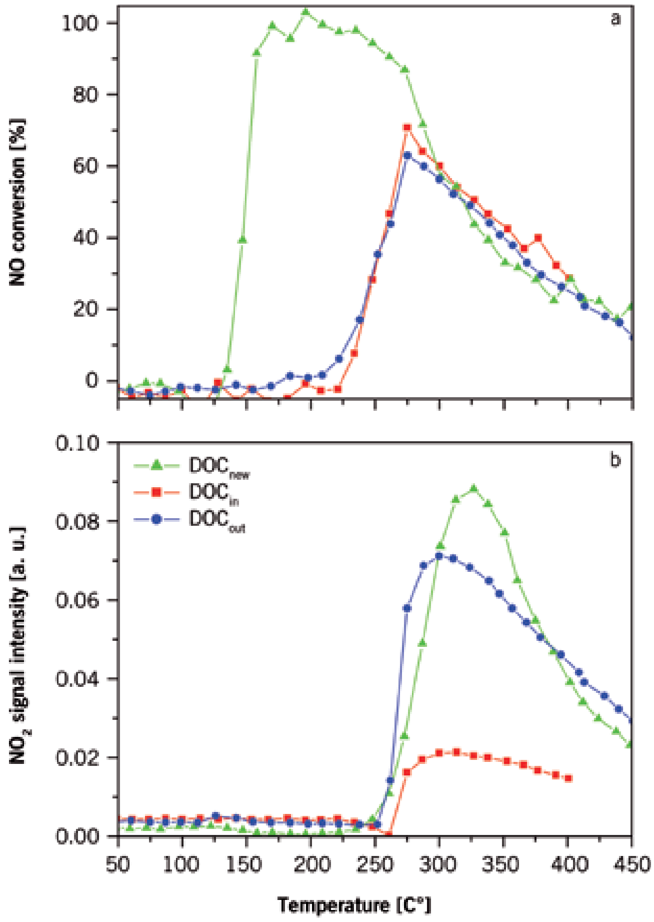

❽ NO conversion (a) and NO_2 formation (b) on DOC$_{new}$ (green), DOC$_{in}$ (red) and DOC$_{out}$ (blue) – model exhaust gas composition: 250 ppm NO, 1200 ppm propene, 300 ppm propane, 3000 ppm CO, 11 vol.% O2, 25 vol.% CO_2, balance N_2

DRIFTS measurements confirmed the different structures. The particle structure is correlated with the presence of phosphorous in the wash coat. Pt-P interactions result in round Pt agglomerates during sintering.

XANES measurements revealed that for DOC$_{new}$ platinum is present both in metallic as well as in oxidized form. In case of DOC$_{in}$ and DOC$_{out}$ platinum is almost exclusively present in metallic form.

Catalytic activity of DOC$_{in}$ and DOC$_{out}$ was investigated with a model exhaust gas. All samples showed almost identical activity with regard to HC and CO conversion. DOC$_{in}$ showed substantially lower NO_2 formation than DOC$_{out}$. This circumstance can be attributed to the differences in the structure of the platinum particles.

REFERENCES

[1] Nakane, T.; Ikeda, M.; Hori, M.; Bailey, O.; Mussmann, L.: Investigation of the aging behaviour of oxidation catalysts developed for active DPF regeneration systems. In: SAE Paper 2005-01-1759

[2] Twigg, M.V.: Roles of catalytic oxidation in control of vehicle exhaust emissions. In: Catal. Today 117 (2006), S. 407-418

[3] Lox, E.S.J. in: Ertl, G. et al. (Eds.): Handbook of heterogeneous catalysis – second, completely revised and enlarged edition. Weinheim: WILEY-VCH Verlag, 2008

[4] Neyestanaki, A.K.; Klingstedt, F.; Salmi, T.; Murzin, D.Y.: Deactivation of postcombustion catalysts, a review. In: Fuel 83 (2004), S. 395-408

[5] van Basshuysen, R.; Schaefer, F.: Handbuch Verbrennungsmotoren – 2. verbesserte Auflage. Braunschweig/Wiesbaden: Friedr. Vieweg & Sohn Verlagsgesellschaft mbH, 2002

[6] Winkler, A.; Ferri, D.; Aguirre, M.: The influence of chemical and thermal aging on the catalytic activity of a monolithic diesel oxidation catalyst. In: Appl. Catal. B: Environmental 93 (2009), S. 177-184

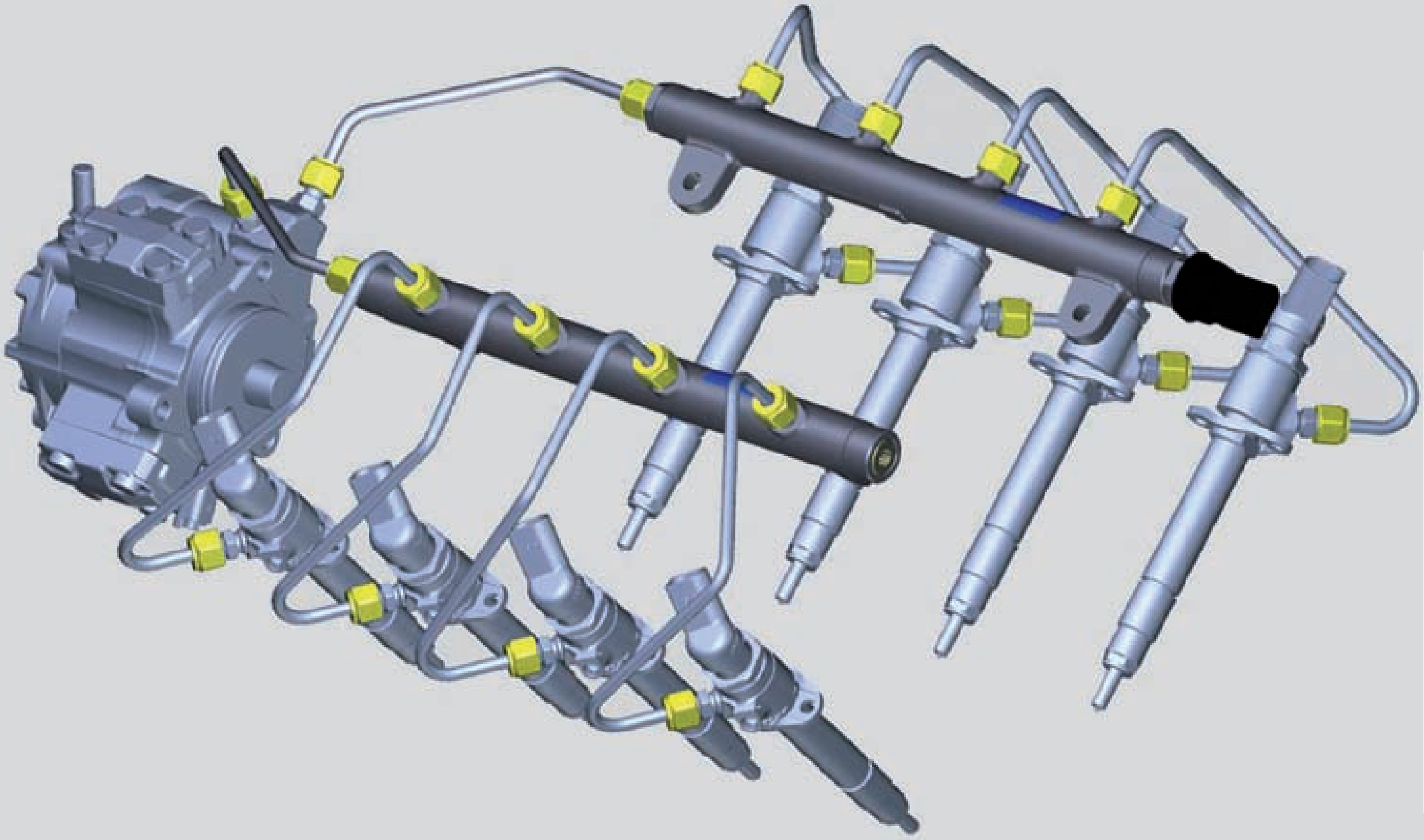

SIMULATION OF DIESEL COMMON RAIL INJECTION SYSTEMS

The Common Rail Diesel Injection Systems are complex systems with many influencing parameters. A major challenge is to meet the multiple injection quantity tolerances stringently. In order to optimize the cost, narrow tolerances must be avoided as much as possible. In this context, it is important to distinguish between important and unimportant parameters. The numerical simulation offers thereby decisive advantages which is proven in this article by University of Applied Sciences Regensburg and Continental.

AUTHORS

PROF. DR.-ING. FREDRIK BORCHSENIUS
works on the Development of Simulation Software at the University of Applied Sciences Regensburg (Germany).

DR.-ING. DANICA STEGEMANN
is System Simulation Expert at Continental, Division Powertrain, in Regensburg (Germany).

DIPL.-MATH. (FH) XAVER GEBHARDT
is Pump Simulation Expert at Continental, Division Powertrain, in Regensburg (Germany).

M. SC. JIGNESH JAGANI
is Injector Simulation Expert at Continental, Division Powertrain, in Regensburg (Germany).

DR.-ING. ANATOLIY LYUBAR
is Computer Modelling Expert at Continental, Division Powertrain, in Regensburg (Germany).

Simulation has become essential in the development of complex products. During the quotation, simulation helps to ensure feasibility. Subsequently, the simulation accompanies development, particularly in the early sample phases, and gives impetus to the adjustment of the most influencing parameters to ensure the functioning and adherence to specified limits. Advantages of the simulation are:

: early evaluation of a concept
: better understanding of the functionality, by separation of influencing parameters.

The simulation works as a "mathematical loupe" with which the innermost physical relationships can be illuminated, especially the areas which are not accessible with measurement techniques. The sound understanding of the physical connections is a prerequisite for the goal-oriented development.

However, in practice the potential of the simulation is restricted by

: high computation time, especially for large models
: restriction of the available licenses.

Due to these problems, at Continental, in addition to commercial programs, a free simulation software HSSIM (Hydraulic System Simulation) is also used. With this program, the problem of time consuming computation is solved. For example, simulations of the complete fuel injection systems, as well as optimization of Piezo Common Rail Injectors with the help of genetic algorithms.

THE COMPUTATIONAL PROGRAM HSSIM

HSSIM is a new development on the basis of the program HYSIM, which was developed at the Technical University of Munich [1]. HSSIM consists of a solver and a graphical user interface. While developing the solver, the main objective was the realization of low computation time even for large systems. For this purpose, the core is written in C + +. The graphical user interface is developed in JAVA and storage of all data in XML file. The user interface supports hierarchical models, so that complex systems can be clearly composed by subsystems, thus partial models (e.g. injector) are also used in other simulation models.

MATLAB interface is available for the parameter variations. It makes possible to

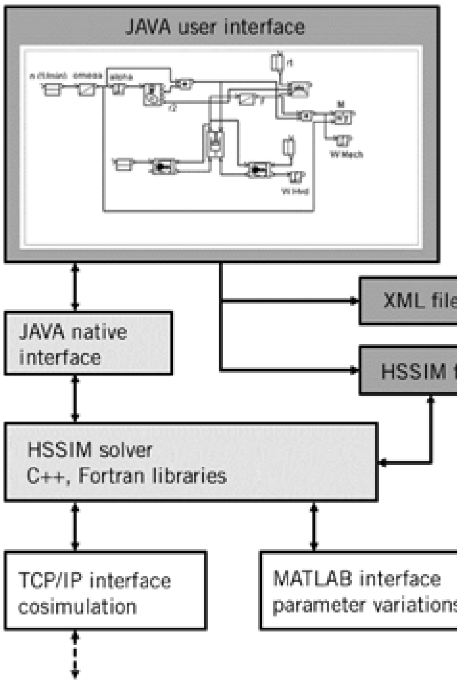

❶ Computational Program HSSIM

run algorithms such as optimization methods, where control of simulation is implemented in MATLAB. TCP/IP interface is available for the Co-simulation of HSSIM with other programs. For example, coupled simulations (HSSIM with Fluent) are carried out to optimize the dynamics of pump valves. ❶ shows the program structure schematically. HSSIM runs under Windows and Linux.

PIEZO COMMON RAIL INJECTOR PCR2

❷ shows the working principle of 2nd Generation Piezo Common Rail Injector of Continental and a corresponding HSSIM model. The opening and closing of the injector occurs via a hydraulic servo system with a Piezo actuator, [2].

The HSSIM model consists of basic electrical, mechanical and hydraulic components. The triggering of the Piezo actuator is carried by a power amplifier model. Due to the dynamic control, the mass and elasticity of all the moving parts are taken into account. The parameters (mass and stiffness) are obtained from FEM simulations. Hydraulic components are validated with 3D-CFD simulations, such as flow rate and flow forces on the nozzle needle. An injector is described by approximately 60 coupled differential equations.

❸ shows the comparison of measured and simulated injection quantity characteristics for low, medium and high rail pressure.

The characteristic of PCR2-Injectors is to be improved with the help of numerical optimization. Due to nonlinearities, classical optimization methods are ruled out, since they do not find global optimum. Genetic algorithms are able to identify a global optimum, but only with a high cost of computation.

The idea of genetic algorithms is to fit a “injector-population” via successive selection, inheritance and mutation. The good injectors with high probability and bad injectors with low probability are selected. This selection prevents sticking of the optimization algorithm in a local minimum [3].

The quality of an Injector is described by the evenness of the injection quantity characteristic. The smoother the curves, the lower the sensitivity to parameter variations.

With the help of genetic algorithm, the injection quantity characteristic of PCR2-Injector was smoothed, ❹. Thereby ten parameters were varied. For the optimization of the curves 540,000 simulations were necessary. A simulation takes about 1 s, the entire cycle on a computer takes about six days.

In Linux, the simulations can be distributed over multiple processors. With 18 processors, the time is reduced to less than nine hours (overnight).

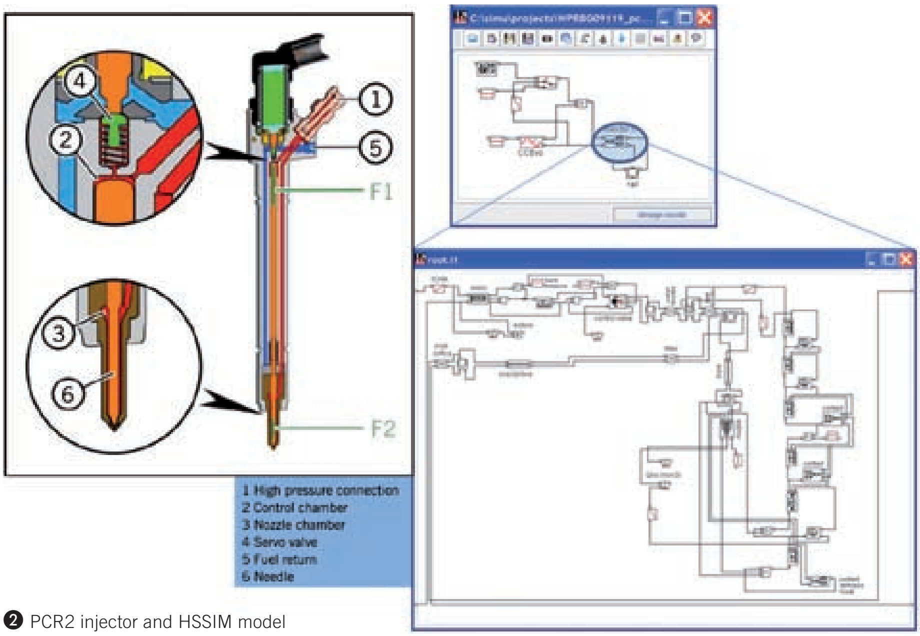

❷ PCR2 injector and HSSIM model

COMMON RAIL V8 SYSTEM

In this section, a HSSIM simulation model for the 8-cylinder system is described with a simulation example.

The model is hierarchical and mainly consists of components

- common rail pump with three pistons and flow control valve
- eight PCR2 injectors at two rails
- power stage (ECU)
- pressure control.

❺ shows the top level of the HSSIM model. The model is described by approximately 600 differential equations.

The pressure is built by a 3-piston high pressure pump with flow rate control. The rail pressure is constantly being compared with the set-point and adjusted by a PI controller. The controller output is connected to the flow control valve of the pump.

The pump model includes high pressure cylinders with inlet and outlet valves. The valve models are also designed with CFD simulations.

The pump has two high pressure ports, connected to the two rails. The pipes connecting the Pump-Rail and Injector pipes are FEM models, to realize the effect of pressure waves. For the damping of pressure waves, orifice at the Rail outlet can be considered. At each Rail, 4 complete Injector Models are connected. The injectors are triggered via power stage models (ECU), which are available for each bank.

The following example is used to estimate the influence of pre and post injections on the injection quantity of other injector. With late post-injection, it comes almost simultaneous to pre-injection of another injector. If the injectors are on the same bank, then reciprocal influence of the injection quantities are expected. In order to quantify this effect, the injection quantities of complete system are calculated and compared with the individual Injector simulations. The individual Injector simulation considers pressure waves that lead to quantity deviations for the multiple injections, but not the interaction with other injectors.

The entire injection system consisting of a pump, ten pipes, two rails and eight PCR2 injectors with electronic control units can be simulated within a few hours. As an operating point, a triple injection (Pre, Main and Post injection) at maximum pressure is selected.

The fire order contains two successive injections on the same bank (rail). All other injections are alternating between the banks. In the simulation model, the two successive injectors on one bank are called injector 1 and injector 2. The pres-

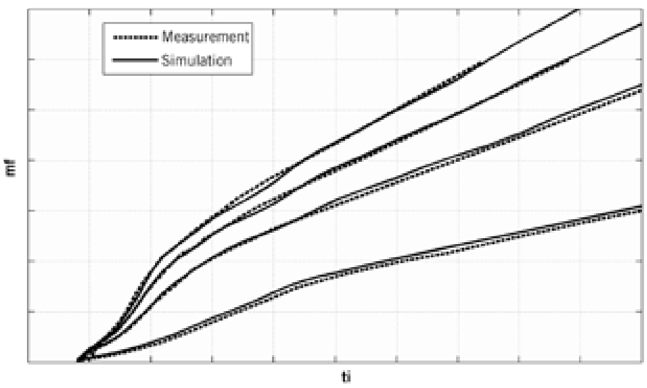

❸ Injection quantity characteristic for low, medium, high rail pressure

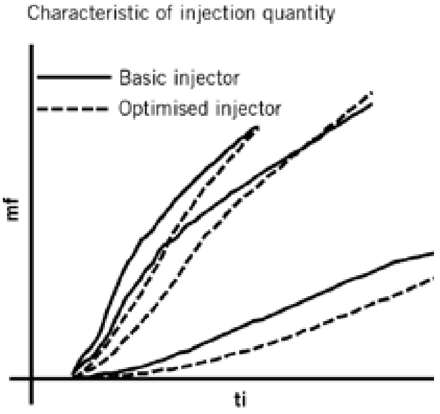

❹ Optimized injection quantity characteristic

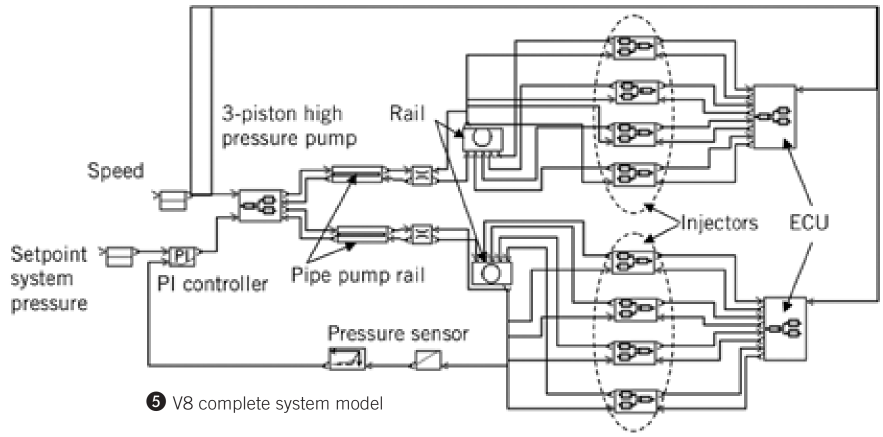

❺ V8 complete system model

sure waves induced by injector 1 influence the injection of injector 2. The resulting mass deviations shall be calculated. The available quantity correction function is not taken into account.

In order to cover different operating conditions, the start of the third injection is varied.

❻ shows the chronological variation of the post injection in eight stages. The point of the pilot injection and main injection are defined. The stability of the pilot injection in the complete system is determined by varying the post injection.

In ❼ the results of single injector simulation and the results of complete system simulation are compared. It is clearly visible that one can compare deviation of post-injection quantities with each other. This itself justifies the high influence of the main injection on subsequent injections. Since the main injection leads to the largest pressure drop, it has the greatest influence. The following post injection is mainly influenced by the main injection. This effect is nearly the same for all injectors.

The pre injection quantity in the single injector simulation model is not disturbed by any previous injection. Therefore the quantity for all injections is equal. Here it is clear that the complete system is required for the investigation of quantity deviations of pre-injection. Injector 1 shows, in comparison to the injector 2, a different behavior in injection quantities deviation. The pilot injection quantity from injector 1 differs through the predominant pressure waves in the Injector pipes and Rail. These pressure conditions are caused by the pump and from previous injections. The pre-injection by injector 1 is hardly affected by the injections on the other bank, just before Injector 1. The behavior is different at injector 2, where the pre-injection is directly influenced by the injection of Injector 1, because both the injectors are on the same bank.

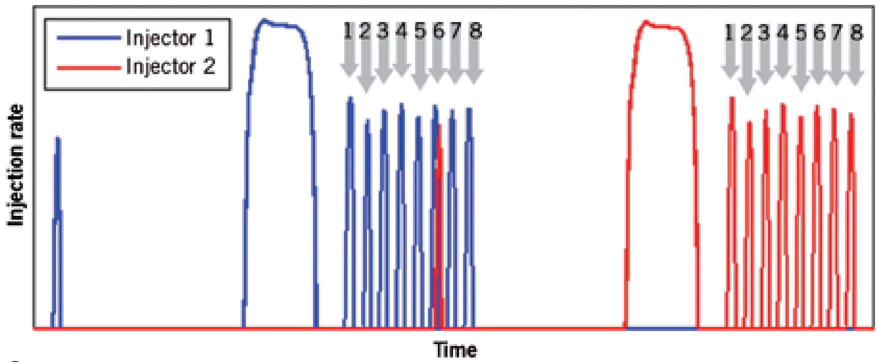

❻ Timing variation of post-injection (without injection quantity correction function)

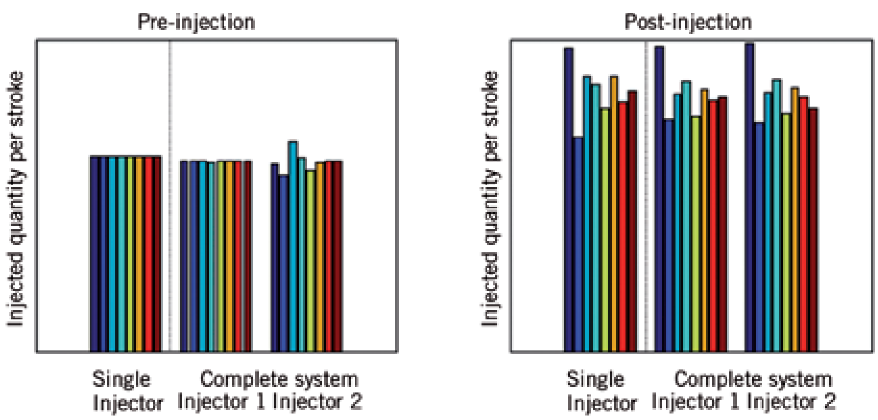

❼ Injection quantity deviation due to variation of post-injection

CONCLUSION

The computational program HSSIM is an alternative for commercially available injection system simulation programs, which is especially advantageous for computing time consuming simulations.

REFERENCES

[1] Pfeiffer, F.; Borchsenius, F.: New Hydraulic System Modelling. In: Journal of Vibration and Control, 10: 1493.1515, Sage Publications 2004

[2] Egger, K.; Warga, J.; Klügl, W.: Neues Common-Rail-Einspritzsystem mit Piezo-Aktorik für Pkw-Dieselmotoren. In: MTZ 9/2002 Jahrgang 63

[3] Gebhardt, X.: Optimierung der Dynamik eines Piezo-Injektors mit Hilfe von numerischer Simulation und mathematischen Optimierungsalgorithmen. Diplomarbeit Hochschule Regensburg, 2008

PEER REVIEW ATZ | MTZ

PEER REVIEW PROCESS FOR RESEARCH ARTICLES IN ATZ AND MTZ

STEERING COMMITTEE

ADVISORY BOARD

Scientific articles of universities in ATZ Automobiltechnische Zeitschrift and MTZ Motortechnische Zeitschrift are subject to a proofing method, the so-called peer review process. Articles accepted by the editors are reviewed by experts from research and industry before publication. For the reader, the peer review process further enhances the quality of the magazines' content on a national and international level. For authors in the institutes, it provides a scientifically recognised publication platform.

Therefore, since the No. 4 issues of 2008, ATZ and MTZ have the status of refereed publications. The German association "WKM Wissenschaftliche Gesellschaft für Kraftfahrzeug- und Motorentechnik" supports the editors in the introduction and execution of the peer review process. The WKM has also applied to the German Research Foundation (DFG) for the magazines to be included in the "Impact Factor" (IF) list.

In the ATZ | MTZ Peer Review Process, once the editors has received an article, it is reviewed by two experts from the Advisory Board. If these experts do not reach a unanimous agreement, a member of the Steering Committee acts as an arbitrator. Following the experts' recommended corrections and subsequent editing by the author, the article is accepted.

THE SEAL OF APPROVAL FOR SCIENTIFIC ARTICLES IN MTZ.
MTZ PEER REVIEW
REVIEWED BY EXPERTS FROM RESEARCH AND INDUSTRY.

AUTHORS

DR.-ING. JOHANNES SCHICKER
is Scientist in the Group Modeling and Simulation of Division V.2 at the Federal Institute for Material Research and Testing (BAM) in Berlin (Germany).

DR.-ING. RAINER SIEVERT
is Scientist in the Group Modeling and Simulation of Division V.2 at the Federal Institute for Material Research and Testing (BAM) in Berlin (Germany).

DR.-ING. BERNARD FEDELICH
is Head of the Working Group Modeling and Simulation of Division V.2 at the Federal Institute for Material Research and Testing (BAM) in Berlin (Germany).

DR.-ING. HELLMUTH KLINGELHÖFFER
is Head of the Working Group Mechanical Behaviour of Metals at the Federal Institute for Material Research and Testing (BAM) in Berlin (Germany).

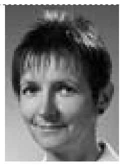

PRIV.-DOZ. DR.-ING. BIRGIT SKROTZKI
is Head of Division V.2 at the Federal Institute for Material Research and Testing (BAM) in Berlin (Germany).

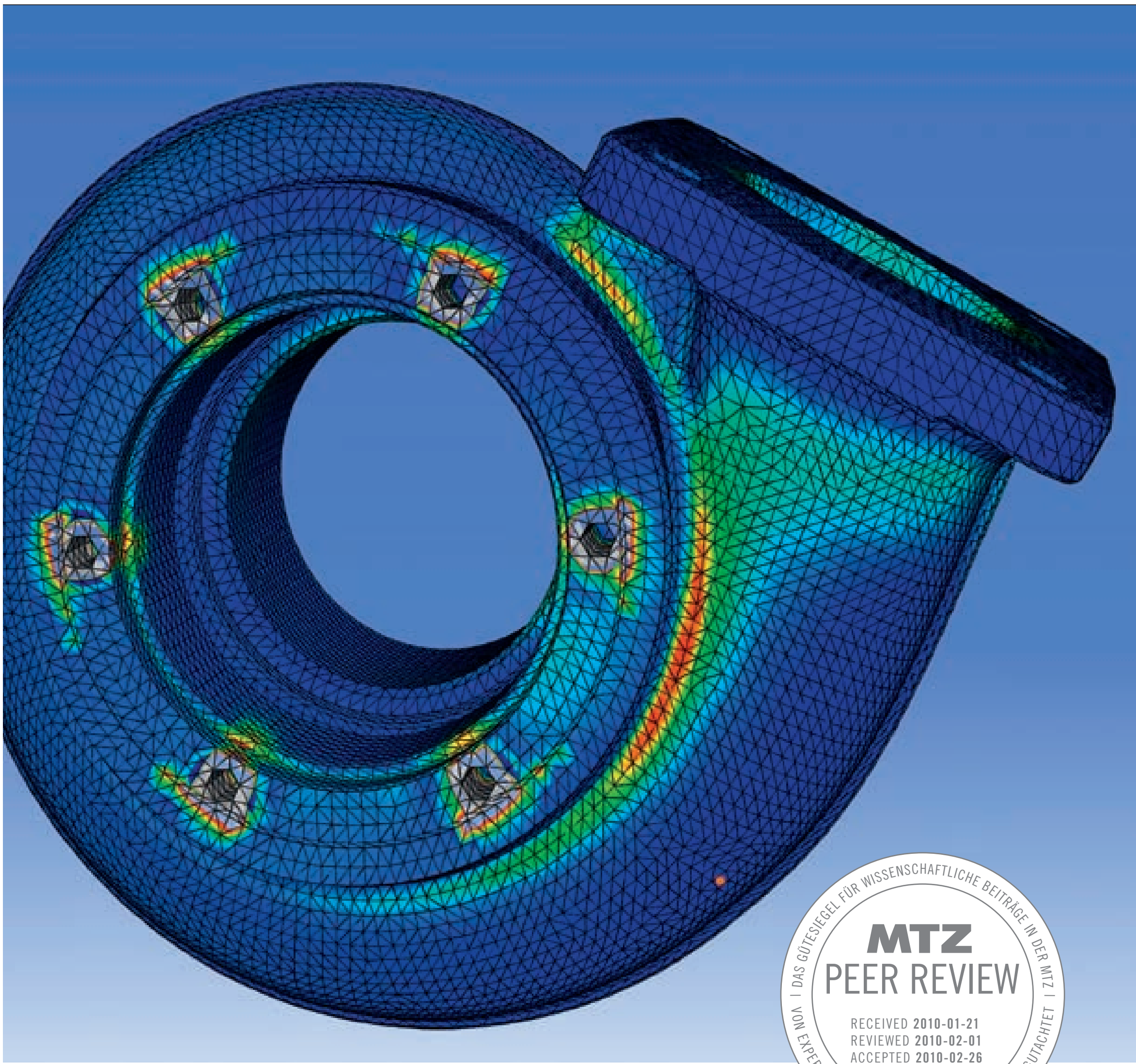

DAS GÜTESIEGEL FÜR WISSENSCHAFTLICHE BEITRÄGE IN DER MTZ | VON EXPERTEN AUS FORSCHUNG UND INDUSTRIE BEGUTACHTET

MTZ PEER REVIEW

RECEIVED 2010-01-21
REVIEWED 2010-02-01
ACCEPTED 2010-02-26

FAILURE ESTIMATION OF THERMO-MECHANICALLY LOADED HOT PARTS IN TURBOCHARGERS

Components directly exposed to the exhaust-gas streams of combustion engines are increasingly thermo-mechanically loaded. A keystone for dimensioning is the calculated failure prediction. Within the FVV research project No. 916 ("Hot Parts"), a model for the calculated simulation of thermo-mechanical fatigue was developed for the cast iron material SiMo 4.05 in the division Mechanical Behaviour of Materials at the Federal Institute for Material Research and Testing (BAM). Using this model, the location and the time of the occurrence of first cracks in exhaust-gas turbocharger housings may be estimated in good approximation.

1 INTRODUCTION

Due to decreasing engine displacement, casings of exhaust-gas turbochargers and other components, which are directly exposed to exhaust-gas streams of combustion engines, are subjected to increasing thermal and mechanical loadings. The gas temperature at the entry point of the turbine reaches today up to 970 °C. Thereby, the temperature difference inside a unit may be up to 800 K in the stationary phase. During the next years the gas inlet temperature shall increase up to 1050 °C [1].

Dimensioning of such parts is mostly still performed by empirical methods amended by calculations using finite elements and an elastic or elastic-plastic material law. Though the locations of high loading may be reasonably determined in doing so, the life time may only insufficiently be estimated. It ends with the initiation of cracks as a result of the interaction of superposed temporally shifting thermal and mechanical loads. Already shortly after their first forming, cracks grow through the wall of the casing leading to leakage. To estimate when the first critical cracks develop in casings of exhaust-gas turbochargers as a result of such loadings, a model for calculation was developed. It was calibrated using the frequently applied cast iron material EN GJS XSiMo 4.05. The model was then verified for a casing of an exhaust-gas turbocharger under near reality test conditions.

2 MATERIAL CHARACTERISATION

Next to the testing program consisting of tensile, relaxation, life cycle fatigue (LCF) and thermo-mechanical fatigue (TMF) tests for determining the parameters of the deformation and damage models, the accomplished investigation of the material also included metallographic and microscopic investigations prior to and after crack development. Furthermore, thermal-physical properties of the material were identified, such as the coefficient of thermal expansion, the density, the conductivities of temperature and heat and the specific heat. Also, the Young's and shear moduli were determined as functions of temperature and the transversal contraction was calculated.

The tests to determine the model parameters were performed using machined round specimens. Tensile tests at room temperature, relaxation and LCF tests at various temperatures ranging between room temperature and 800 °C and TMF tests were carried out. The latter focused on 180° out of phase loading, since this represents the typical cycle for heating of a component under constrained strain condition. Furthermore, this represents the most damaging loading case for the surveyed material.

Relaxation tests were loaded under strain control up to 2 % elongation, arrested at this strain for up to 200 h while measuring the resulting stresses. Isothermal LCF tests were carried out under stain control, partially with hold time in compression for 180 s. The number of cycles to failure was defined at 20 % load drop in the tensile regime. TMF tests were carried out with temperature rates of 5 K/s using variations of temperature in the scope from 300 to 800 °C. The loading was imposed with a strain ratio of R = -1 and the loading was imposed 180°-out-of-phase with constant strain rate and hold times of 180 s at maximum temperature.

Life time investigations for calibrating the material model parameters were basically performed with specimens with the casting skin removed due to machining. Components, however, were not refinished after casting for cost and manufacturing reasons, that means their casting skin remains on the surface. Therefore, the question whether and to which amount cracks develop earlier in casting skins than in refinished surfaces is essential to predict product life of components. Therefore, a testing configuration was chosen in which the effect of casting skin can be investigated on specimens. A four-point bending test turned out to be applicable. Test pieces with rectangular cross sections were used and the casting skin was preserved on the tensile side for some of the specimens. The test results showed that specimens without casting skin endured about 4 to 5 times as many bending cycles until failure compared to specimens with casting skin. An explanation for the earlier failure of the specimens with casting skin could be found in the surface layer of the casting skin, which dif-

A) MECHANICAL ITEMS AND OTHER VARIABLES	
ε_{in}, $\dot{\varepsilon}_{in}$	inelastic strain tensor, tensor of the inelastic strain rate
p, $\dot{p}$	accumulated inelastic equivalent strain, inelastic equivalent strain rate
$\dot{p}_0$	scaling constant
σ, σ'	stress tensor, deviator of the stress tensor
$\mathbf{X}$, $\mathbf{X}_1$, $\mathbf{X}_2$	tensor of the inner back stress, components
X_{eq}	equivalent back stress
r, $\dot{r}$	dimensionless variable to calculate isotropic hardening, its rate
α_i, $\dot{\alpha}_i$, i = 1,2	kinematic hardening tensors, their rates
D, $\dot{D}$, ΔD	damage variable, 0 ≤ D ≤ 1, damage rate, damage increase damage variable, 0 ≤ D ≤ 1, damage rate, damage increase
$T(\sigma_{max})$	temperature at maximum stress
B) MATERIAL SPECIFIC PARAMETERS	
k	initial yield strength
R	increase of yield strength due to isotropic hardening
K	viscosity coefficient
n	flow exponent
Q, b, f, q	material specific parameters to describe isotropic hardening
a_i, c_i, d_i, m_i mit i = 1, 2	material specific parameters to describe kinematic hardening
A, m_l, n_l	material specific parameters of damage development
$E(T)$	temperature related Young's modulus
C) OTHER FORMULA SYMBOLS	
N_f, N_f^{exp}, N_f^{sim}, N_f^{SWT}	cycles of failure, experimentally determined, determined by simulation, by SWT estimation

❶ Explanation of used formula symbols

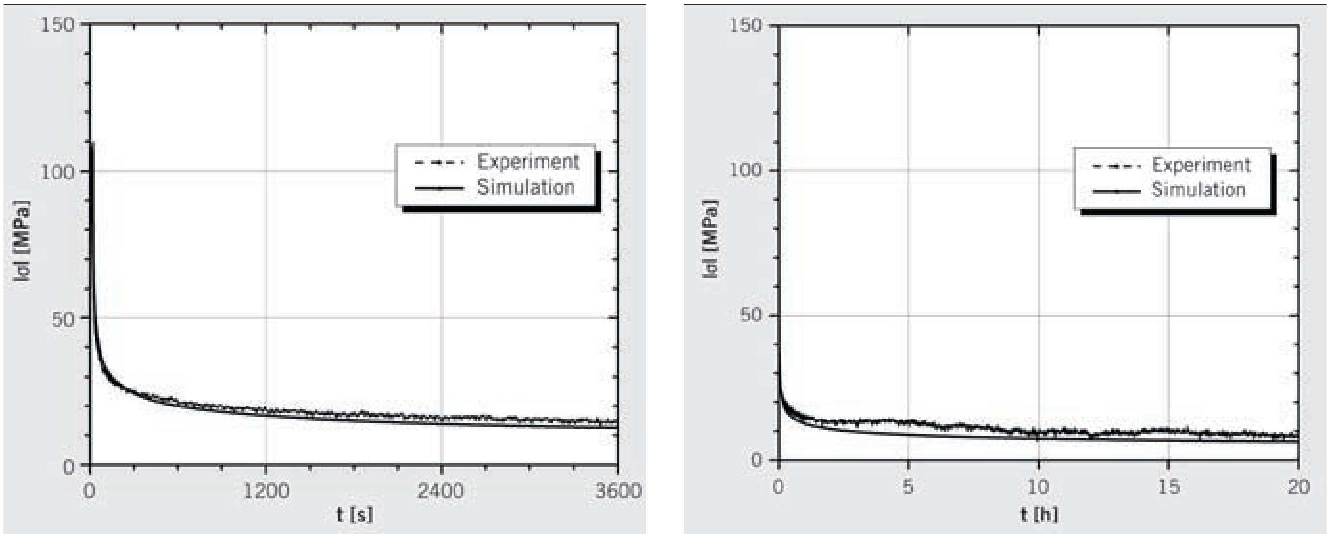

❷ Stress relaxation at 700 °C (comparison of experiment and simulation after 1 h (left) and 20 h (right))

fers from the homogeneous base material. In this layer the graphite pebbles of the base material are missing. Instead, the graphite appears as lamellae which can lead little cracks into the inner structure.

3 MODEL

The model consists of two components. In a first step a model is formulated to describe high temperature deformation behaviour under complex multiaxial thermo-mechanical loading. In a second step an incremental local damage rule is developed, which gathers the life time consumption resulting from the loadings at the corresponding location. By integration over the time the accumulated damage can be determined and thus the time span until a critical damage occurs may be estimated.

The critical region of a structure is finally obtained by comparing the damage values of all locations of the structure. The damage rule and the deformation model are implemented into a so called material routine of a finite element program. The routine is used to calculate the strains and stresses at an integration point as a result from external loadings.

A variant of the model of Chaboche [2] was used to describe the stress and strain behaviour. This model was developed for high temperature behaviour of metals, and, next to the phenomena of cyclic plasticity, that means the dependency of the deformation rate from the level of the stresses, it is able to describe stress relaxation during strain controlled arrests as well as creep. The underlying equations of the model partly represent evolution equations of inner variables. So, the inelastic deformation rate results from the flow rule:

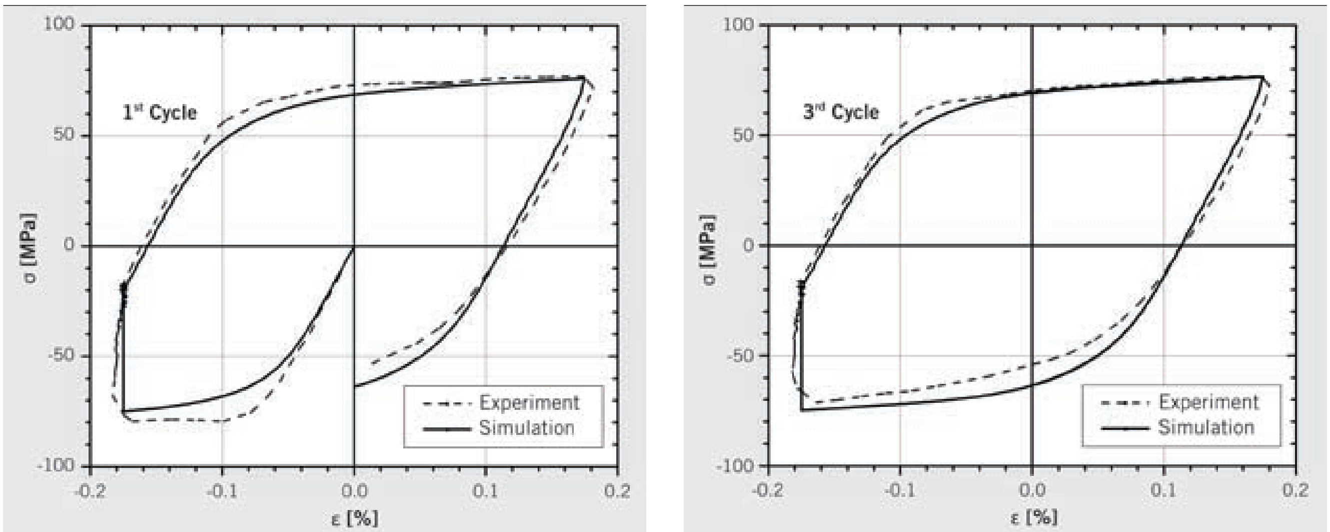

❸ Hysteresis of the first (left) and a saturated cycle 3 (right) of a strain controlled LCF test at 700 °C with 180 s hold in compression (comparison of experiment and simulation)

EQ. 1	$\dot{\varepsilon}_{in} = \frac{3}{2}\left\langle \frac{J_2(\sigma' - \mathbf{X}) - (k + R)}{K} \right\rangle^n \frac{\sigma' - \mathbf{X}}{J_2(\sigma' - \mathbf{X})}$

Plastic flow occurs only when the yield surface is exceeded, that means if the term in angular brackets is greater than zero. The initial yield stress k, the increase of the yield stress as a result of hardening R, the flow exponent n, and the viscosity coefficient K are material parameters, ❶. The direction of flow is determined by the deviation of the stress deviator σ' from the inner back stress **X**. The function J_2 is defined as:

EQ. 2	$J_2(\mathbf{A}) = \sqrt{\frac{3}{2}}\,\|\mathbf{A}\|$

The isotropic increase of the flow resistance R is formed using a dimensionless variable r:

EQ. 3	$R = Q(T)r,\ 0 \leq r \leq 1$

for which again an evolution equation is used:

EQ. 4	$\dot{r} = b(1\text{-}r)\,\dot{p} - f\,r^q,\ r(t = 0) = 0$

The variable R specifies isotropic widening of the elastic domain, whereas the back stress **X** in Eq. 1 corresponds to the centre of this domain in the space of the stress deviator. To capture the different gradients within one hysteresis more precisely, **X** is split into two components:

EQ. 5	$\mathbf{X} = \mathbf{X}_1 + \mathbf{X}_2 \text{ mit } \mathbf{X}_i = \frac{2}{3}\,a_i\,\alpha_i,\ i = 1{,}2$

Each of them consists of a material specific parameter a_i with the dimension of a stress and a dimensionless tensor valued inner variable α_i. The latter depends on an evolution equation for its rates $\dot{\alpha}_i$:

EQ. 6	$\dot{\alpha}_i = c_i\,\dot{\varepsilon}_{in} - \frac{3}{2}\,c_i\,\frac{\mathbf{X}_i}{a_i}\,\dot{p} - \frac{3}{2}\,d_i\left(\frac{J_2(\mathbf{X}_i)}{a_i}\right)^{m_i}\frac{\mathbf{X}_i}{J_2(\mathbf{X}_i)}$

with the initial conditions $\alpha_i\,(t = 0) = \mathbf{0}$. The exponents m_i and the factors c_i and d_i as well as the parameters Q, b, f and the exponent q are material specific; and $\dot{p}$ is the equivalent inelastic strain rate, which is being calculated from the inelastic deformation rate $\dot{\varepsilon}_{in}$ through:

EQ. 7	$\dot{p} = \sqrt{\frac{2}{3}}\,\|\dot{\varepsilon}_{in}\|$

Its time integral gives the accumulated inelastic equivalent strain p. A complete description of the model can be found in [3].

From incremental crack growth equations for creep fatigue failure [5, 6], an evolution equation due to a critical crack length can be found for the life time consumption in dependency on the inelastic strain and its growth in the distant field of the crack. Here, as in [4] and [5], the inelastic strain is replaced by the inner back stress **X** which is suitable for the behaviour of cast material. Finally, the following evolution equation for the life time consumption is derived:

EQ. 8	$\dot{D} = \frac{dD}{dt} = \left(\frac{X_{eq}}{A(T)}\right)^{m_l(T)}\left(\frac{\dot{p}}{\dot{p}_0}\right)^{n_l(T)}\dot{p}_0,\ X_{eq} := \sqrt{\frac{3}{2}}\,\|\mathbf{X}\|$

It is formulated using the von Mises equivalent inelastic strain rate $\dot{p}$ of Eq. 7, and the equivalent back stress X_{eq}. Herein, $\dot{p}_0$ is a scaling constant and A, m_l and n_l are material parameters. Using Eq. 8 the growth of damage per time increment is determined. The accumulated damage reaches its limiting value of 1 as soon as a critical macroscopic crack develops. In cyclically repeated loadings as they appear in temperature loaded exhaust-gas turbochargers the number of load cycles to failure N_f then results from the increase of damage ΔD during one saturated cycle:

EQ. 9	$\Delta D \cdot N_f = 1$

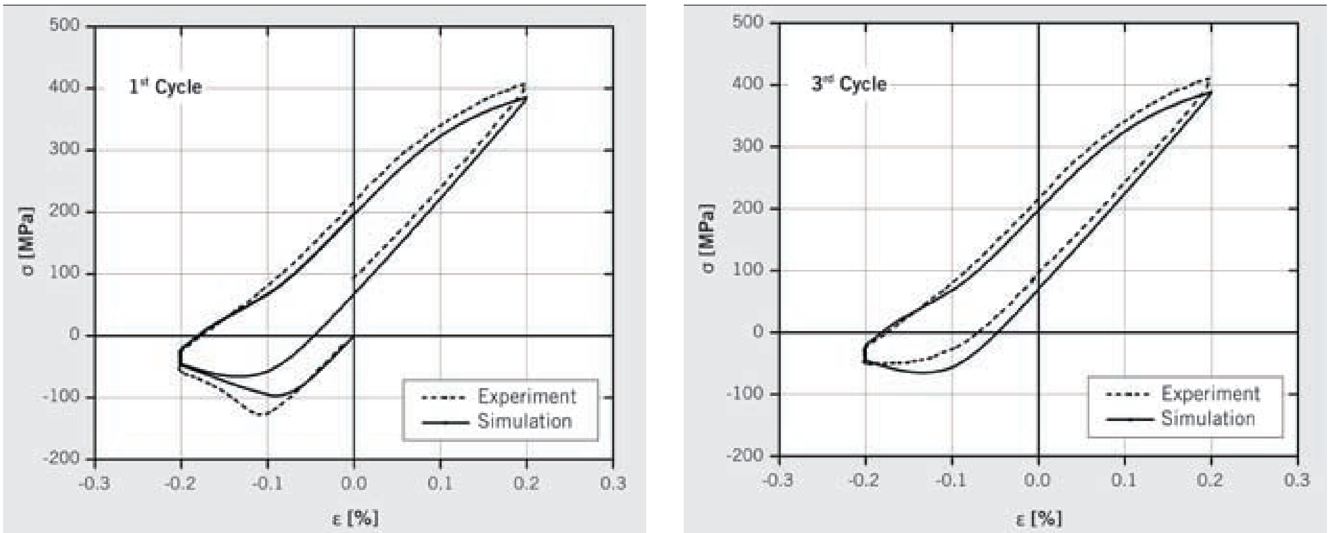

❹ Hysteresis of the first (left) and a saturated cycle 3 (right) of a non isothermal TMF 180° OP test with 180 s hold at 700 °C (comparison of experiment and simulation)

4 ADJUSTMENT OF THE MATERIAL-SPECIFIC MODEL PARAMETERS AND VALIDATION OF THE MODEL

To adjust the parameters of the deformation model to the mechanical tests the model equations are used in their uniaxial form. Then, the parameters are adjusted to reproduce the behaviour of uniaxial relaxation tests and cyclic LCF and TMF tests as well as possible. ❷ displays the stress relaxation behaviour of a compression test at 700 °C for 1 and 20 h, respectively, ❸ the hysteresis of a strain controlled LCF test at 700 °C with 180 s hold in the compression regime. ❹ shows the hysteresis of a non isothermal TMF 180° out of phase (OP) test with 180 s hold at 700 °C.

Tests on machined specimens were simulated to adjust the parameter values of the deformation and damage model. The resulting life time estimations of isothermal LCF and TMF tests are depicted in ❺. The open symbols represent tests used for the calibration procedure.

These were LCF tests with and without hold time up to 500 °C, above 500 °C without hold, and TMF tests with hold. If tests had been repeated, then they had been used for the numerical optimisation as well. They can be identified by the identical value of N_f^{sim}. The model was not adjusted to the fatigue tests represented by filled symbols in ⑤. Their life time predictions are verifications. These verifications include five different TMF tests (90° and 180° OP with different strain and temperature ranges) and isothermal LCF tests. However, isothermal high temperature LCF loading are considered to be irrelevant for the dimensioning of components, since they are generally thermo-mechanically strained. This shows, however, that the influence of hold times is overemphasised for isothermal LCF loadings at high temperatures (grey symbols), and that the model systematically underestimates the life times of these loading conditions. But, ignoring these less relevant tests for the component design, the life time discrepancies between simulation and experiment of all other tests lie inside a factor of 2.

In the practice of component design of cyclically loaded parts, frequently the approach of Smith, Watson and Topper (SWT) [7] is used for life time estimations. It supposes that the number of cycles to failure is a function of strain amplitude, maximum stress and Young's modulus. The function itself is determined by pretests. To compare both methods for the estimation of the number of cycles until failure, the SWT parameters:

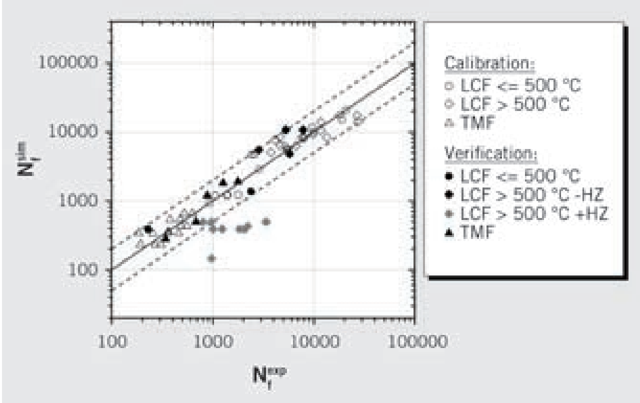

❺ Comparison of by simulation determined versus experimentally determined cycles of failure; the open symbols represent test used for the calibration procedure; the model was not adjusted to the tests represented by the filled symbols; these serve only for comparison

EQ. 10

$$P_{SWT} = \sqrt{\sigma_{\max}\, \varepsilon_a\, E(T(\sigma_{\max}))}$$

were calculated for those tests in ⑤, which had been used to calibrate our model. They are depicted in ❻ versus their cycle number of failure. From these a trend-function was established using a straight line in the double-logarithmic diagram, ⑥.

Then, for all tests in ⑤ the numbers of cycles of failure N_f^{SWT} were estimated by using this SWT trend function. According to ⑤, the calculated cycle numbers are plotted versus their experimentally found cycles to failure in ❼. In this case, the predictions show obviously a wider scatter than a factor of 2. This results from different testing temperatures and loading types, which are not accounted for by the SWT function, Eq. 10.

5 VERIFICATION ON A COMPONENT

To verify the applicability of the method in practice and for additional verification of the model parameters, a computer aided simulation was carried out on a component and the results were compared to those of a rig test. The company BorgWarner Turbo Systems provided casings of exhaust-gas turbochargers and examined

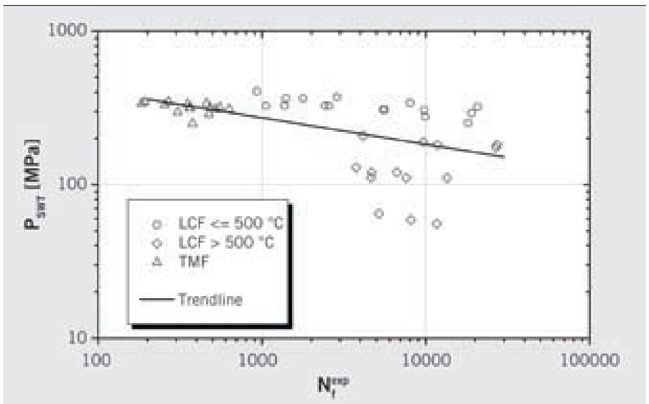

❻ P_{SWT} values of the tests used for model calibration and the trend line of these values

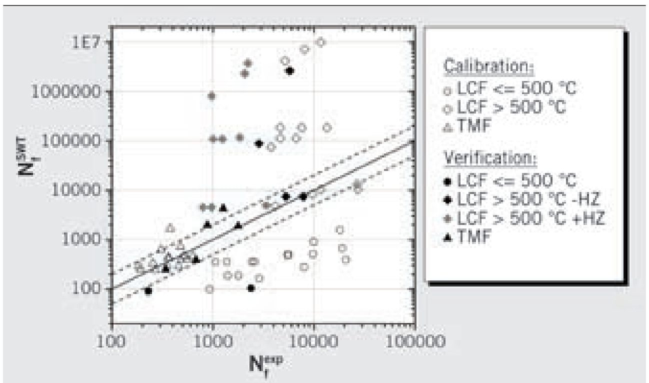

❼ Number of cycles to failure by P_{SWT} estimation versus experimentally determined; the P_{SWT} function was fitted by use of the open symbols (compare to ❻)

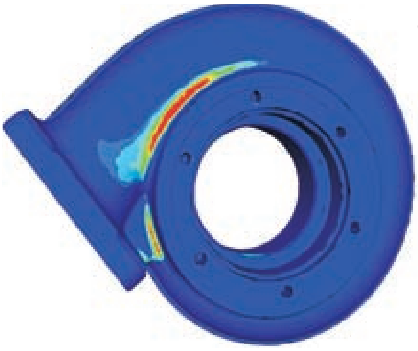

❽ Positions of damage (red area) in the simulation

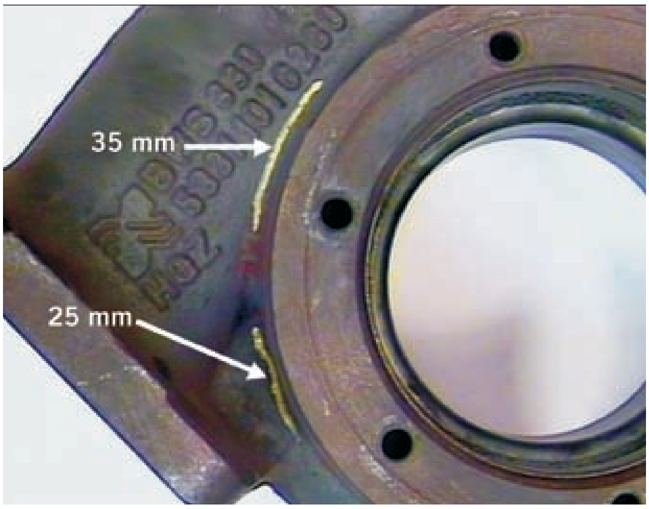

❾ Dyed cracks in the test casings

them on their own test rig. In the tests hot and cold air of 800 and 100 °C was blown through the casings alternating for 5 min, while the temperature development was recorded at various points of the casings. In periodic intervals the casings were dismounted and examined for cracks.

For the simulation the casings were meshed from CAD data. Then, using a CFD analysis the temperature development inside the casing wall was calculated, compared to the recorded temperatures and stored for a FE analysis as a function of location and time. The FEM simulation was performed by the commercial program Abaqus [8] extended by the material module which was developed at BAM and using the model parameters determined for the investigated material. The positions of the calculated highest damage in the simulation correspond perfectly with those where the first cracks had been found in the casings, ❽ and ❾.

The simulation as well as a metallographic examination of the casings after cracking showed that the cracks always initiated from the surface. The calculated time for appearance of first cracks provided about 4 times as many cycles compared to their occurrence in the rig test. If one takes into account the results of the investigation of the casting skin, namely that refinished surfaces, on which the model parameter identification is based, have a four to five times higher life expectancy, then the simulation reproduces almost exactly the real life time of the components with a discrepancy of about 10 %.

6 SUMMARY

Within the FVV research project No. 916 (“Hot Parts”), the division Mechanical Behaviour of Materials at the Federal Institute for Material Research and Testing (BAM) investigated an approach to estimate the life time of hot components in exhaust-gas turbochargers. The presented method for estimating the life time of thermo-mechanically loaded hot part components proved to be stable and applicable in the design practice. The calculation time using the presented model is comparable to the one using an elastic-plastic material law.

The life time determined by simulation proved to be superior to that determined by empirical methods and got good results in direct comparison with rig tests, if the different surface properties were taken into account. Besides the schematic mode of calculation, an advantage of this approach results from the fact, that the damage value at every point of the structure merely increases monotonically, and thus, the most strained position can be found easily.

REFERENCES

[1] Simon, V.; Oberholz, G.; Mayer, M.: Exhaust Gas Temperature 1050°. BorgWarner Turbo Systems, 2000, http://www.turbos.bwauto.com/service/default.aspx?doctype=12
[2] Chaboche, J.-L.: Cyclic Viscoplastic Constitutive Equations. Part I: A Thermodynamically Consistent Formulation. In: J Appl Mechanics 60 (1993), pp. 813 – 821
[3] Schicker, J.; Sievert, R.; Fedelich, B.; et al.: TMF-Lebensdauerberechnung für Abgasturbolader-Heißteile. Abschlussbericht, Heft 902 - 2010, Forschungsvereinigung Verbrennungskraftmaschinen e. V., Frankfurt/Main, 2010
[4] Sommitsch, C.; Sievert, R.; Wlanis, T.; et al.: Modelling of Creep-Fatigue in Containers during Aluminium and Copper Extrusion. In: Comp Mater Sci 39 (2007), pp. 55 – 64
[5] Yeh, N. M.; Krempl, E.: An Incremental Life Prediction Law for Multi-axial Creep-Fatigue Interaction and Thermomechanical Loading. In: McDowell, D. L.; Ellis, R.: Advances in Multiaxial Fatigue. ASTM STP 1191 (1993), pp. 107 – 119
[6] Majumdar, S.; Maiya, P. S.: A Mechanistic Model for Time-Dependent Fatigue. In: J Eng Mater-T 102 (1980), pp. 159 – 167
[7] Smith, K. N.; Watson, P.; Topper, T.-H.: A Stress-Strain Function for the Fatigue of Metals. In: J Mater 5 (1970), pp. 767 – 778
[8] Abaqus Inc.: Abaqus User’s Manual. Version 6.7. Providence, RI, USA, 2007. See also http://www.abaqus.com

THANKS

The research centre expresses its thanks to BorgWarner Turbo & Emissions Systems for performing the thermo-shock tests on turbine casings. The authors express their thanks to the Research Association for Combustion Engines (FVV, Frankfurt) for the selection of topics of this research project No. 916 as well as to the Federal Ministry of Economics and Technology (BMWi) for financial support via the German Federation of Industrial Research Associations (AiF, No. 14924N). The project was attended by an accompanying board of the FVV under the leadership of Dr. H. Haase. Special thanks of the authors go to this board for its wide support.